

**Domestic Electric Water Heater Control for Peak Shaving & Frequency
Control**

by

Sheng Xiang

Master of Engineering, Hefei University of Technology, 2014

A Thesis Submitted in Partial Fulfillment
of the Requirements for the Degree of

Doctor of Philosophy

in the Graduate Academic Unit of Electrical and Computer Engineering

Supervisors: Liuchen Chang, Ph.D., Electrical and Computer Engineering
Chris Diduch, Ph.D., Electrical and Computer Engineering
Examining Board: Julian Meng, Ph.D., Electrical and Computer Engineering
Julian Cardenas, Ph.D., Electrical and Computer Engineering
Suprio Ray, Ph.D., Faculty of Computer Science

External Examiner: Steven Wong, Ph.D., Natural Resources Canada

This thesis is accepted by the
Dean of Graduate Studies

THE UNIVERSITY OF NEW BRUNSWICK

February, 2021

©Sheng Xiang, 2021

ABSTRACT

The traditional operation paradigm in power systems is to dispatch controllable generators to follow a variable electricity demand. In such a way, the objective of real-time generation/load balance is achieved. The power system infrastructure is designed to meet the highest level of demand; consequently, it is underutilized during off-peak periods. Hence, peak shaving helps to reduce capital investment, operating, and maintenance costs. With the increasing penetration of renewable energy resources (RERs), the requirement for traditional generators to provide electricity is decreasing, then on-line generators' reserves are decreasing. Hence, RERs require additional reserves to defend the fluctuating generation. Therefore, additional ancillary service resources are required, such as frequency control services.

Conceptually, to control some loads to follow power production is possible, which was proposed in the 1980s, to help to provide peak shaving and ancillary services. The advantages of a domestic electric water heater (DEWH) make it a primary candidate for direct load control (DLC). The operation of a conventional DEWH is dependent on its internal thermostat, which reacts to water temperature directly and is uncontrollable. An external relay can be installed to exercise control on conventional DEWHs, but the internal end-user comfort may not be guaranteed under the relay control without temperature measurements.

In the thesis, an individual DEWH state estimation method is introduced to provide a reference for selecting control actions. Based on hot-water consumption patterns and characteristics of hot-water consumption activities, the worst cases are considered to maintain the end-user comfort without temperature measurements.

A customer satisfaction prediction index (CSPI) is proposed to gauge the comfort level of DEWH users, without temperature measurements, and is generated by a time-varying weight matrix. Subsequent hot-water consumption is considered in the CSPI. A peak shaving algorithm based on the CSPI is proposed in the thesis.

As DEWHs are resistance heating devices, they can be used to provide frequency control services for utilities. DEWHs can be aggregated as a virtual frequency control provider (VFCP) to provide frequency control under normal and contingency conditions, and the available capacity is estimated and sent to the system operator (SO) for its controls. Two control algorithms are proposed to provide frequency control services by the VFCP.

The results of this thesis show that: (1) The end-user comfort can be maintained without temperature measurements with the proposed individual DEWH state estimation method. (2) The proposed peak shaving method reduces morning peak by 24.0%, and evening peak by 31.3%. (3) The VFCP can be an effective resource to provide frequency control in power systems under different situations.

ACKNOWLEDGEMENTS

This thesis summarizes most of my research works during the last 4 years as a Ph.D. student at the Emera & NB Power Research Centre of Smart Grid Technologies of University of New Brunswick (UNB). There are many people to thank for their help and support during this time.

First and foremost, I would like to express my deepest gratitude to my supervisor, Dr. Liuchen Chang for allowing me to pursue my Ph.D. at UNB. He has been an exemplary supervisor who allowed me a lot of freedom in my research and was there to support and advise me. Without his endless, valuable supervision and persistent help, this dissertation would not be finished.

Special thanks go to Prof. Yigang He from the School of Electrical Engineering and Automation, Hefei University of Technology (HFUT) for being effectively my supervisor when I was studying in HFUT. My research was started by his supervision and help.

Another special thanks go to Dr. Bo Cao from UNB for a significant part of the Ph.D. studies, he had helped me to improve my papers and thesis all the time, I have to say, that is quite a hard job. I benefited a lot from the inspiring discussions with Dr. Bo Cao, and Dr. Riming Shao. Special thanks go to Dr. Chris Diduch for his help.

I am grateful to Dr. Julian L Cardenas Barrera, who had helped me a lot with my

experiments on water heater and simulations on our platform. Dr. Eugene F. Hill, who had given me a lot of help in my research. My appreciation to my roommates and friends, Xun Gong and Guanhong Song, they helped me a lot during the last 4 years. I consider it an honor to work with all the people in UNB, it is hard to list all their names here. They have provided their help, insights, and suggestions with kindness, which are precious to me.

Last but not least, I owe a big thanks to my family for their guidance and love, for their supports and understandings. My friends in China and Canada were an endless resource of energy and happiness, and I would like to thank them for being companions in my life. Last but not least, I am deeply grateful for the love, support, and patience of my Yoda.

Table of Contents

ABSTRACT	ii
ACKNOWLEDGEMENTS	iv
List of Tables.....	xi
List of Figures	xii
List of Abbreviations	xv
List of Symbols	xvii
1 Introduction.....	1
1.1 Background.....	1
1.1.1 Peak Shaving.....	1
1.1.2 Frequency Control.....	2
1.1.3 Direct Load Control for Peak Shaving & Frequency Control	5
1.2 Literature Review	8
1.2.1 State Estimation of Individual DEWH.....	8
1.2.2 Direct Load Control Algorithms for Peak Shaving	10
1.2.3 Direct Load Control Algorithms for Frequency Control.....	12
1.3 Objectives.....	15
1.4 Methodologies and Contributions.....	17
1.4.1 State Estimation of Individual DEWH.....	17

1.4.1.1 Methodology	17
1.4.1.2 Contributions.....	21
1.4.2 Peak Shaving Algorithm.....	22
1.4.2.1 Methodology	22
1.4.2.2 Contributions.....	24
1.4.3 Frequency Control Algorithm.....	25
1.4.3.1 Methodology	25
1.4.3.2 Contributions.....	28
1.5 Thesis Organization	28
2 State Estimation for Individual DEWHs.....	30
2.1 Introduction	30
2.1.1 DEWH Without Control.....	31
2.1.2 DEWH with Control.....	35
2.2 Hot-Water Consumption	37
2.2.1 Hot-Water Consumption Patterns	37
2.2.2 Hot-Water Consumption Activities.....	40
2.3 Worst Cases Analysis.....	42
2.3.1 Scenario I.....	44
2.3.2 Scenario II.....	46

2.3.2 Scenario III	46
2.3.3 Worst Case Assumptions.....	47
2.3.3.1 Assumption 1: Start Temperature	48
2.3.3.2 Assumption 2: Volume of a Hot-Water Consumption Activity.....	48
2.3.3.3 Assumption 3: Duration of a Hot-Water Consumption Activity	49
2.3.4 Fuzzy Logic Based Activity Identification.....	50
2.4 State Estimation for Individual DEWHs.....	51
2.5 Case Study Results.....	56
2.5.1 Test DEWH Structure	56
2.5.2 Performance on End-User Comfort	58
2.5.3 Control DEWH with State Estimation Method	62
2.6 Conclusion.....	65
3 Peak Shaving.....	67
3.1 Introduction	67
3.2 Temperature Drop Weight Matrix	68
3.3 Customer Satisfaction Prediction Index.....	70
3.4 Proposed Peak Shaving Algorithm.....	77
3.5 Case Study Results.....	83
3.5.1 Peak Shaving.....	86

3.5.2 End-User Comfort.....	91
3.5.3 Randomness of Human Behaviors	93
3.6 Conclusion.....	96
4 Frequency Control	98
4.1 Introduction	98
4.2 Virtual Frequency Control Provider	102
4.3 Proposed Frequency Control Algorithm	107
4.3.1 Frequency Control with Tolerance.....	107
4.3.2 Frequency Control with Adaptive Criterion.....	112
4.4 Case Study Results.....	119
4.4.1 Frequency Control Under Normal Conditions.....	122
4.4.1.1 For Renewable Generation	122
4.4.1.2 Regulation Services	128
4.4.2 Frequency Control Under Contingency Conditions.....	132
5 Conclusions and Future Work.....	135
5.1 Summary of this Thesis.....	135
5.2 Conclusions	136
5.3 Future Work.....	138
References	139
Appendix I Solution of the Objective Function	153

Appendix II Analysis of the Maximum Ramp-Down Power Is Increased by the Adaptive	
Criterion	155
Curriculum Vitae	

List of Tables

Table 1.1 States of DEWH.....	8
Table 1.2 Classification of AEL.....	26
Table 1.3 Classification of Controllable DEWHs	27
Table 2.1 Length of Heating Durations under Control.....	65
Table 3.1 Available Control Commands	69
Table 3.2 Parameters of DEWHs in Case Study	83
Table 3.3 Electricity Consumption.....	89

List of Figures

Figure 1.1 Peak shaving and valley filling.....	2
Figure 1.2 Response time of different frequency control services.....	5
Figure 1.3 Diagram of a DEWH with an external relay	7
Figure 1.4 Block diagram of DEWH controls providing services in a power system	16
Figure 1.5 Block diagram of the proposed state estimation method	20
Figure 1.6 Available control actions on the relay, DEWH states, and demand response .	22
Figure 2.1 Hysteresis control process of DEWH	34
Figure 2.2 DEWH temperature and power demand without hot-water consumption.....	35
Figure 2.3 Example of relay control.....	36
Figure 2.4 Seasonal influence on hot-water consumption patterns [62]	38
Figure 2.5 Probability of consumed hot-water volume by activities	41
Figure 2.6 Cumulative probability of each activity.....	41
Figure 2.7 Example of hot-water consumption activities	44
Figure 2.8 Minimum temperature with the flow rate at 5 <i>lpm</i>	45
Figure 2.9 Minimum temperature with the duration at 5 minutes	46
Figure 2.10 Minimum temperature with the start temperature at the lower limit.....	47
Figure 2.11 Membership function	50
Figure 2.12 Flow chart of the proposed state estimation method	52
Figure 2.13 Investigated DEWH.....	57
Figure 2.14 Diagram of the three-element water heater	57
Figure 2.15 24 hour hot-water consumption on the DEWH.....	58

Figure 2.16 Hourly hot-water consumption and pattern.....	59
Figure 2.17 Temperature and current of the DEWH	59
Figure 2.18 Measured and estimated temperature in the first duration	60
Figure 2.19 Measured and estimated temperature in the second duration.....	61
Figure 2.20 Measured and estimated temperature in the third duration	62
Figure 2.21 Temperature comparison.....	63
Figure 2.22 DEWH states of both cases	64
Figure 3.1 Temperature and power demand during a heating duration.....	71
Figure 3.2 Current of the DEWH during each case study	73
Figure 3.3 Temperature of the DEWH during each case study	73
Figure 3.4 Example of an activity	75
Figure 3.5 Temperature and power demand with control actions.....	76
Figure 3.6 Pseudocode of the proposed algorithm.....	77
Figure 3.7 Comparison of the real DEWH and its simulated model.....	84
Figure 3.8 Hot-water consumption of the DEWHs system in three workdays.....	85
Figure 3.9 Power consumption of the DEWHs system	86
Figure 3.10 Hourly electricity consumption	88
Figure 3.11 Percentage of DEWHs in Zone 2 during each hour.....	90
Figure 3.12 Percentage of DEWHs in Zone 3 during each hour.....	91
Figure 3.13 Maximum temperature drops of the DEWHs system.....	92
Figure 3.14 A DEWH information during control.....	93
Figure 3.15 Maximum hot-water consumption excessive of the patterns	94
Figure 3.16 Percentage of DEWHs whose hot-water consumption exceeds patterns.....	95

Figure 4.1 Frequency control in power systems	99
Figure 4.2 Framework of the VFCP	103
Figure 4.3 Available control action relates to AEL and relay state	105
Figure 4.4 Schematic representation of FCWT.....	110
Figure 4.5 Pseudocode of FCWT	111
Figure 4.6 Schematic representation of FCWA	114
Figure 4.7 Pseudocode of FCWA.....	115
Figure 4.8 Diagram of IEEE 34-bus system	120
Figure 4.9 Power system operation states and required services	121
Figure 4.10 Frequency and generation without the VFCP in CYME	122
Figure 4.11 Frequency and generation with the VFCP in CYME	123
Figure 4.12 Actual and forecast renewable generation	124
Figure 4.13 Charging/discharging power of the VFCP	124
Figure 4.14 Tracking errors of the two proposed algorithms	125
Figure 4.15 Available capacities of the VFCP.....	126
Figure 4.16 Regulation services by the VFCP	128
Figure 4.17 Available ramp-up and ramp-down capacities	129
Figure 4.18 Frequency of the test model	131
Figure 4.19 Maximum temperature drop during regulation	131
Figure 4.20 Frequency and generation in CYME after a contingency event.....	133
Figure 4.21 Discharging power of the VFCP for the contingency event	133
Figure 4.22 Available capacities of the VFCP.....	134

List of Abbreviations

ACE	area control error
AEL	Available energy level
BESS	battery energy storage system
CREST	Centre for renewable energy systems technology
CSPI	customer satisfaction prediction index
DEWH	domestic electric water heater
DLC	direct load control
DTFC	direct temperature feedback control
EV	electric vehicle
FCWT	frequency control with tolerance
FCWA	frequency control with adaptive criterion
HVAC	heating, ventilation, and air conditioning
ITFC	indirect temperature feedback control
<i>lpm</i>	liters per minute
NS	Nova Scotia
PFC	primary frequency control
PJM	Pennsylvania-New Jersey-Maryland
PV	photovoltaics
RER	renewable energy resource
REU	residential end use
RMS	root-mean-square

SFC	secondary frequency control
SO	system operator
SOC	state of charge
TFC	tertiary frequency control
TOD	time-of-day
TOU	time-of-use
VFCP	virtual frequency control provider
VPP	virtual power plant

List of Symbols

A	surface area of DEWH
ACE	area control error
AEL	available energy level in DEWHs
\mathbf{AEL}	set of DEWH AELs
\mathbf{B}	set of DEWHs should be turned back to maintain the end-user comfort
β	proportional factor
c	specific heat capacity of water
C	DEWH is controllable or uncontrollable
\mathbf{C}^k	controllability set each DEWH at the k^{th} sample
C_{SPI}	the priority of control
\mathbf{CS}^k	control signals for DEWHs at the k^{th} sample
\mathbf{D}^k	set of D_{elap} at the k^{th} sample
$D_{ava,on}$	the available duration for DEWH to keep on by the estimation method
$D_{ava,off}$	the available duration for DEWH to keep off by the estimation method
D_{cum}	cumulative heating duration since DEWH thermostat turns on
D_{elap}	elapsed time since DEWH thermostat turns on
D_{full}	estimated heating duration
D_{off}	off-heating duration
$D_{off,max}$	maximum off-heating duration without hot-water consumption
D_{on}	heating duration

$D_{on,min}$	minimum heating duration without hot-water consumption
D_{part1}	heating duration let DEWH heating to its lower limit
D_{part2}	heating duration let DEWH heating from its lower limit to upper limit
F	flow rate of draw out hot-water
$f_{measure}$	measured frequency
f_o	nominal frequency
\mathbf{G}_{CSPI}^k	<i>CSPI</i> set of each DEWH at the k^{th} sample
K	K-factor of control area
I	line flow
I_{max}	maximum limitation of the line flow
I_{min}	minimum limitation of the line flow
\mathbf{M}	set of thermostat states
$maxP_{cha}$	maximum charge power
$maxP_{dis}$	maximum discharge power
P	electricity power
\mathbf{P}	set of rated power of DEWHs
ρ	density of water
P_1	one part of P_{down}
ΔP	desired correcting power
ΔP_{adjust}	adjusted power
P_{actual}	actual power
P_{avg}	average power

P_{back}	increased power from set B
P_{base}	baseline demand of the VBPS
$P_{measure}$	instantaneous measured active power
P_{down}	decreased power
$P_{down,max}$	maximum ramp-down power
P_g	real power of a generator
$P_{g,max}$	maximum real power of a generator
$P_{g,min}$	minimum real power of a generator
P_{obj}	objective power demand
$P_{program}$	programmed exchange power with neighboring control areas
P_{rate}	rated power of DEWH
P_{Ref}	reference power
P_{VFCP}	demand of the VBPS
P_{up}	increased power
$P_{up,max}$	maximum ramp-up power
Q	thermal energy stored in DEWH
Q_{con}	consumed thermal energy
Q_g	reactive power of a generator
$Q_{g,max}$	maximum reactive power of a generator
$Q_{g,min}$	minimum reactive power of a generator
Q_{heat}	thermal energy from electricity
Q_{in}	thermal energy from inlet cold-water

Q_{loss}	standby heat loss
Q_{use}	thermal energy for hot-water consumption
R	thermal resistance of the insulation material
RS	set of relays states
R_S	external relay state
RMS	tracking error
S	set of DEWH states
T	internal temperature of DEWH
Δt	time interval
T_{aa}	estimated temperature after an activity
T_{am}	ambient temperature
T_{body}	suitable water heater temperature for the human body
T_{change}	temperature change
T_{end}	final internal temperature of DEWH
TH	temperature upper limit
Thm	thermostat state
T_{in}	temperature of inlet cold-water
TL	temperature lower limit
T_o	difference between T_{start} and TL , $T_{start} - TL$
T_{out}	draw out hot-water temperature
T_r	integration time constant
T_{start}	internal temperature when an activity starting to occur

T_{tole}	tolerance temperature
V	tank volume of DEWH
$V_{activity}$	volume of a hot-water consumption activity
V_{actual}	volume of actual hot-water consumption
V_{add}	available additional hot-water consumption without affect the end-user
V_{bus}	bus voltage
$V_{bus,max}$	maximum limitation of the bus voltage
$V_{bus,min}$	minimum limitation of the bus voltage
$V_{pattern}$	volume of hourly hot-water consumption
V_{un}	volume of unexpected hot-water consumption
w	temperature drop rate
W	weight matrix of w

1 Introduction

1.1 Background

A fundamental responsibility of a power system operator (SO) is to balance generation and load in real-time [1]. Global electricity demand has experienced significant growth for decades, e.g., an increase of 4% (900TWh) in the year 2018 and 3.9% in 2019 [2]. Traditionally, the power system infrastructure is designed to meet the highest level of load [3]. More generators, transmission lines, and transformers are required to match the electricity demand growth and maintain the generation/load balance.

1.1.1 Peak Shaving

The power system is underutilized during off-peak periods due to high peak-valley gap. The peak-valley gap of the power demand is as high as 40% to 50% in some cities of industrialized countries [4], and keeps growing [5]. To make full use of the system infrastructures, the peak-valley gap should be reduced. Peak shaving is a way to reduce such gap by reducing the demand during peak periods [6], as shown in Figure 1.1. Such reduction will lower the requirement of the installed capacity, leading to reduced costs for infrastructure and maintenance.

Implementing peak shaving will benefit not only power enterprises but also customers. The time-of-use (TOU) electricity price reflects the cost of producing electricity based on intra-day consumption demand [7], [8]. The TOU price is the highest during peak periods and

the lowest during valley periods (as shown in Figure 1.1). For example, the electricity price during valley periods (\$ 0.065 per kWh) is about half of that during peak periods (\$0.134 per kWh) in Ontario, Canada. Peak shaving can be used to reduce load demand during high price periods, thus resulting in economic benefits for industrial, commercial, and residential customers. Therefore, peak shaving methods are favorable for both power system enterprises and customers.

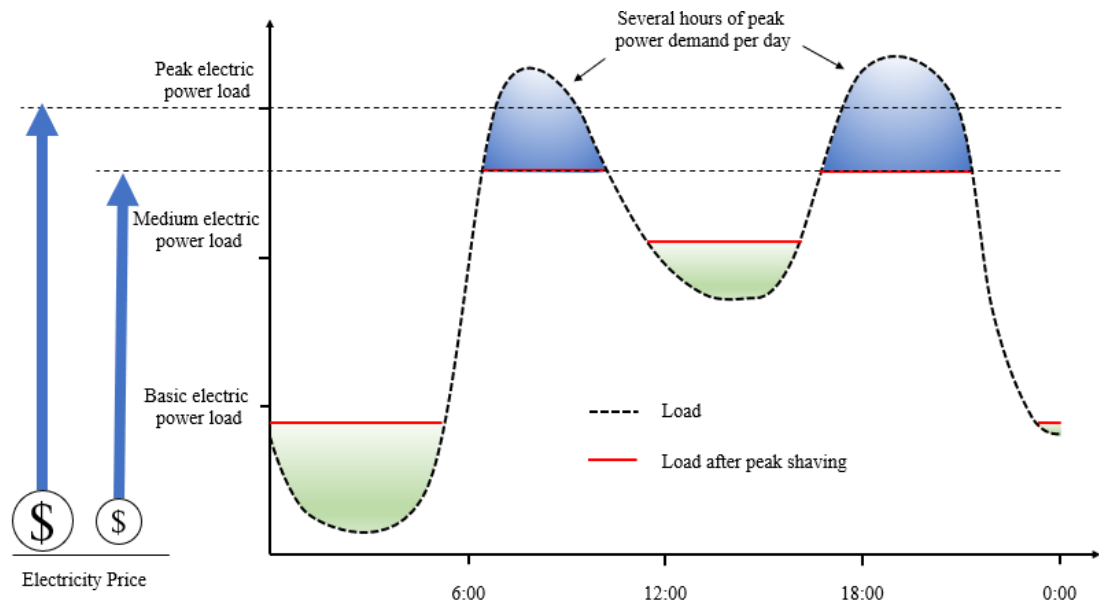


Figure 1.1 Peak shaving and valley filling

1.1.2 Frequency Control

Over the past decades, the share of renewable energy resources (RERs), such as wind and solar power [9]–[12], is rapidly increasing in electricity markets. The installed capacity of global RERs has been increased by more than 5% in 2017, three times higher than the increment of the total energy consumption. The newly installed renewable capacity will

grow by nearly 4% globally in 2020, reaching almost 200 GW of accumulative installed capacity, and the RERs are expected to reach more than 15% of total energy consumption in 2025 [13]. The increasing use of RERs has three merits: a) generating electricity that produces no greenhouse gas emissions from fossil fuels; b) utilizing sustainable energy that never runs out; and c) requiring less maintenance than traditional generators. These merits make RER a wise choice for power systems.

However, the greatest disadvantage of RER is that the energy supply is less stable than that of conventional generators [14]. Because RERs rely upon the weather conditions, i.e., wind turbines need wind to turn the blades. These weather conditions are highly variable leading to volatile RER generation. Hence, many researchers work on wind and photovoltaics (PV) generation forecast [15]–[18]. The fluctuating RER generation poses challenges to power system balancing.

Grid frequency reflects the instantaneous generation/load balance in the power system. The frequency is required to remain close to its nominal value (such as 50 Hz in China and 60 Hz in North America). When the generation exactly meets the demand, the frequency is at its nominal value. When the generation becomes lower than the demand, the frequency decreases from its nominal value. When the generation becomes higher than the demand, the frequency increases from its nominal value. The frequency control services are provided by generators or flexible loads in traditional power systems [19]–[22].

The power system frequency can be controlled in three steps: primary, secondary, and

tertiary frequency control:

- **Primary frequency control (PFC)** is designed to stabilize the frequency when unbalance conditions occur between generations and loads. PFC is the first active response of resources to arrest the grid frequency deviations. The grid frequency is maintained within permissible limits, but a steady-state deviation from the nominal frequency remains. The response time of the PFC is typically less than 30 seconds [23].
- **Secondary frequency control (SFC)** is used to restore the grid frequency to its nominal value after the PFC. The active power is modified by a centralized controller. The SFC is typically completed within 15 minutes [23].
- **Tertiary frequency control (TFC)** is introduced to the system if the grid frequency still cannot be restored after the SFC [22], [24]. The TFC is the automatic or manual change in the working points of the participating generating units.

The relationship among the three frequency control methods is shown in Figure 1.2.

The number and magnitude of grid frequency deviations are increased due to the increasing penetrations of volatile RERs. More frequency control reserves are therefore required [25]. However, the percentage of conventional generators in power systems is reduced by the increasing RERs, then the frequency control reserve capacity is decreased. Therefore, additional resources are required to provide frequency control services.

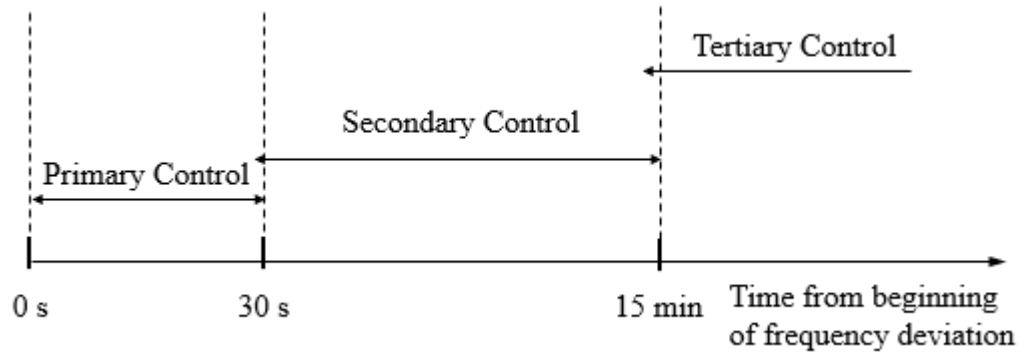


Figure 1.2 Response time of different frequency control services

1.1.3 Direct Load Control for Peak Shaving & Frequency Control

Thermostatic loads can be used as flexible energy resources. The loads include heating, ventilation, and air conditioning (HVAC) units, domestic electric water heaters (DEWHs), and refrigerators [26]–[31]. They can be directly controlled without affecting the end-user comfort due to their thermal inertia. Such direct load control (DLC) can change daily load profiles for peak shaving, and regulate real-time electric power for frequency control [28]–[31].

Electricity consumption by DEWHs has taken up a high percentage of total consumption in the local power system, e.g. 18% in the U.S. [32] and 19% in Canada [33]. The residential electricity consumption is highly dependent on the consumption of DEWHs [34], [35], and the peak periods in the power system demand are approximately the same with the peak periods of DEWH consumption [32]. Furthermore, the high thermal inertia of hot-water tanks offers a huge potential of modifying their duty cycles without affecting the end-user comfort [36]. Hence, DEWH is a good candidate for DLC.

The pilot program of the U.S. Department of Energy had controlled water heaters with temperature sensors to provide load shift and curtailment services, which had shown the potential of water heater control in power systems [37]. Two pilot studies were completed in 2015, which controlled water heaters based on temperature information and showed positive results in providing ancillary services [38]. CanmetENERGY had a program on Energy Research and Development, which demonstrated the demand response potential of water heaters based on temperature measurements [39]. Washington State University Energy program also controlled water heaters with temperature measurements to provide services [40]. The potential of water heaters was verified through these programs.

DEWHs are typically controlled by a hysteresis controller using an internal thermostat based on a preset temperature setpoint and a dead band (including both lower and upper temperature limits). When the temperature falls below the lower limit, the DEWH turns on and keeps heating until the temperature reaches its upper limit. Then, the DEWH turns off and a new cycle begins. The hysteresis controller guarantees the end-user comfort. Smart water heaters have controllable setpoints and can be controlled on/off at any time [41]–[43]. However, smart water heaters are rarely deployed in practice due to high costs. Thus, only conventional DEWHs are considered in the thesis. The setpoints and dead bands of conventional DEWHs are uncontrollable; therefore, an external relay is installed to exercise controls.

Figure 1.3 shows the diagram of a one-element conventional DEWH with an external relay,

the external relay is connected in series with the DEWH. The setpoint is normally set manually and is rarely changed in practice. When the relay is on, the on/off state of DEWH is consistent with that of its local thermostat. When the relay is off, the DEWH is off. Hence, when the local thermostat is on, the control on a DEWH can reduce the electricity demand by turning off the external relay. When the local thermostat is off, the external relay cannot change the electricity demand [44]–[46]. Such on/off state logics of the DEWH and the external relay are summarized in Table 1.1.

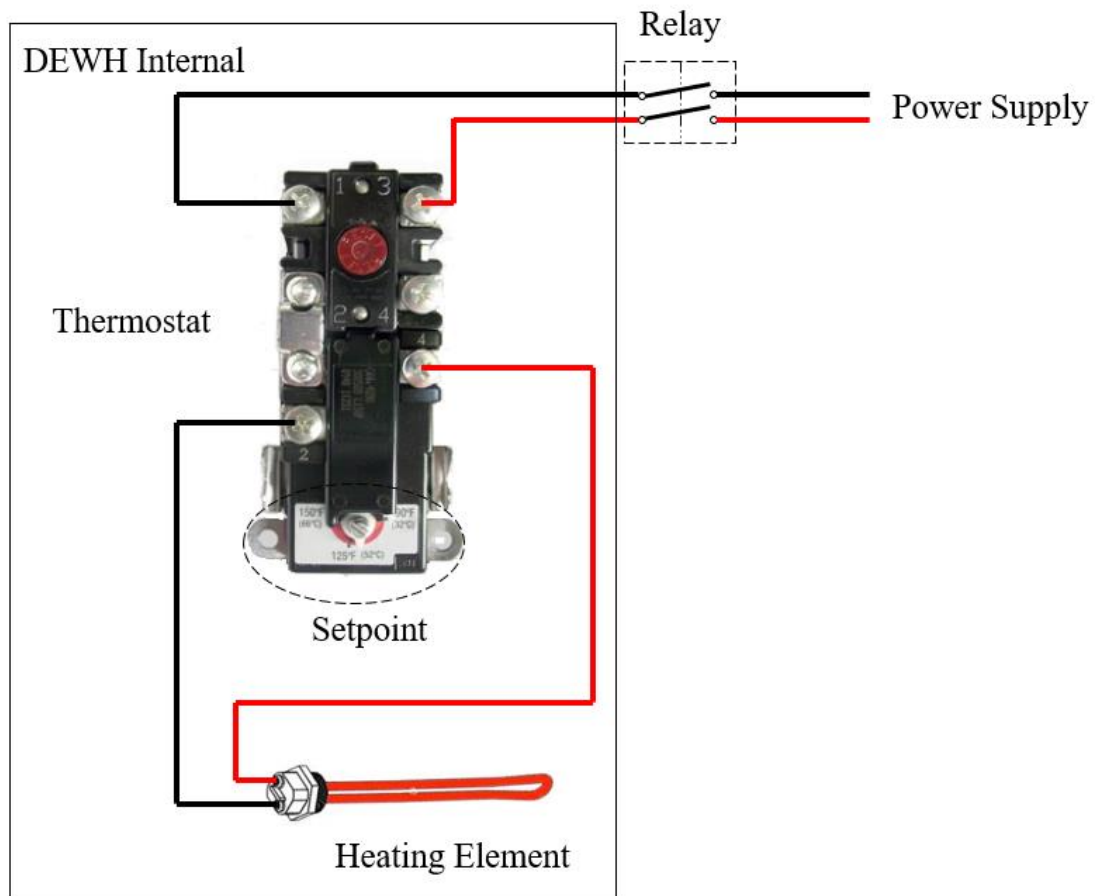


Figure 1.3 Diagram of a DEWH with an external relay

Table 1.1 States of DEWH

DEWH States		Relay States	
		ON	OFF
Thermostat States	ON	ON	OFF
	OFF	OFF	OFF

When the external relay is on, the hysteresis controller works as usual to maintain the end-user comfort. However, when the relay is off, the DEWH can no longer heat water and the end-user comfort guaranteed by the hysteresis controller is lost. Hence, maintaining the end-user comfort with the external relay is the main challenge when controlling conventional DEWHs. In [28], [29], [32], [47], [48], real-time temperature measurements are used to control DEWHs. However, temperature measurements require to add temperature sensors on each DEWH, which increase the costs for equipment and the requirement for communication infrastructures. Hence, DEWH temperature measurements are impractical for cost reasons. To maintain the end-user comfort without temperature measurements is one of the main objectives of the thesis.

1.2 Literature Review

1.2.1 State Estimation of Individual DEWH

External relays as that shown in Figure 1.3 may lead to the loss of end-user comfort which is originally guaranteed by DEWHs' local thermostats; and it is also costly to implement temperature measurements. Hence, DEWH states should be estimated and provide a reference during control to maintain the end-user comfort.

Some existing DEWH control algorithms were based on temperature measurements or controllable setpoints [28], [29], [32], [47], [48]. Real-time temperature measurements were used to estimate human behaviors. Therefore, DEWHs could be pre-heated before large hot-water consumption activities occurred.

In [28], the hot-water consumption was estimated and forecasted based on given water usage patterns and the measured temperature information. Subsequently, the control decisions were generated by a reinforcement learning method to minimize economic costs. Up to 50 temperature sensors were implemented and certain water usage was assumed.

Net-zero energy buildings in the Netherlands were demonstrated in [49]. Smart meter data for domestic hot-water consumption were collected for these buildings. Then online optimization models were built to represent occupant behaviors based on this information. Finally, the data-driven optimal heating schedules were generated automatically.

Roma Spur et al. [50], [51] extracted hot-water consumption profiles based on temperature measurements or flow rates and durations of hot-water consumption. Then occupant behaviors were calculated. Sufficient time to reheat the water before the next demand occurrence was reserved to maintain the end-user comfort.

All in all, the consideration of subsequent hot-water consumption helps to generate more effective control actions on DEWHs, but temperature measurements during control are impractical. Hence, an individual DEWH state estimation is required, not only to estimate

the DEWH state to maintain the end-user comfort without temperature measurements, but also to take into account the effects of hot-water consumption.

1.2.2 Direct Load Control Algorithms for Peak Shaving

There were different control strategies for controlling DEWHs for peak shaving. *Nehrir et al* assigned the water heaters in an area into several blocks and controlled each by different fuzzy controllers [52]. The utility distribution profiles were leveled via shifting the DEWH peak demand to off-peak periods. These fuzzy logic controllers needed the temperature information, utility power demand, and customers' preferences, which were designated by the maximum and minimum temperatures for DEWHs.

In [53], a hardware design of smart home energy management system was proposed with the applications of communication and sensing technologies. Then a machine learning algorithm was used to control water heaters and other devices to reduce total electricity costs. Human activities, water heater temperature, customer preferences, and other information were required.

Khalid et al introduced Q-learning and action-dependent heuristic dynamic programming that reduced the peak demand and the economic cost [32]. A state-space model was defined. The states were the temperature of hot-water, instantaneous hot-water consumption flow rate, and estimated grid load. Three membership functions were used to convert the three states to linguistic representations that were compatible with the Q-

learning based approach.

Ruelens et al developed an agent with 50 temperature sensors and a backup controller that overrules the control actions to maintain the end-user comfort, with a reinforcement learning method to reduce costs [28]. Auto-encoders were applied to explore a small-dimensional representation that reduced the number of temperature sensors used. They also used a model-free Monte-Carlo method that uses a metric based state-action value function or Q-function in [29].

All above-mentioned peak shaving methods were based on the control of conventional DEWHs. These methods needed temperature measurements. Some other researchers had developed the methods for smart DEWHs. The end-user comfort was maintained by an internal hysteresis controller, so these methods would not require temperature measurements. *Diao et al* adjusted temperature settings to reduce DEWH demand and peak demand in power systems [41]. The setpoints were set at low values during peak periods to reduce the peak demand, and the local hysteresis controllers were automatically applied to maintain the end-user comfort.

Ning Lu et al discussed setpoint control strategies for DEWHs in a competitive electricity market [54]. The power consumption was shifted from high price periods to low price periods by varying the setpoints. The daily day-ahead market price curve was used to find the economically optimized control strategies with all physical constraints satisfied.

Kondoh et al [55] modified circuit of a conventional water heater with an additional lower thermostat, then the water heater was controlled without temperature measurements. However, it was impractical to modify water heaters to make their thermostats controllable. Others [56] assumed the local controller had highest priority, then the devices could respond to control commands if they temperatures were in the deadband; it was impossible for conventional devices.

Overall, the existing methods were mostly based on temperature measurements or direct adjustments of DEWHs' temperature setpoints. The end-user comfort was maintained by the temperature information or the local hysteresis controller. However, all of them are not suitable for the conventional DEWHs without temperature measurements and without modifications on the internal circuits. Therefore, a new algorithm is proposed for peak shaving in the thesis.

1.2.3 Direct Load Control Algorithms for Frequency Control

Compared with using traditional generators, using loads to provide ancillary services may offer higher efficiency and lower costs [57]. The DLC must deliver a reliable resource to the power system while simultaneously maintaining a level of service commensurate with customer expectations. This characteristic distinguishes it from conventional generation-based control approaches [57]. Frequency control is one of the most important ancillary services. Hence, many researchers are working on developing frequency control methods with controllable loads.

In [41], *Diao et al* employed a centralized and two decentralized controllers to provide frequency support following generators' trips. The centralized controller assumed no communication delay and the control signals could be a sinusoidal wave or step change to adjust setpoints of DEWHs. The two types of decentralized controllers were: a) temperature setting droop and randomized threshold; b) reconnection delay. All the controllers controlled setpoints to respond to frequency variations.

Zeyad et al introduced a hierarchal control for a group of DEWHs to provide different dynamic frequency services. Two decision layers were used: the aggregator layer and the device control layer [58]. The aggregator layer received states of devices from the device control layer. The device control layer used the temperature information to respond from DEWHs with higher to lower temperatures when a frequency drop occurred.

Khalid et al in [59] used DEWHs for frequency control in a small residential type PV-diesel hybrid mini-grid through the varying setpoints and a droop factor to adjust the power demand of DEWHs to respond to the grid frequency deviations.

Ali et al presented a cost-effective modification of the operation of the lowest heating element of a DEWH to allow the DEWH to participate in frequency control regulation [60]. Two proportional loops regulating the temperature and grid frequency were operated in parallel with a modified lowest heating element, or a proportional loop regulating the rate-of-change of the grid frequency. When the grid frequency was high, the element was

turned on to increase the power demand to restore the generation/load balance. When the grid frequency was low, the element was turned off to decrease the power demand to restore the generation/load balance. The element would remain off until the frequency regulating loop reached equilibrium with the temperature regulating loop.

Tasisuke et al in [61] employed electric vehicles (EV) and water heaters to reduce the required capacity of the battery energy storage system (BESS). The power of water heaters was decreased into the range of $90\% \pm 10\%$ of the rated power to respond to control signals, and this was achieved by controlling the voltage. These water heaters were divided into several groups and controlled in each group in different periods.

Vrettos [22] introduced DEWHs to provide the SFC, with the measured temperature information to quantify the energy stored in DEWHs. Then a direct temperature feedback control (DTFC) method was proposed to respond to frequency variations for the SFC. An indirect temperature feedback control (ITFC) method did not directly require temperature information. However, the ITFC still required temperature measurements to detect the event when the temperature reaches the upper or lower temperature limit. Hence, the temperature measurements were required. An aggregated power feedback control method was proposed without temperature measurements, which did not require feedbacks from individual water heaters. However, the water heaters were bidirectionally controlled for DTFC, ITFC and the aggregated power feedback control method. In other words, the thermostat was controllable. These methods were not appropriate for conventional DEWHs. A stochastic blocking control method was also proposed with a broadcast control

parameter, in which the water heaters were blocked or released by comparing the broadcast control parameter and a generated uniformly distributed random number. It did not require temperature measurements or other information from individual water heaters. However, the end-user comfort was not considered, and may be affected during control.

In [62], a control algorithm was proposed based on the estimation of reserve capacity. The proposed algorithm did not require temperature measurements. A preset time constraint was applied to guarantee customers' comfort during control and to calculate the ramp-up/ramp-down reserves. However, how to build the preset time constraint was not presented.

All in all, the previous methods were mostly based on the temperature measurement or direct control of DEWH's internal thermostats. However, all of them are not suitable for the conventional DEWHs without temperature measurements and without modifications on the internal circuits. Therefore, new algorithms are needed for frequency control.

1.3 Objectives

The limitations of the previous DEWH controls motivate us to design control algorithms for peak shaving and frequency control with conventional DEWHs without temperature measurements, and meanwhile the end-user comfort should be maintained. Specifically, the research objectives of this thesis research are divided into the following sub-objectives:

- (1) Propose a new state estimation method for an individual DEWH to evaluate the available capacity and reference the information for control, which can handle uncertainty and randomness of human behaviors on conventional DEWHs. Thus the end-user comfort can be maintained without temperature measurements.
- (2) Develop a control algorithm for peak shaving based on the information obtained from the proposed state estimation method for individual DEWHs.
- (3) Design two control algorithms to provide frequency control services for utilities under normal and contingency conditions.

A block diagram in the context of DEWH control in the power system is shown in Figure 1.4, where DEWHs are aggregated as a distributed resource in the power system. Virtual power plant (VPP) presented in Figure 1.4 works as a centralized controller for the

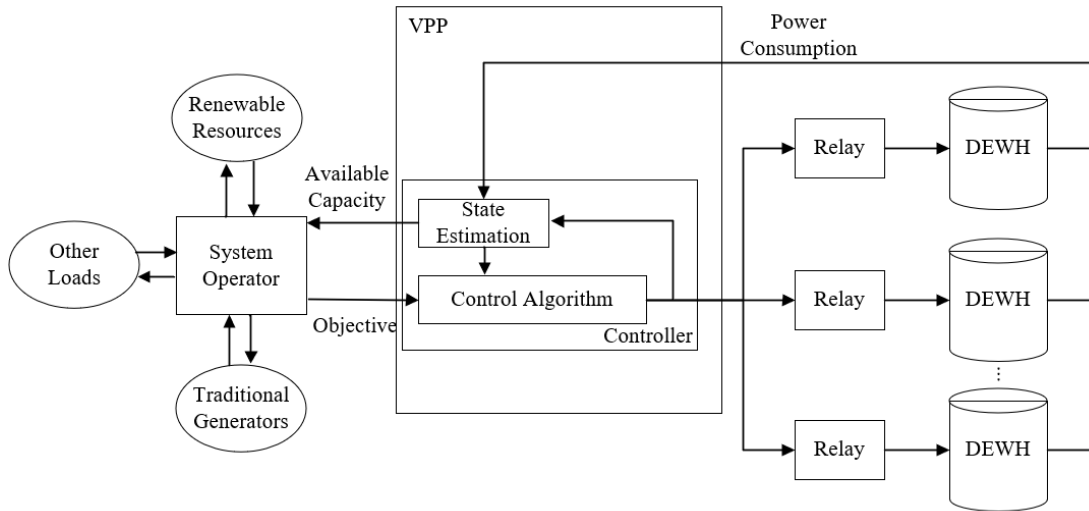


Figure 1.4 Block diagram of DEWH controls providing services in a power system

distributed DEWHs. The state estimation block in the VPP corresponds to the proposed individual DEWH state estimation method to estimate DEWH states and provide the available capacity information to the SO. The peak shaving or frequency control services are provided by the control actions generated from control algorithms.

1.4 Methodologies and Contributions

1.4.1 State Estimation of Individual DEWH

1.4.1.1 Methodology

In practice, most people have behavioral habits which result in corresponding hot-water consumption patterns [63]–[66]. These hot-water consumption patterns can be used for the individual DEWH state estimation, which can be used to estimate the hot-water consumption.

As Table 1.1 shows, the on/off state of a DEWH is dependent on the relay state and the on/off state of the DEWH's thermostat. The control signal determines the on/off state of the relay and can be directly obtained from the controller. Hence the relay does not need a measurement. The DEWH state can be identified through the household power measurement by using smart meters data and load disaggregation methods [34], [67]; assuming completely accurate in the thesis. The thermostat state is unknown but can be deduced by the DEWH state and the relay state:

(1) When the relay remains on, the DEWH is directly turned on and off by its internal thermostat, i.e., the thermostat state is the same with the DEWH state which is known.

(2) When the relay remains off, the DEWH keeps off regardless of the thermostat state.

The thermostat state is assumed to keep its previous state:

- a. If the previous state of thermostat is off, the DEWH cannot be controlled to change the load demand. Hence, the DEWH is not a candidate for controls.
- b. If the previous state of thermostat is on, the DEWH can be controlled to change the load demand. The thermostat state is on.

When the relay is on and the thermostat turns from on to off, the DEWH stops heating, meaning that the DEWH temperature has reached its upper limit. When the relay is on and the thermostat turns from off to on, the DEWH begins heating, meaning that the DEWH temperature has reached its lower limit. These two rules can be used to adjust the estimation results, which helps to maintain the end-user comfort.

The internal temperature of a DEWH is dependent on its rated power, on/off state, tank volume, standby heat loss, inlet cold-water temperature, and hot-water consumption. The information except the hot-water consumption is knowable. The unknown hot-water consumption has huge impact on the DEWH state.

Hot-water consumption activities, such as tap, bath and shower, have different volumes of hot-water usage, flow rates, and durations [63], [64], [68], [69]. These differences can be

used to identify hot-water consumption activities based on template patterns. Then the identified activities can be used to estimate DEWH states.

The diagram of the proposed state estimation method is shown in Figure 1.5.

To maintain the end-user comfort without temperature measurements, the worst cases (which causes the internal temperature to be the lowest) should be considered as described in the following:

- (1) The activity with large hot-water consumption volume is identified from the hot-water consumption patterns by a fuzzy logic function. Based on hourly hot-water consumption patterns, the available activities are identified by mapping their characteristics with the patterns. Since drawing out a large volume of hot-water in a short duration will cause a large temperature drop, the maximum possible temperature drop will be assumed by taking the available large volume hot-water consumption activity into account.
- (2) The consumed thermal energy associated with each type of hot-water consumption activity is assumed to be constant. When an activity occurs, the different thermal energy stored in the DEWH will lead to different minimum temperatures; less thermal energy leading to a lower minimum temperature. The identified activity is assumed to occur instantaneously when the thermostat turns on. When the thermostat remains on, the identified activity is assumed to occur at the earliest

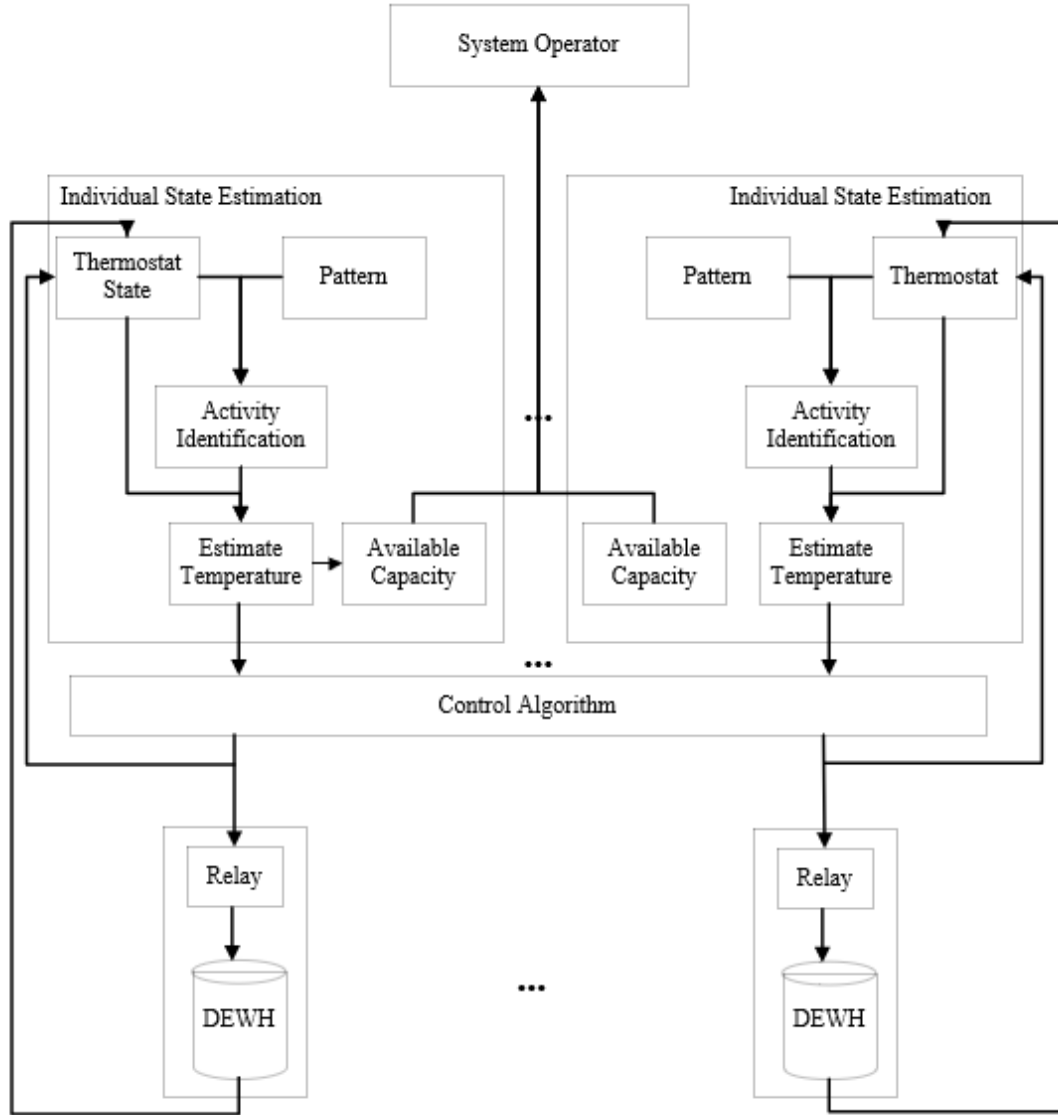


Figure 1.5 Block diagram of the proposed state estimation method

available occurrence time.

- (3) For the same hot-water consumption activity, the minimum temperature may be lower with a fast flow rate. The same hot-water consumption leads to a lower temperature with a faster flow rate. Hence, the activity duration should be assumed to be small.

With the above three worst case assumptions, hot-water consumption activities and their occurrence times can be estimated. Then the temperature of the DEWH can be estimated, which will be the reference to maintain the end-user comfort during control. The available on duration (the heating duration until the temperature reaches its upper limit) and off duration (the off-heating duration until the temperature drops too low) can be calculated. The on and off durations decide the available capacity for controls. The capacity should be provided to the SO.

1.4.1.2 Contributions

The research into the proposed state estimation method for individual DEWHs has led to the following contributions:

- (1) Estimate the state of individual conventional DEWHs without temperature measurements. The estimated information includes the temperature and available on/off durations for controls.
- (2) Maintain the end-user comfort for the control of conventional DEWHs. While the end-user comfort guarantee from the hysteresis controller in the conventional DEWH is lost when the relay keeps off, the estimated information based on the developed method is used to provide a reference to maintain the end-user comfort without temperature measurements.

1.4.2 Peak Shaving Algorithm

1.4.2.1 Methodology

With the external relay, the available control actions and the effects on DEWH's states are shown in Figure 1.6. The DEWH keeps off when the thermostat is off, they are uncontrollable. The control actions are useful to DEWHs which thermostats are on.

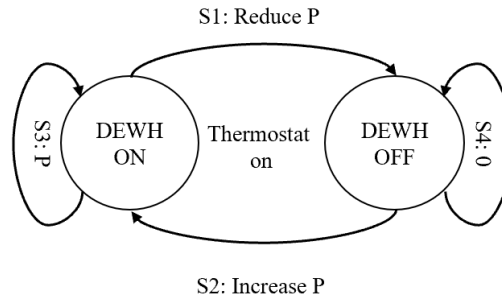


Figure 1.6 Available control actions on the relay, DEWH states, and demand response

The demand can be controlled with the following four control actions: (1) when the relay control signal is switched from on to off (S1), the DEWH will be turned off and its demand will be decreased by P (the rated power of the DEWH); (2) when the relay control signal is switched from off to on (S2), the DEWH will be turned on and its demand will be increased by P ; (3) when the relay control signal remains on (S3), the DEWH will stay on and its demand will remain P ; (4) when the relay control signal remains off (S4), the DEWH will stay off and its demand will remain zero.

When the DEWH thermostats are on and the end-user comfort is satisfied, the DEWHs can

be turned off by S1 and kept off by action S4 for certain durations, to reduce demand. When the end-user comfort is not satisfied, the DEWHs must be powered by action S2 to start heating water, then kept heating up by action S3.

With the estimated information from the proposed state estimation method for an individual DEWH, the temperature can be estimated. To maintain the end-user comfort during control, a minimum temperature is selected when the DEWH must be turned on. This minimum temperature is called the tolerance temperature in this thesis [70]. If the estimated temperature is higher than the tolerance temperature, the end-user comfort is regarded as maintained. A lower tolerance temperature can provide a larger control capacity, but would result in more negative impacts on the end-user comfort. The temperature for the end-user comfort should be no less than 40 °C [71], pointing to the minimum value of the tolerance temperature.

As in the previous descriptions, the subsequent hot-water consumption is very important for the control and end-user comfort. Hence, the subsequent hot-water consumption in combination with the estimated temperature, is considered to generate appropriate control actions on DEWHs. A weight matrix is introduced to express the temperature drop caused by the subsequent hot-water consumption and standby heat loss. A customer satisfaction prediction index (CSPI) is proposed to express the priority of control with the weight matrix.

The required thermal energy by hot-water consumption activities should remain unchanged

because human behaviors are not affected by controls. Therefore, more DEWHs reaching their upper temperature limits at the beginning of peak periods will help to achieve the objective of peak shaving.

The peak shaving algorithm is to generate appropriate control signals based on DEWH CSPIs and relay states. The end-user comfort will be maintained by turning on the relays of those DEWHs whose CSPIs are low.

The proposed control algorithm has the similar ability on peak shaving with that of a benchmark algorithm, DTFC [22]. Meanwhile, the proposed algorithm does not require temperature measurements which are a must-have for the DTFC, and has a better performance in maintaining the end-user comfort.

1.4.2.2 Contributions

The contributions of the proposed peak shaving algorithm in the thesis are:

- (1) The subsequent hot-water consumption is modeled as a weight matrix by which thermal energy can be prepared against large hot-water consumption activities. The prepared energy can help avoid significant DEWH temperature drop and thus maintain the end-user comfort.
- (2) The proposed algorithm enables a successful management on uncontrollable

DEWH thermostats, leading to the increase of the peak shaving capacity.

- (3) An error reduction method is proposed to reduce the estimated errors without temperature measurements.

1.4.3 Frequency Control Algorithm

1.4.3.1 Methodology

In power systems, a power mismatch can be caused by the variations of generations or load demands, which leads to a grid frequency deviation. Frequency control services are activated to reduce and eventually eliminate the frequency deviation. For conventional generation-based control approaches, the power mismatch and frequency deviation are eliminated by the increase/decrease of the generation. The power mismatch and frequency deviation can also be recovered by the decreased/increase of the load demand, which is the load-based control approach.

DEWHs can be aggregated as a frequency control service resource in power systems, which is called a virtual frequency control provider (VFCP) in this thesis. Due to the delays of more than seconds in communications and controls of DEWHs, the VFCP is used to provide SFC in this thesis.

The VFCP consists of a number of DEWHs, a centralized controller, and a capacity calculator. The centralized controller controls DEWH demands to respond to the frequency

control requirements from the SO. The capacity calculator is used to calculate the available ramp-up and ramp-down capacities of the VFCP. The capacities will be sent to the SO.

To respond to the frequency control requirement, the demand of the VFCP should be increased/decreased. Only these DEWHs of which thermostats are on can be controlled to increase/decrease their demands. An available energy level (AEL) in a DEWH is introduced to show the stored energy in the controllable DEWH for frequency control and maintain the end-user comfort. The AEL is dependent on the DEWH temperature, as shown in Table 1.2. If the DEWH temperature is equal to its lower limit, the AEL is defined as zero. If the DEWH temperature is higher than the lower limit, the AEL is positive. If the DEWH temperature is lower than the lower limit, the AEL is negative.

Table 1.2 Classification of AEL

DEWH Temperature	AEL
$> \text{lower limit}$	> 0
$= \text{lower limit}$	$= 0$
$< \text{lower limit}$	< 0

Then these controllable DEWHs can be classified into four groups based on their AELs and relay states, as shown in Table 1.3. Group 1 includes DEWHs of which relays are on and AELs are positive. Group 2 includes DEWHs of which relays are on and AELs are not positive. Group 3 includes DEWHs of which relays are off and AELs are higher than a threshold. Group 4 includes DEWHs of which relays are off and AELs are not higher than

the threshold. A threshold is employed to maintain the end-user comfort, which relates to the tolerance temperature in Section 1.4.2.

Table 1.3 Classification of Controllable DEWHs

Group	Group 1	Group 2	Group 3	Group 4
Relay	ON	ON	OFF	OFF
AEL	> 0	≤ 0	$> \text{threshold}$	$\leq \text{threshold}$

The DEWHs in Group 4 must be turned on to maintain the end-user comfort. Then, the frequency control requirement should be adjusted due to the increased demand of DEWHs in Group 4. The adjusted requirement is the frequency control requirement minus the demand of DEWHs in Group 4. If the adjusted requirement is negative, the VFCEP is required to reduce its demand through turning off DEWHs in Group 1. If the adjusted requirement is positive, the VFCEP is required to increase its demand through turning on DEWHs in Group 3.

A novel algorithm is proposed for frequency control based on the above descriptions. In addition, an improved algorithm is also proposed to increase the frequency control reserve of the VFCEP. An IEEE 34-node test model is employed to test the frequency control performances of the VFCEP with both control algorithms. The end-user comfort is maintained with both algorithms in the case studies. The maximum temperature drop is reduced by the improved algorithm.

1.4.3.2 Contributions

The contributions of the proposed algorithms in the thesis include:

- (1) A VFCP framework is proposed as a frequency control resource in power systems. The VFCP demand is increased/decreased by controlling these controllable DEWHs.
- (2) Two frequency control algorithms are proposed to provide frequency control services by the VFCP.

1.5 Thesis Organization

The rest of the thesis is divided into the following chapters:

- **Chapter 2** develops an individual DEWH state estimation method without temperature measurements. Based on hot-water consumption patterns and characteristics of hot-water consumption activities, a fuzzy logic membership function is introduced to estimate hot-water consumption activities. The worst case assumptions to estimate DEWH's states and maintain the end-user comfort are also introduced.
- **Chapter 3** introduces a novel peak shaving algorithm for control of conventional DEWHs. A weight matrix is proposed to consider the subsequent hot-water consumption, and the CSPI is proposed to express the priority of control based on

the weight matrix. According to the CSPI and relay states, these controllable DEWHs are divided into two groups, each group is sorted by the CSPI. With the control actions, more thermal energy can be stored in DEWHs before the beginning of peak periods, and the demand can be reduced by following the sorted order during peak periods. To maintain the end-user comfort, on-signals are sent to the DEWHs whose CSPIs are not satisfied. The results show the peak demand is significantly reduced and the end-user comfort is maintained.

- **Chapter 4** proposes two frequency control algorithms to provide SFC services with DEWHs. A VFCEP is introduced as a frequency control resource. The VFCEP is estimated and sent the available capacity for frequency control. The control actions are generated to respond to frequency deviations under normal and contingency conditions. The algorithms are dependent on the estimated information for control. The performances of the two algorithms are demonstrated in simulation studies.
- **Chapter 5** summarizes the key findings of this thesis and suggests directions for future work.

2 State Estimation for Individual DEWHs

2.1 Introduction

With the external relays to control conventional DEWHs in the thesis, maintaining the end-user comfort without temperature measurements is important. Hence, it is necessary to estimate the DEWH states before controlling the DEWH. The estimated state information includes the temperature and available durations for the DEWH to keep on or off. The estimated information is used to conduct on/off control to DEWHs, providing peak shaving or frequency control services without affecting the end-user comfort.

The chapter introduces the estimation of the DEWH states without temperature measurements. If the external relay is turned off which keeps the DEWH off, the internal temperature can be lower than its lower limit, then the end-user comfort may be affected. In this situation, the relay should be turned on to heat water to avoid affecting the end-user comfort. To maintain the end-user comfort without temperature measurements, the worst cases are used to estimate the minimum temperature of DEWHs, then the estimated results can be used as references for control.

The organization of this chapter is as follows: the process of the DEWH without control is presented in Section 2.1.1. The process of the DEWH with control is presented in Section 2.1.2. Hot-water consumption patterns and activities are analyzed in Section 2.2. Potential worst cases are analyzed, whereby the worst case assumptions for the proposed state

estimation method are obtained in Section 2.3. A fuzzy logic hot-water consumption activity identification method is introduced in Section 2.3 too. The proposed state estimation method for individual DEWH is described in Section 2.4. Finally, the experimental results are presented in Section 2.5.

2.1.1 DEWH Without Control

The thermal energy stored in a DEWH through hot-water in the tank is converted from the electrical energy by heating elements. When the end-user draws out hot-water from the DEWH, thermal energy decreases. The stored thermal energy is decreased gradually and persistently by the standby heat loss, due to the imperfect insulation of the tank. The hot-water consumption and standby heat loss cause the DEWH temperature to drop.

The thermal energy stored in a DEWH is represented by the internal temperature of the DEWH:

$$Q(t) = c\rho VT(t) \quad (2.1)$$

where Q is the thermal energy stored in the DEWH, c is the specific heat capacity of water, ρ is the density of water, V is the volume of the tank, and T is the internal temperature of the DEWH.

DEWHs are resistive devices, and the electrical energy converts to the thermal energy through heating elements. Hence, when ignoring the grid voltage variations, the thermal energy from the electrical energy can be written as:

$$Q_{heat}(t) = P(t)\Delta t \quad (2.2)$$

where Q_{heat} is the thermal energy from electricity, P is the power of the DEWH which is the rated power P_{rate} when the DEWH is on or 0 when the DEWH is off, and Δt is the time interval. When the DEWH is on, the thermal energy from the electrical energy is increased with a constant rate.

The standby heat loss is a transfer of internal thermal energy from the tank to the ambient environment, this is due to the internal temperature of DEWH being higher than the ambient environment. The standby heat loss is dependent on the thermal insulation material, the surface area of the tank, and the difference between the internal and ambient temperatures. Hence, the standby heat loss can be written as:

$$Q_{loss}(t) = A \frac{T(t) - T_{am}(t)}{R} \Delta t \quad (2.3)$$

where Q_{loss} is the standby heat loss, A is the surface area of the DEWH, R is the thermal resistance of the insulation material, and T_{am} is the ambient temperature around DEWH.

The standby heat loss is independent of the DEWH state. Generally, the tanks have good insulation performances; therefore, the standby heat loss is limited [72]. In addition, the standby heat loss can be regarded as a constant, in the sense that the variations of standby heat loss caused by the changes of the internal and ambient temperature are negligible.

The draw out thermal energy is dependent on the volume and temperature of the draw out hot-water, and it can be expressed as:

$$Q_{use}(t) = c\rho V_{use}(t)T_{out}(t) \quad (2.4)$$

where Q_{use} is the draw out thermal energy with hot-water consumption, V_{use} is the volume of draw out hot-water, and T_{out} is the temperature of draw out hot-water.

The cold-water flows into the tank at the same time as the end-user uses hot-water, and the cold-water volume is the same as the consumed hot-water. Hence, the thermal energy by the inlet cold-water is:

$$Q_{in}(t) = c\rho V_{use}(t)T_{in}(t) \quad (2.5)$$

where Q_{in} is the thermal energy with the inlet cold-water, and T_{in} is the temperature of inlet cold-water.

According to Equations (2.1) - (2.5), the temperature change in a time interval is dependent on the electrical energy from power systems, the hot-water consumption, and the standby heat loss, which can be expressed as Equation (2.6) [70].

$$\Delta T(t) = \frac{P(t)}{c\rho V} \Delta t + \frac{A}{c\rho V R} (T_{am}(t) - T(t)) \Delta t + \frac{V_{use}(t)}{V} (T_{in}(t) - T_{out}(t)) \quad (2.6)$$

Without any control action, the DEWH is directly controlled by its hysteresis controller based on a temperature setpoint and a dead band. The hysteresis process is shown in Figure 2.1.

The state of the local thermostat is controlled by the hysteresis controller. If the temperature reaches or becomes lower than the lower limit, the thermostat turns on to heat the DEWH

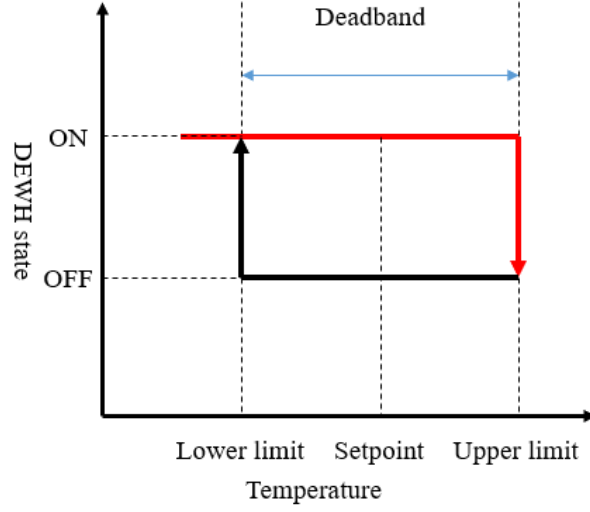


Figure 2.1 Hysteresis control process of DEWH

till the temperature reaches the upper limit. The thermostat state can be expressed as:

$$Thm(t) = \begin{cases} 1, & T(t) \leq TL \\ 0, & T(t) \geq TH \\ Thm(t-1), & otherwise \end{cases} \quad (2.7)$$

where Thm is the thermostat state, TL is the lower limit, and TH is the upper limit.

The power demand of the DEWH is based on its thermostat state, and can be written as:

$$P(t) = P_{rate}Thm(t) \quad (2.8)$$

where P_{rate} is the rated power of the DEWH.

When there is no hot-water consumption, the DEWH temperature is increased or decreased with approximately constant rates. The demand of the DEWH is maintained at its rated power when the DEWH is on, as shown in Figure 2.2. Without hot-water consumption, the required heating duration for the DEWH temperature to increase from the lower limit to the upper limit is minimum; the duration for the DEWH to turn on again is maximum. We

denote the minimum on duration by $D_{on,min}$, and the maximum off duration by $D_{off,max}$.

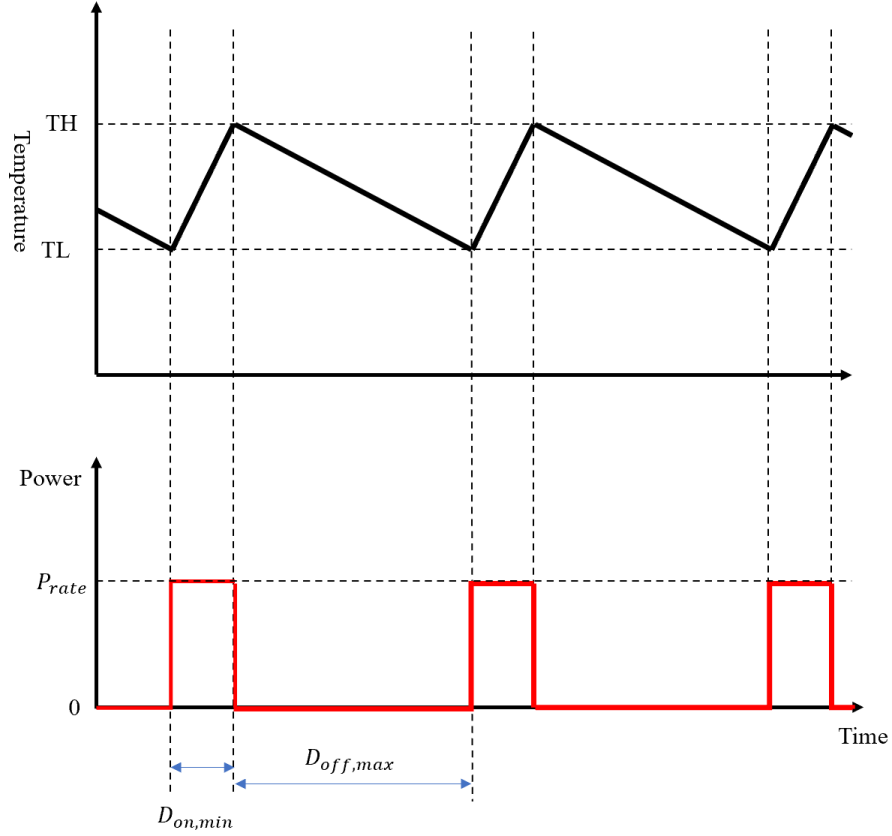


Figure 2.2 DEWH temperature and power demand without hot-water consumption

2.1.2 DEWH with Control

With the external relay controlling DEWH, the power demand will be modified by the relay, and Equation (2.8) can be re-written as:

$$P(t) = R_S(t)P_{rate}Thm(t) \quad (2.9)$$

where R_S is the state of the external relay, $R_S = 1$ when the relay is on or $R_S = 0$ when the relay is off.

A simple example is presented in Figure 2.3 which shows a basic idea of DLC on DEWHs. As the thermostat of a conventional DEWH is uncontrollable and the external relay cannot directly control the thermostat state, the prerequisite of controlling the conventional DEWH is to remain its thermostat on. When the internal temperature is increased to a certain value, the relay can be turned off to reduce the power demand till the temperature reaches the lower limit. The number of heating cycles in Figure 2.2 is fewer than that in

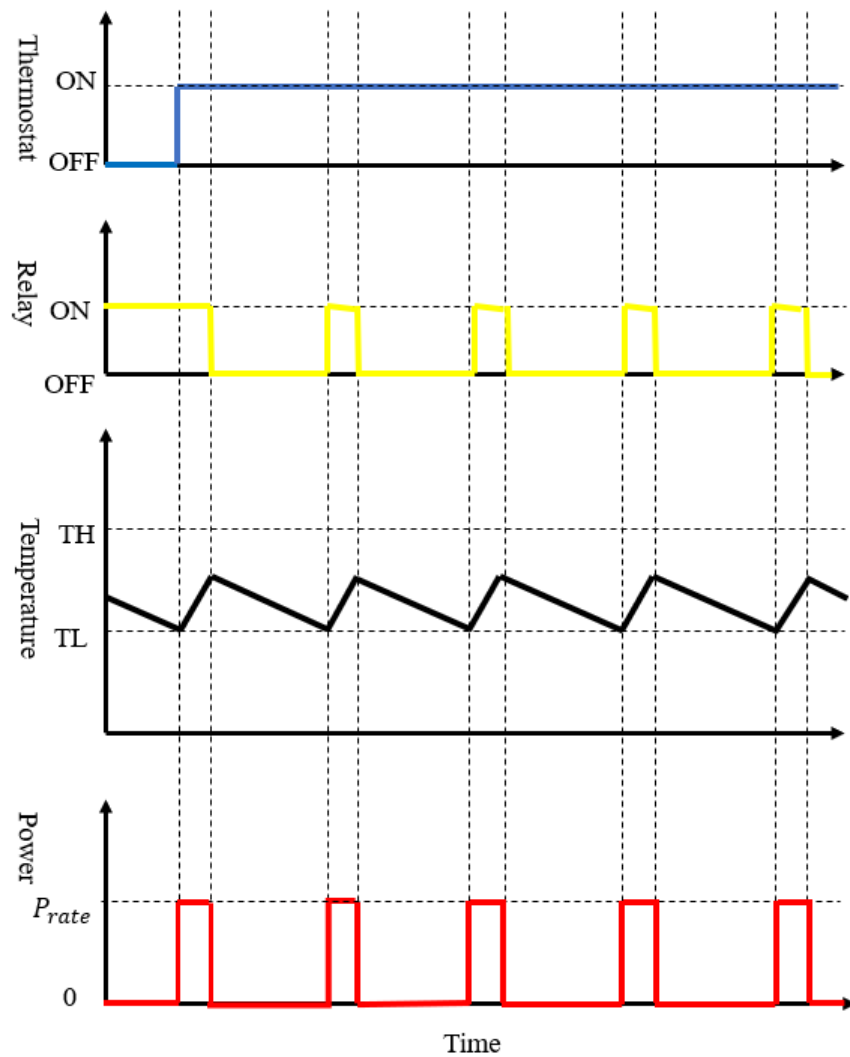


Figure 2.3 Example of relay control

Figure 2.3, while the heating durations are longer. As such, the electric power is shifted by DLC. The consumed electrical energy for both cases, in the long run, should be approximately equal because the DLC does not affect the end-user behaviors, the hot-water consumption and consumed thermal energy should not be changed.

Whenever the thermostat is on and the internal temperature satisfies the end-user comfort, the DEWH can be turned off by the external relay to reduce the power demand. The relay should be turned on when the internal temperature drops below the end-user comfort level, and these DEWHs with the low temperatures should not be turned off. The main objective of the proposed state estimation method is to estimate the DEWH temperature, whereby the DEWH's eligibility for on or off control actions is determined.

2.2 Hot-Water Consumption

2.2.1 Hot-Water Consumption Patterns

As seen in Equation (2.6), the temperature change of a DEWH is dependent on the hot-water consumption. However, it is hard to know the volume and occurrence time of hot-water activities, this is because of the randomness of human behaviors.

Fortunately, most people have behavioral habits and there exist patterns for hot-water consumption [63]–[66]. The patterns are dependent on seasons and weather. Seasonal influence on the hot-water consumption patterns is shown in Figure 2.4, which is from Residential End-Use Monitoring Program Report, New Zealand, and Australian

governments [73]. Seasonal hot-water consumption data for Canada does not appear to be available [66].

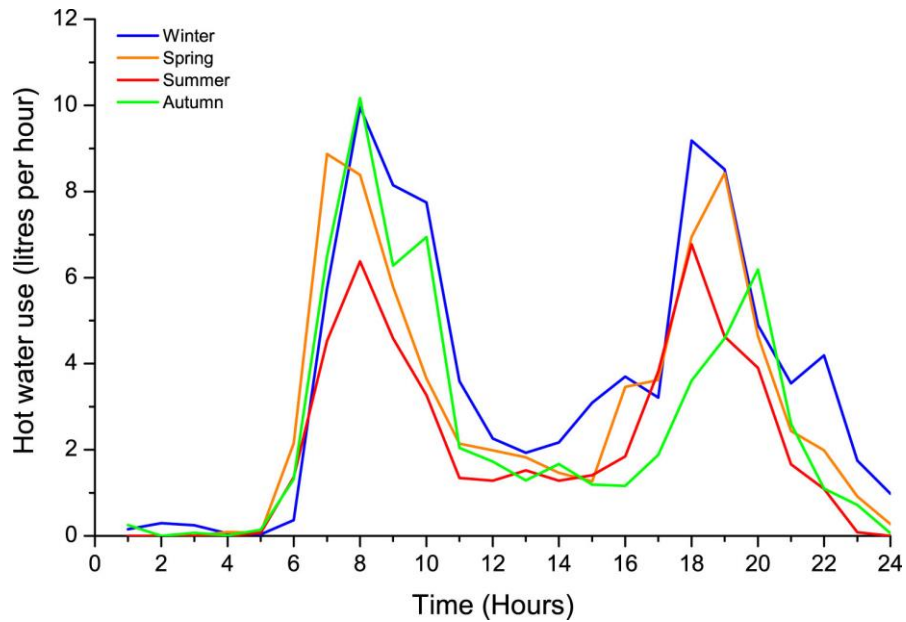


Figure 2.4 Seasonal influence on hot-water consumption patterns [62]

In addition to climate and season effects, the hot-water consumption patterns are also affected by other factors, such as the number of occupants (more occupants, more hot-water consumption), the ages of occupants (teenagers prefer longer average shower times, while young children have a high frequency of baths), and household incomes.

To obtain hot-water consumption patterns, temperature-based event inference methods and flow trace signature analysis methods are employed. Flow measurements are made when hot-water left the tank, and temperature measurements are made at the main pipes [63], [64], [66]. The temperature-based event inference method involves temperature

measurements as close as possible to specific end uses, with flow measurements at the water outlet [74]. However, many sensors are installed for temperature-based event inference methods and flow trace methods, which is impractical.

The hot-water consumption can be estimated by the on/off durations of DEWHs [75]–[77]. Without hot-water consumption, V_{use} in Equation (2.6) is zero. The total heating duration is $D_{on,min}$, and the temperature is increased from the lower limit to the upper limit. Then we have:

$$TH - TL = \frac{P_{rate}}{c\rho V} D_{on,min} + \frac{A}{c\rho VR} (T_{am} - T) D_{on,min} \quad (2.10)$$

When the actual heating duration is D_{on} , the volume of hot-water consumption during D_{on} is V_{use} , the temperature is increased from the lower limit to the upper limit, then:

$$TH - TL = \frac{P_{rate}}{c\rho V} D_{on} + \frac{A}{c\rho VR} (T_{am} - T) D_{on} + c\rho(T_{out} - T_{in}) \frac{V_{use}}{V} \quad (2.11)$$

Combine Equation (2.10) and (2.11). Then, the volume of hot-water consumption during D_{on} is:

$$V_{use} = \frac{(P_{rate} + A/R(T_{am} - T))}{c\rho(T_{out} - T_{in})} (D_{on} - D_{on,min}) \quad (2.12)$$

When the actual off duration is D_{off} , the volume of hot-water consumption during this off duration is:

$$V_{use} = \frac{A/R(T_{am} - T)}{c\rho(T_{out} - T_{in})} (D_{off} - D_{off,max}) \quad (2.13)$$

With this method [75]–[77], hourly hot-water consumption patterns can be built from the historical data in practice.

2.2.2 Hot-Water Consumption Activities

The domestic hot-water consumption is defined through a set of water fixtures including basins (clothes washing included), kitchen sinks, baths, and showers in [69]. In [64], the domestic hot-water consumption is classified into showers, taps, clothes washers, baths, and dishwashers. *DeOreo et al* classify hot-water consumption activities into showers, clothes washers, dishwashers, taps, and baths [63].

The thesis classifies the hot-water consumption activities into showers, baths, clothes washers, dishwashers, and taps. Washing machines are normally used once a week [66]. Dishwashers consume about 3.5 gallons water per cycle [78], and a regular cycle can last for two hours or more [79]. The impact on a DEWH is small during the cycle. Therefore, washing machines and dishwashers are not considered for daily hot-water consumption in the thesis. Daily dish and clothes washing tasks by hand are classified into taps. In the thesis, domestic hot-water consumption is by three fixtures: tap, shower, and bath.

In [68][69], the Centre for Renewable Energy Systems Technology (CREST) had built the relationship between hot-water consumption activities and their consumed volumes, as

shown in Figure 2.5. The average hot-water volume consumed by each activity can be calculated by expectation: 2.3 liters by a tap activity, 25.7 liters by a shower activity, and 73.3 liters by a bath activity.

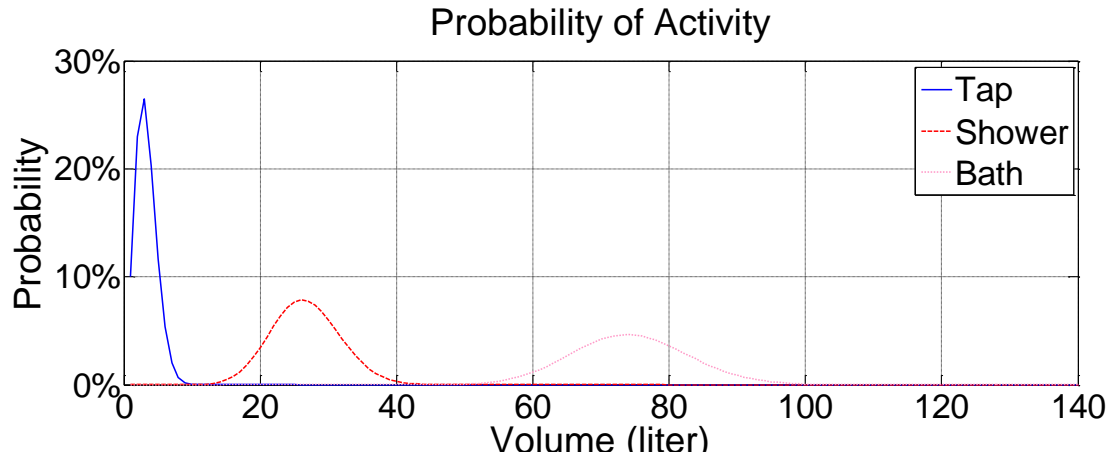


Figure 2.5 Probability of consumed hot-water volume by activities

The cumulative probability of each activity consuming at least a certain volume is shown in Figure 2.6. For example, the cumulative probability of a shower activity consuming no more than 20 liters is 10%. The probability of a bath consuming no more than 60 liters is

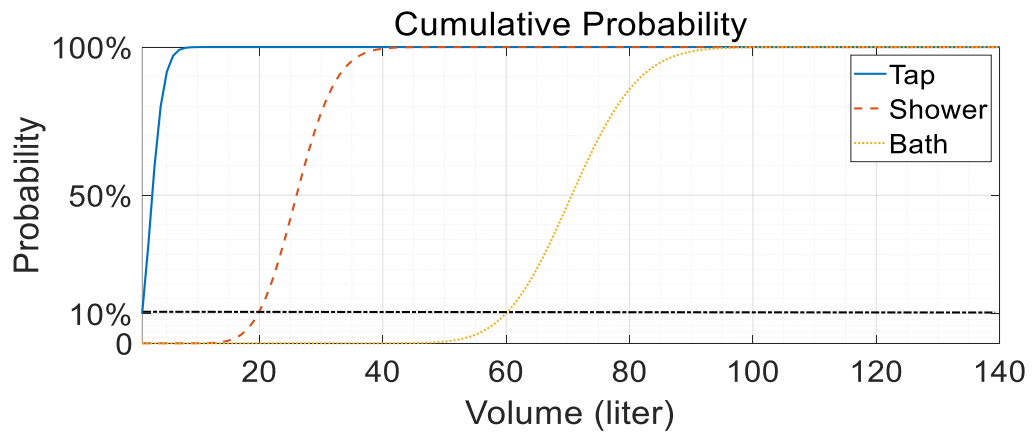


Figure 2.6 Cumulative probability of each activity

10% too. The probability of a shower activity with no more than 40 liters hot-water consumption is 99.7%. The probability of a bath activity with no more than 97 liters hot-water consumption is 99.7%.

According to the residential end use (REU) 1999 report [80] and REU 2016 [64], although showers, taps, and baths vary, the average consumed volume of each activity is almost the same. Based on the analyses results in [63], [69], the average flow rate for tap activities is 3.54 liter per min (*lpm*), and 9.26 *lpm* for showers and baths.

Hence, the three hot-water consumption activities have different durations and volumes, the effects on the DEWH temperature are different too. A higher hot-water draw out flow rate leads to a faster temperature drop. A larger volume of hot-water consumption leads to a larger temperature drop too.

2.3 Worst Cases Analysis

Worst cases are introduced to take into account the hot-water consumption activities that will cause the temperature to drop to the minimum value, which may affect the end-user comfort. The hot-water consumption under the worst cases is used to estimate the DEWH state, in an effort to avoid affecting the end-user comfort during control. The estimated information is provided for control, which includes the temperature of the DEWH, and the durations for the DEWH that remains on or the relay that remains off without affecting the end-user comfort. The end-user comfort can be guaranteed so long as it can be satisfied

under the worst cases.

Equation (2.6) shows that the temperature change of a DEWH is dependent on the hot-water consumption. Different volumes and occurrence times have different effects on temperature variations. Hence, the worst case analysis consists of volumes and occurrence times for hot-water consumption.

According to Equation (2.6), it is noteworthy that when the hot-water consumption is large enough (flow rate is high), the temperature keeps dropping even though the DEWH is heated. The standby heat loss is negligible when compared to the loss caused by the large hot-water consumption. Subsequently, the temperature drops during heating when the flow rate satisfies:

$$F \geq \frac{60P_{rate}}{c\rho(T_{out} - T_{in})} \quad (2.14)$$

where F is the draw out hot-water flow rate in lpm , and P_{rate} is the rated power of the DEWH. For example, when P_{rate} is 3 kW, and the difference between the outlet and inlet temperature is 40 °C, the temperature keeps dropping during heating when the flow rate is higher than 1.1 lpm . If P_{rate} is 9 kW, the temperature keeps dropping when the flow rate is higher than 3.3 lpm . Given the average flow rates of hot-water consumption activities in Section 2.2, the flow rates in practice will cause sustained temperature drops during heating. Hence, the internal temperature may get lower than the lower limit TL .

In Figure 2.7, a specific hot-water consumption activity, i.e., bath, consumes 90 liters and

the temperature reaches its lower limit during the activity. The temperature keeps dropping as the high flow rate has a more dominant cooling effect over heating the DEWH. The minimum temperature is lower than the lower limit. When a hot-water consumption activity occurs with a low flow rate and short duration, e.g. tap, the temperature will be increased by heating the DEWH. The activity has a limited impact on the internal temperature.

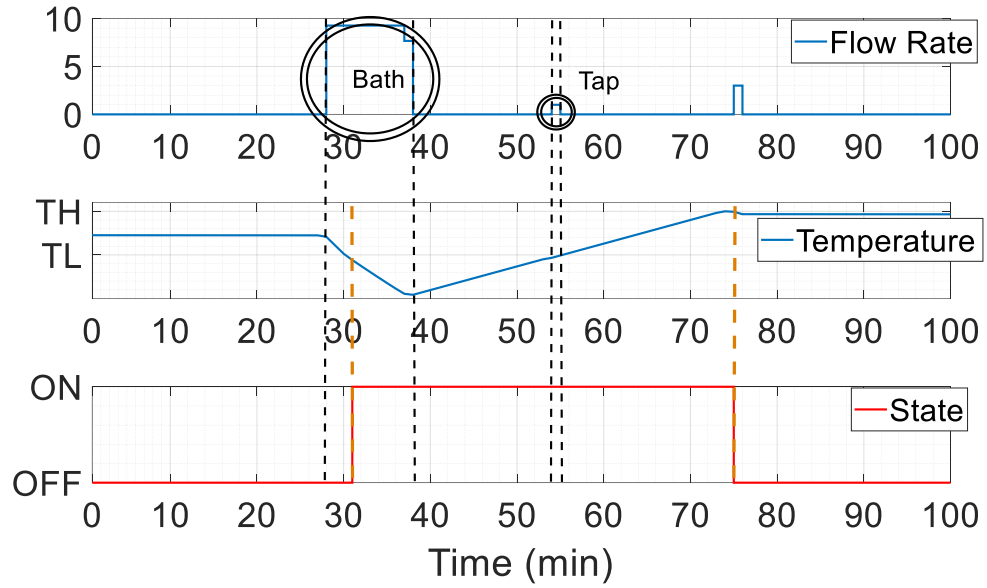


Figure 2.7 Example of hot-water consumption activities

2.3.1 Scenario I

Suppose that the flow rate remains constant for the whole duration of an activity. The total temperature change is:

$$T_{change} = \left(\frac{P}{c\rho V} + \frac{A}{c\rho VR} (T_{am} - T) + \frac{F}{V} (T_{in} - T_{out}) \right) D_{activity} \quad (2.15)$$

where T_{change} is the total temperature change during the activity, and $D_{activity}$ is the

duration of the activity.

When the flow rate F satisfies Equation (2.14), the temperature keeps dropping even the DEWH is heated. The minimum temperature decreases with the increase of $D_{activity}$. The total consumption volume of the activity increases with the increase of $D_{activity}$.

The temperature after the hot-water consumption activity can be expressed as:

$$T = T_{start} + T_{change} \quad (2.16)$$

where T_{start} is the temperature of the DEWH when the activity starts.

Figure 2.8 shows the minimum temperature with different durations and T_o (T_o is the difference between T_{start} and the lower limit, $T_o = T_{start} - TL$). The flow rate is 5 *lpm*. $D_{activity}$ varies from 0 to 10 minutes, and T_o varies from 0 to 5°C. The minimum

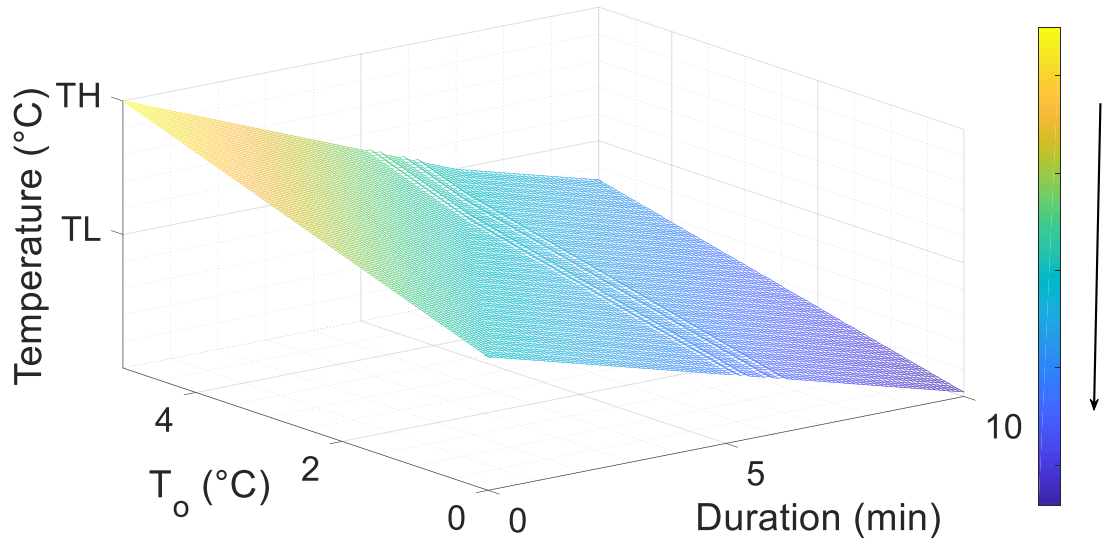


Figure 2.8 Minimum temperature with the flow rate at 5 *lpm*

temperature decreases with the decreasing T_{start} and the increasing $D_{activity}$. The worst case occurs when $D_{activity}$ is 10 minutes and T_{start} is at the lower limit.

2.3.2 Scenario II

When the activity duration $D_{activity}$ remains constant, different flow rates lead to different volumes of hot-water consumption. Figure 2.9 shows the minimum temperature with different flow rates and T_o . $D_{activity}$ is 5 minutes for all the cases in this figure. The flow rate F varies from 0 to 10 *lpm*, and T_o varies from 0 to 5°C. The minimum temperature decreases with the decrease in T_{start} and the increase in the flow rate. The worst case occurs when the F is 10 *lpm* and T_{start} at the lower limit.

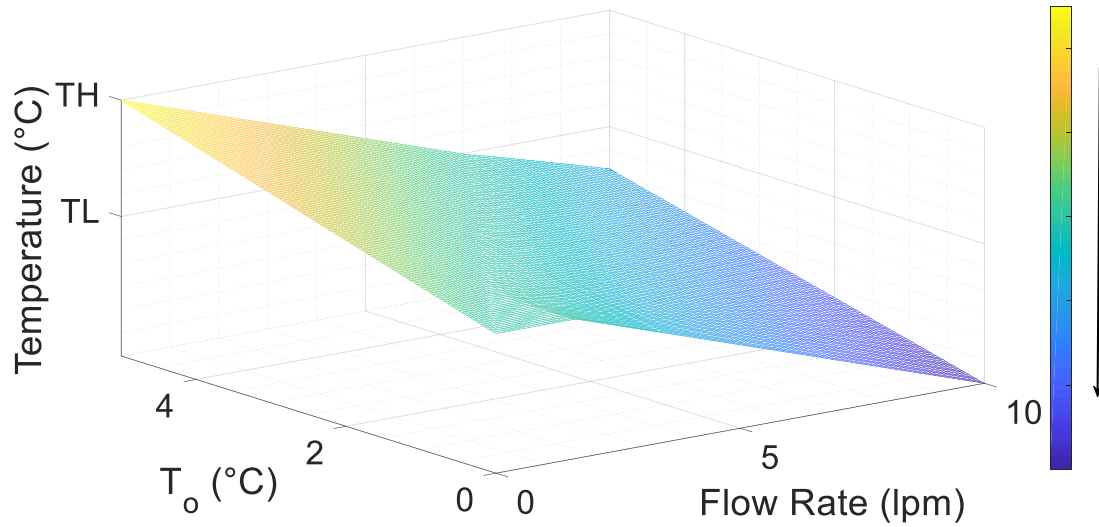


Figure 2.9 Minimum temperature with the duration at 5 minutes

2.3.2 Scenario III

When the temperature T_{start} is a constant, different flow rates and durations lead to different volumes of hot-water consumption and temperature drops. Figure 2.10 shows the minimum temperature with different flow rates and durations. T_{start} is at the lower limit. The flow rate varies from 0 to 10 *lpm*, and $D_{activity}$ varies from 0 to 10 minutes. The minimum temperature decreases with the increase in the flow rate and duration. The worst case occurs when the F is 10 *lpm* and $D_{activity}$ is 10 minutes.

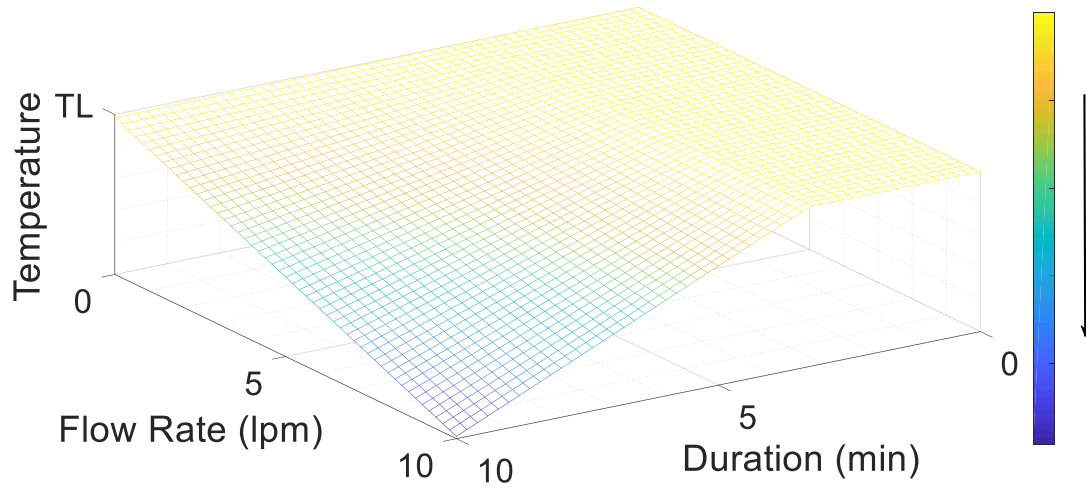


Figure 2.10 Minimum temperature with the start temperature at the lower limit

2.3.3 Worst Case Assumptions

All the above worst cases show that the minimum temperature decreases with the increase in the flow rate and duration of an activity, and the decrease in the temperature at the beginning of the activity. Due to the lack of temperature measurements, the temperature at the beginning of the activity T_{start} is unknown. Due to the randomness of human behaviors, the flow rate and duration are also unknown. Hence, the worst case assumptions are

introduced to deal with the unknown information as in the following.

2.3.3.1 Assumption 1: Start Temperature

Only DEWHs with thermostats that are on can be controlled in this research, and their states should be estimated. The DEWHs with thermostats that are off are uncontrollable, and their states will not be estimated until their thermostats turn on.

The state estimation for a DEWH starts when its thermostat turns on and ends when its thermostat turns off. When the thermostat turns on, its temperature has reached the lower limit, hence, the T_{start} is assumed to be its lower limit.

2.3.3.2 Assumption 2: Volume of a Hot-Water Consumption Activity

The volume of a hot-water consumption activity affects the internal temperature, which is dependent on its flow rate and duration. However, both are unknown and vary even for the same kind of activities due to the randomness of human behaviors [63]. Hence, the volume consumed by the same kind of activity varies. In addition, the flow rate itself varies during an activity. Assumption 2 is therefore introduced to estimate the volume of a hot-water consumption activity.

Shower and bath activities consume a large volume of hot-water, and the effect on temperature is significant. Hence, the consumed volume should be decided in order to maintain the end-user comfort and provide available capacity for control. The volumes of

hot-water consumption activities are considered based on the statistical data in [68][69]. As mentioned in Section 2.2.2, a shower activity consumes no more than 40 liters, with a probability of 99.7%. So does a bath activity with no more than 97 liters. The worst case consumption for the shower activity is assumed to be 40 liters. The worst case for a bath activity consumes 97 liters.

The tap activity has minor effects on the DEWH temperature, and is assumed to occur with its average flow rate.

2.3.3.3 Assumption 3: Duration of a Hot-Water Consumption Activity

Given a specified volume of hot-water consumption, the water temperature decreases with a shorter duration of the consumption activity. The change on the temperature can be obtained in the rewritten form of Equation (2.15) as:

$$T_{change} = \left(\frac{P}{c\rho V} + \frac{A}{c\rho VR} (T_{am} - T) \right) D_{activity} + \frac{V_{use}}{V} (T_{in} - T_{out}) \quad (2.17)$$

The minimum value of Equation (2.17) occurs when $\lim (D_{activity}) \rightarrow 0$, meaning the minimum DEWH temperature, i.e., the worst case.

Combining all the three assumptions, the worst case happens when a complete hot-water consumption activity occurs and almost instantaneously ends at the instant when the DEWH reaches its lower limit.

2.3.4 Fuzzy Logic Based Activity Identification

The consumed volume of a bath activity is much more than that of a shower activity. Hence, the DEWH temperature drops even lower when there is a bath activity. Given an hourly hot-water consumption pattern, the intra-hour activities (bath and shower) should be identified. The consumption pattern in Section 2.2.1 is used for the identification.

A fuzzy logic method with a Cauchy distribution membership function [70] (which has a high degree of freedom to adjust the steepness at the crossover points) is used to fuzzily categorize the consumption patterns with associated activities. Based on the statistical data [68][69], the membership function is built and presented in Figure 2.11. As shown in Figure 2.6, a shower activity consumes at least 20 liters. So does a bath with at least 60 liters consumption. Accordingly, the degree of a tap activity is the highest when the hourly hot-water consumption is lower than 20 liters. The degree of a bath activity is the highest when

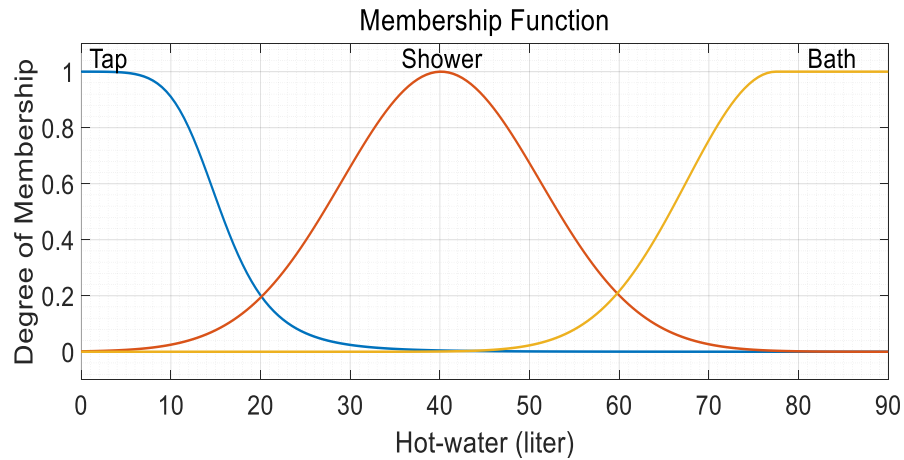


Figure 2.11 Membership function

the hourly hot-water consumption is more than 60 liters.

From the hourly hot-water consumption patterns, the degree of the membership function for each activity can be calculated. The maximum degree can lead to the intra-hour activity identification.

If the hourly hot-water consumption is less than 20 liters, there is no shower or bath activity, and the hot-water is assumed to be drawn out at the average flow rate during this hour. If the hourly consumption is more than 20 liters, the activity can be a shower or a bath, and the consumed volume can be 40 liters for the shower and 97 liters for the bath. If the hourly hot-water consumption demand is smaller than that of the assumed activity, all the hot-water consumption is regarded as all consumed by the activity. If the hourly hot-water consumption is larger than that of the assumed activity, the residual hot-water above of the assumed volume (i.e., 40 liters for shower and 97 liters for bath) is treated as drawn out with an average flow rate during this hour.

2.4 State Estimation for Individual DEWHs

With the assumptions of the hot-water consumption presented above, this section proposes a state estimation method with the structure as shown in Figure 2.12. The detailed process is as follows:

Step 1. Obtain the thermostat state by the DEWH state and the relay state. The DEWH state

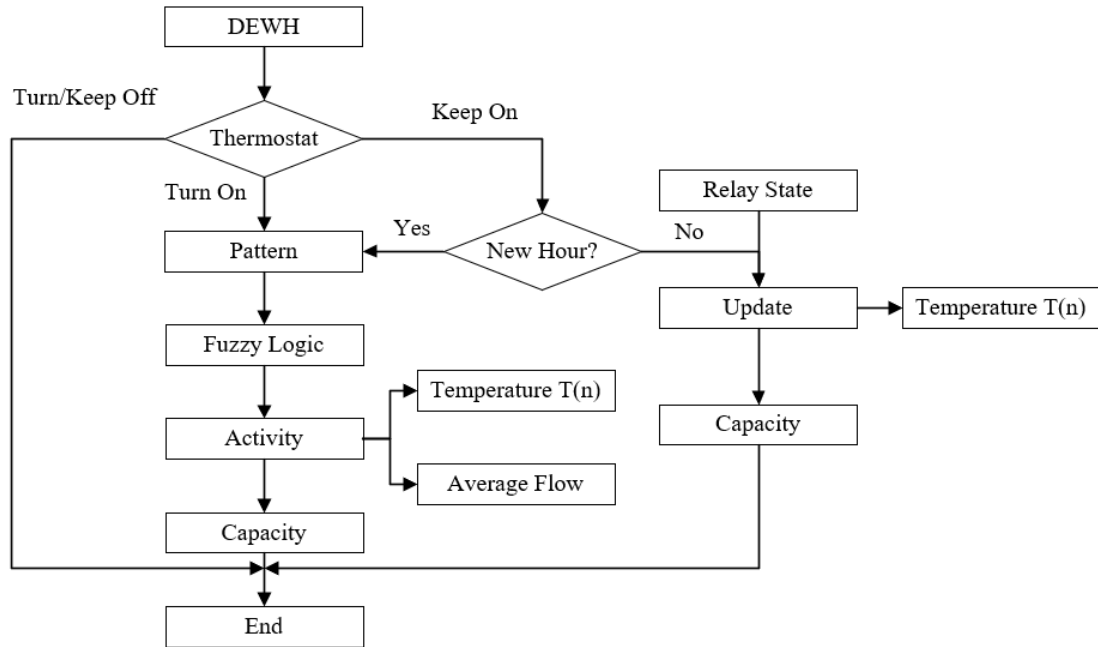


Figure 2.12 Flow chart of the proposed state estimation method

can be identified through the readings of smart meters [67], [76]: 1) if the ramp-up and ramp-down power demands are approximately equal to the rated power of a DEWH, the state of the DEWH turns on/off; 2) if not, the DEWH retains its previous state. The thermostat state is the same as the DEWH state when the relay is on. The relay can only be turned off when its thermostat is on, so the thermostat remains on when the relay is off. The relay state is decided by control actions, which is already known.

If the thermostat remains or turns off, the conventional DEWH is uncontrollable and it does not need state estimation, so go to end; if the thermostat turns on, go to Step 2; if the thermostat remains on, go to Step 3.

Step 2. When the DEWH reaches the lower limit, its thermostat turns on and the DEWH starts heating.

- (a) Identify the hot-water consumption activity and residual hot-water usage with the fuzzy logic membership function. The temperature can be estimated by the worst case assumptions, and can be written as:

$$T(n) = TL + \frac{V_{activity}}{V} (T_{in} - T_{out}) \quad (2.18)$$

where $V_{activity}$ is the consumed volume of the identified activity, n is the n^{th} estimation, TL is the lower limit, V is the tank volume, T_{in} is the temperature of inlet water, and T_{out} is the temperature of the water outlet.

The residual volume of hot-water consumption is drawn out with an average flow rate during the hour, and the average flow rate is:

$$F = \frac{V_{pattern} - V_{activity}}{60} \quad (2.19)$$

where $V_{pattern}$ is the hourly hot-water consumption from the pattern.

- (b) With Equation (2.15), the temperature change rate can be calculated, and the available durations for the DEWH to keep on or off can be:

$$\begin{cases} D_{ava,on}(n) = \frac{TH - T(n)}{\frac{P_{rate}}{c\rho V} + \frac{A}{c\rho VR}(T_{am} - T(n)) + \frac{F}{V}(T_{in} - T_{out})} \\ D_{ava,off}(n) = \frac{T_{tole} - T(n)}{\frac{A}{c\rho VR}(T_{am} - T(n)) + \frac{F}{V}(T_{in} - T_{out})} \end{cases} \quad (2.20)$$

where $D_{ava,on}$ is the available duration for DEWH to keep on, $D_{ava,off}$ is the available duration for DEWH to keep off, TH is the upper limit, P_{rate} is the rated power, A is the surface area of the DEWH, R is the thermal resistance of the insulation material, T_{am} is the ambient temperature around DEWH, and T_{tole} is the minimum temperature to maintain the end-user comfort, when the temperature reaches this value, the DEWH should be turned back on. T_{tole} can be set based on the requirement in practice. In this thesis, T_{tole} is set five degrees below the lower limit, which still satisfies the end-user comfort [70]. The tolerance temperature is no less than the required temperature for hot-water in practice [71]. The available capacity of energy is the rated power multiplied by the available on or off durations.

$$\begin{cases} E_{on}(n) = P_{rate}D_{ava,on}(n) \\ E_{off}(n) = P_{rate}D_{ava,off}(n) \end{cases} \quad (2.21)$$

- (c) The estimated temperature, flow rate, and available on or off durations are sent as outputs of the state estimation method, which marks the end of the state estimation process.

Step 3. The thermostat remains on, the estimated temperature and available on or off durations should be updated.

- (a) Adjust the time. If a new hour begins, the hourly hot-water consumption is changed, and so will be the available activity. Then, the temperature is:

$$T(n) = T(n-1) + \frac{V_{activity}}{V} (T_{in} - T_{out}) \quad (2.22)$$

The new average flow rate is updated with Equation (2.19), then go to Step 2(b). If the time does not enter to a new hour, continue to (b).

- (b) The temperature should be updated with the DEWH state, relay state, and average flow rate of hot-water consumption:

$$T(n) = T(n-1) + \left(\frac{P(n)}{c\rho V} + \frac{A}{c\rho VR} (T_{am} - T(n-1)) + \frac{F}{V} (T_{in} - T_{out}) \right) \Delta t \quad (2.23)$$

where Δt is the time interval between each estimation for the DEWH.

The power demand P is controlled by the relay and the thermostat (which is on), hence, the power demand can be:

$$P(n) = R_S(n)P_{rate} \quad (2.24)$$

where R_S is the relay state, and P is the power demand of the DEWH.

The available on or off durations can be updated with Equation (2.20).

- (c) The estimated temperature, flow rate, and available on or off durations are sent as

outputs of the individual state estimation method, and the state estimation process is ended.

This is the proposed state estimation method for individual DEWHs. DEWH state can be estimated without temperature measurements.

2.5 Case Study Results

In this section, experiments were conducted on an actual DEWH. With the worst case assumptions, the estimated temperature should be lower than the actual temperature to guarantee the end-user comfort. At first, the proposed individual state estimation method was verified when the DEWH was not controlled. Then, a simple control example was implemented to show the ability of load shifting without impact to the end-user comfort during control.

2.5.1 Test DEWH Structure

The investigated DEWH in this research has three heating elements. The rated power of each element is 4500 W, the rated voltage is 240 V, and the tank volume is 279 liters. The DEWH is shown in Figure 2.13. The hot-water is drawn out from the top of the tank, and the cold-water inlet is at the bottom of the tank. Ten temperature sensors are clinging to the surface of the tank from top to bottom with an even distance. The temperature information was employed to verify the proposed method.

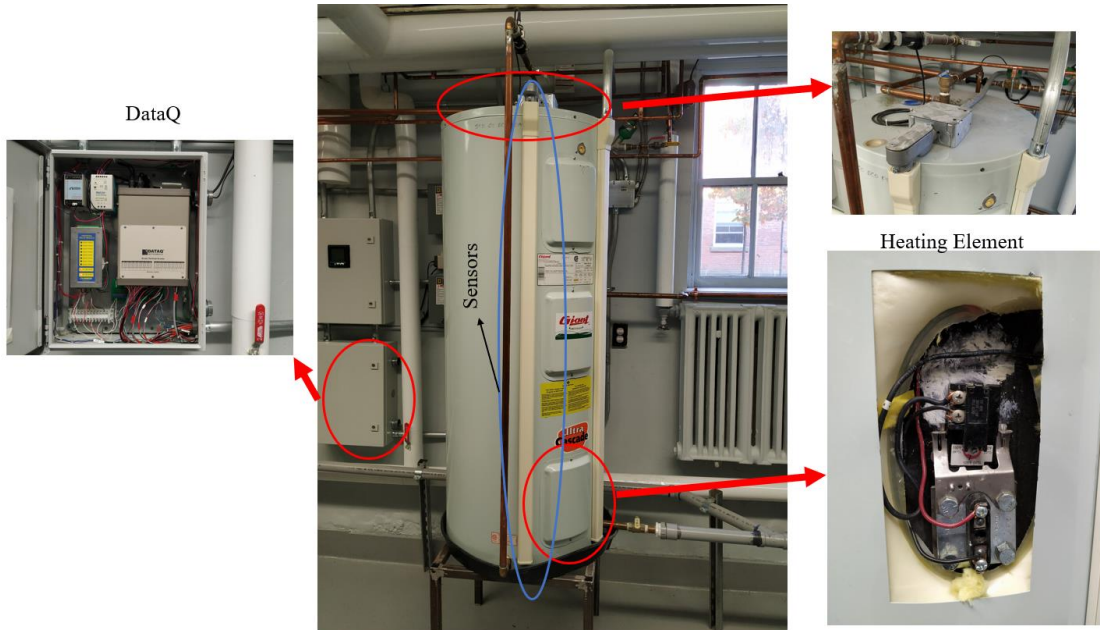


Figure 2.13 Investigated DEWH

The data acquisition (DataQ) instrument is used to control the relay, draw out water flow rate, and measure the inlet/outlet water temperature. All measured information is stored in a database, and control actions are implemented through the database to the DataQ. No more than one heating element can be turned on simultaneously. The diagram of the three-element water heater is shown in Figure 2.14. The priority of the three heating elements is

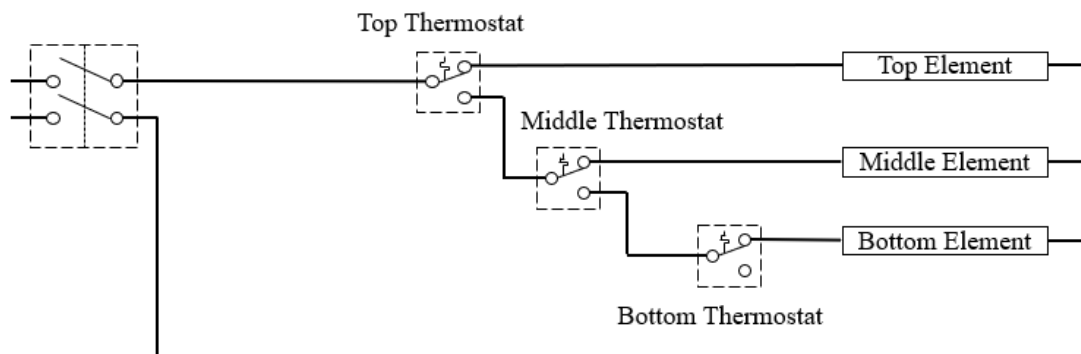


Figure 2.14 Diagram of the three-element water heater

Top element > Middle element > Bottom element. As the three heating elements have the identical rated power, the DEWH is regarded as having a one-element structure. The DEWH is on when either of the three elements is on, and the DEWH is off when all the three heating elements are off.

2.5.2 Performance on End-User Comfort

CREST Demand Model V 2.2 [81] is a high-resolution stochastic model includes a representation of electrical demand and generation (e.g. PV), resident occupancy, hot-water consumption, gas boilers, and so forth. The model is used to generate a 24-hour hot-water consumption for the investigated DEWH. The hot-water usage is shown in Figure 2.15. The hot-water consumption is about 300 liters for 24 hours. The modeled hourly pattern is the pattern shows the hot-water consumption in each hour, which can be obtained from the generated human behavior from the CREST model. Due to the randomness of human behaviors, the actual hot-water consumption should be similar to the hourly pattern,

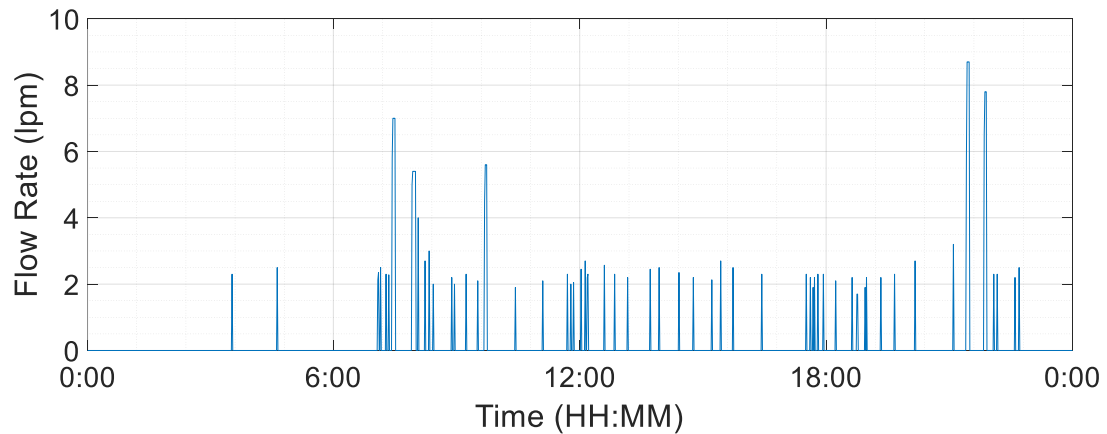


Figure 2.15 24 hour hot-water consumption on the DEWH

but also have some differences as shown in Figure 2.16.

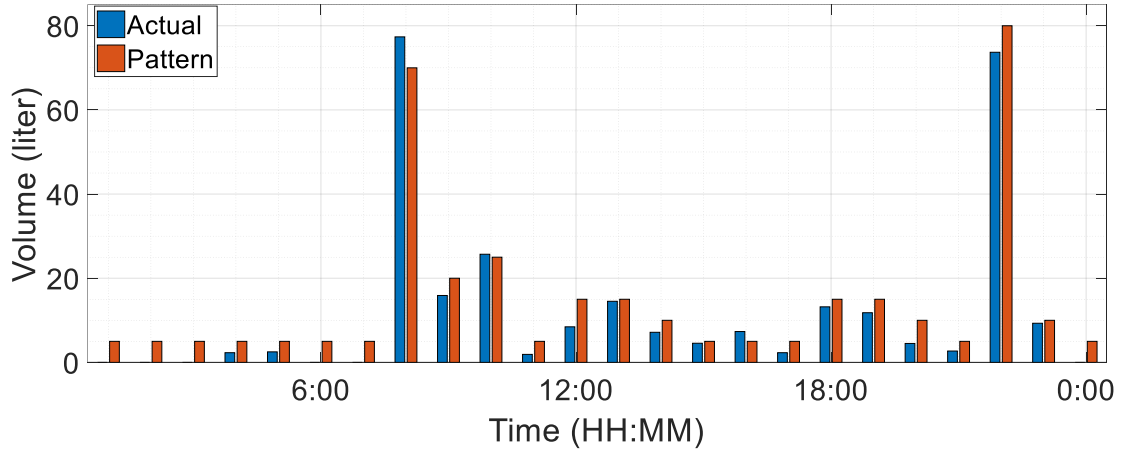


Figure 2.16 Hourly hot-water consumption and pattern

The current and temperature of the DEWH are measured and shown in Figure 2.17, which includes three heating durations, i.e., morning, noon, and evening. The hot-water consumption during the morning and evening heating duration is very large, and the temperature has dropped lower than the lower limit. The first heating duration is from 7:31 to 9:11, the second heating duration is from 12:47 to 13:24, and the third heating duration is from 21:27 to 22:54.

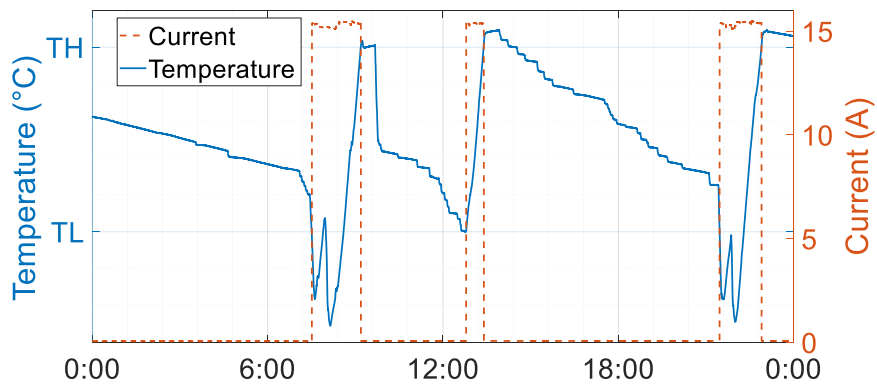


Figure 2.17 Temperature and current of the DEWH

The measured and estimated temperature during the first heating duration is shown in Figure 2.18. The DEWH turns on at 7:31. From the pattern, the hot-water consumption in this hour is 70 liters. With the fuzzy logic function and worst case assumptions, a bath activity with 70 liters is assumed to occur and finish at 7:31. The temperature drops to about 8.78 °C lower than the lower limit. The residual hot-water consumption during this hour is assumed to be zero, and the temperature keeps increasing after 7:31. At 8:00, a new hour begins. The hot-water consumption in this hour is 20 liters. And the hot-water consumption is assumed to draw out with a 0.33 *lpm* flow rate during this hour. It is clear that the increase in the estimated temperature is slower than that in the previous hour. Although the estimated temperature is lower than the measured temperature, it helps to provide a reference for control in an effort to maintain the end-user comfort.

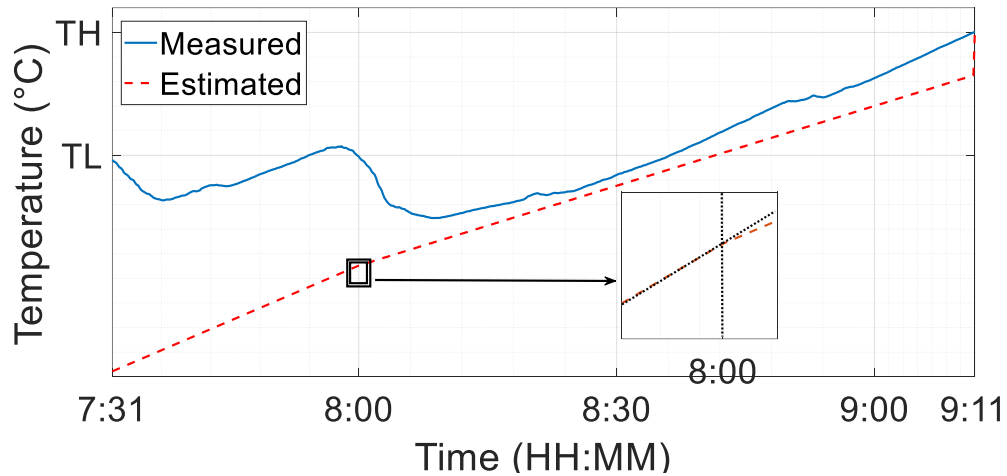


Figure 2.18 Measured and estimated temperature in the first duration

The measured and estimated temperature during the second heating duration is shown in Figure 2.19. The hourly hot-water consumption is less than 20 liters for each hour in this

duration. Hence, the hot-water is assumed to be drawn out with an average flow rate. In the duration, there are some segments that the estimated temperature is higher than the measured temperature. This is because the actual tap activities during these segments consumed more volume than the estimated ones. However, the temperature is always higher than the lower limit during this duration as the hot-water consumption in each hour is small, and the small discrepancies (the estimated temperature being higher than the actual ones) do not affect the end-user comfort during control.

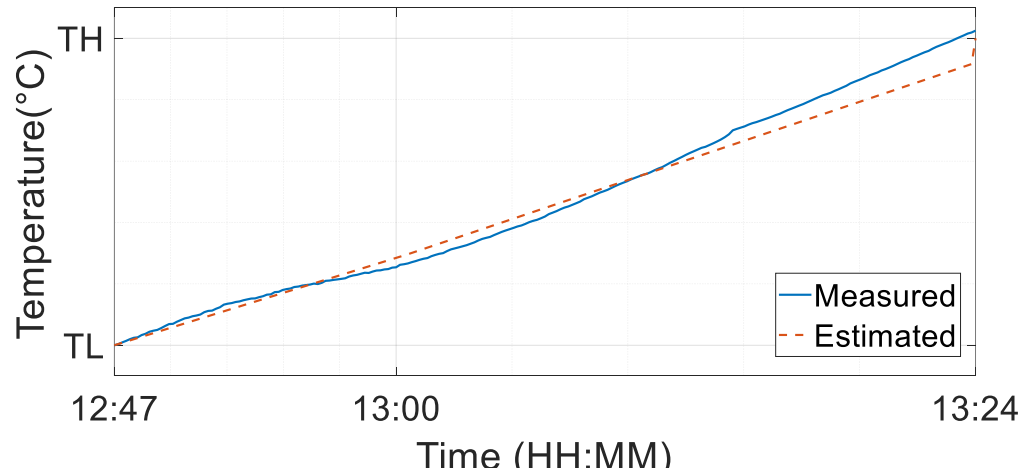


Figure 2.19 Measured and estimated temperature in the second duration

Figure 2.20 shows the measured and estimated temperature during the third heating duration. The hourly pattern indicates an expected hot-water consumption of 80 liters in this hour. A bath activity is assumed to happen at 21:28 with an estimation of hot-water consumption of 80 liters. With the assumed activity, the estimated temperature drops to 10.04 °C lower than the lower limit. The average flow rate is 0 *lpm*. At 22:00, a new hour begins. The average flow rate is 0.167 *lpm*. The increase in the estimated temperature is slower than the previous hour. During the heating duration, the estimated temperature is

lower than the measured temperature. The estimated temperature is used to provide a reference and to maintain the end-user comfort.

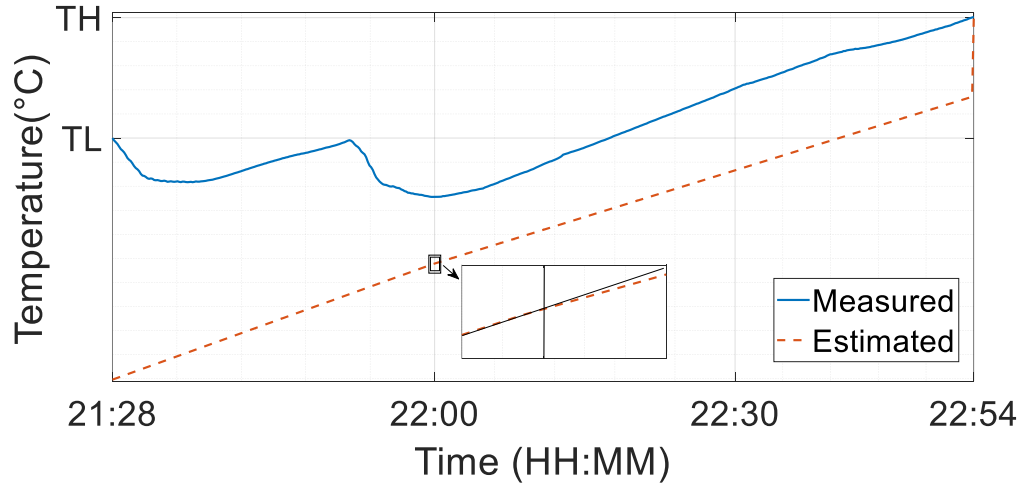


Figure 2.20 Measured and estimated temperature in the third duration

When there is an intense water use such as shower or bath, the temperature may drop to a value lower than the lower limit. The proposed individual state estimation method uses the worst case assumptions to estimate the temperature. The estimated temperatures are lower than the measured values for almost all the durations, which guarantees the end-user comfort without temperature measurements.

2.5.3 Control DEWH with State Estimation Method

A simple control example is tested on the DEWH with the proposed state estimation method for individual DEWHs. There are 80 liters of hot-water consumption between 21:00 and 22:00 in the pattern, and the heating duration is about 87 mins (from 21:27 to 22:54). The objective is to reduce the length of this heating duration.

As DLC does not intend to change human behaviors and the required hot-water consumption should remain unchanged, the required thermal energy should be maintained to avoid affecting the end-user comfort. Hence, more thermal energy stored in the DEWH will help to shorten the heating duration. The higher the temperature at 21:00, the shorter the heating duration. Therefore, the DEWH should be fully heated before 21:00.

Due to the uncontrollability of the internal thermostat, the DEWH should be controlled to keep its thermostat on until the last heating action before 21:00. To maintain the end-user comfort, the DEWH should prepare enough thermal energy for the subsequent hot-water consumption, and keep the temperature higher than the lower limit. The DEWH is heated for several minutes at the beginning of each hour by relay controls. After that, the relay receives off-signals to turn off the DEWH. The temperature is controlled to have a higher value than the lower limit, as shown in Figure 2.21.

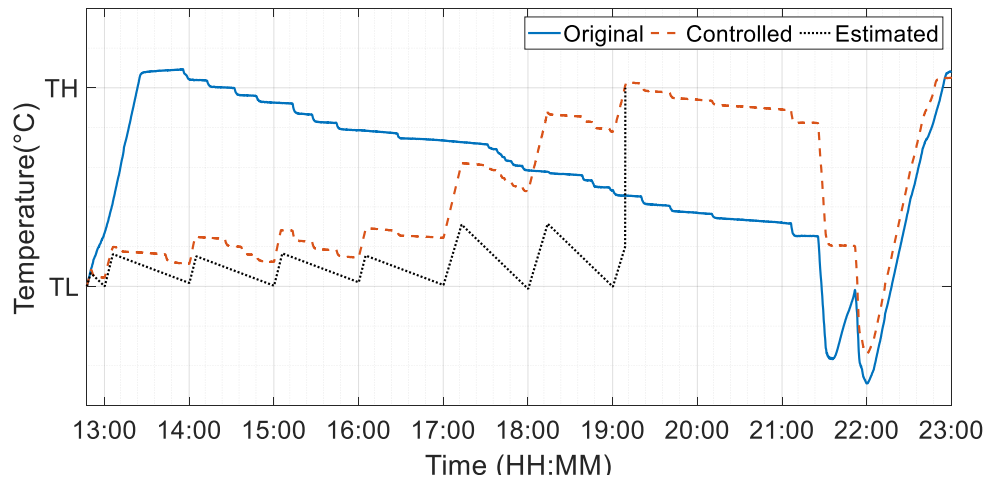


Figure 2.21 Temperature comparison

Figure 2.21 shows the measured temperatures under the original (uncontrolled) and controlled cases as well as the estimated temperature. The actual hot-water consumption is less than that in the pattern, which causes the errors between the measured and estimated temperatures. At 19:09 the DEWH reaches the upper limit, the thermostat of the DEWH turns off. Then, the estimated temperature is adjusted to the upper limit, and the DEWH state does not need to be estimated, because its thermostat is off and the DEWH is uncontrollable. At 21:00, the internal temperature of the controlled case is higher than the original case, which helps to reduce the following heating duration in this hour.

The DEWH states for the original and controlled cases are shown in Figure 2.22. There are two heating durations in the original case: the first duration is about 37 minutes; the second is about 87 minutes; and the total heating time is 124 minutes. There are nine heating durations in the controlled case, the length of each duration is shown in Table 2.1, and the total heating duration is 119 minutes. From Figure 2.21, the average temperature in the

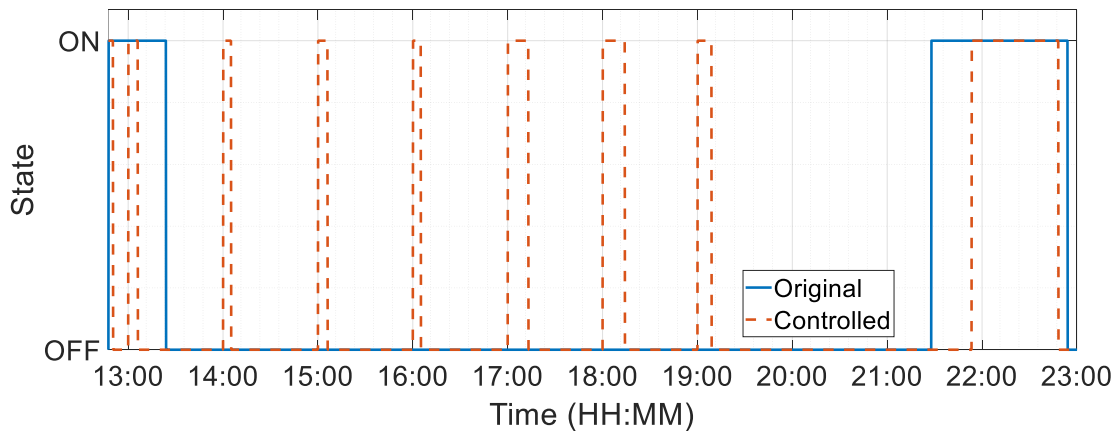


Figure 2.22 DEWH states of both cases

Table 2.1 Length of Heating Durations under Control

Dur.	1	2	3	4	5	6	7	8	9
Leg. (minute)	3	6	6	6	6	13	14	9	56

original case is 3.09 °C higher than the lower limit, and the average temperature in the controlled case is 2.68 °C higher than the lower limit. The standby heat loss increases with the increase of the difference between the DEWH temperature and the ambient temperature. Hence, the standby heat loss of the controlled case is lower than the original case, which causes the reduction of the total heating duration, but the reduction is small.

It is noted that the heating duration after 21:00 is reduced to 56 minutes, which is 31 minutes less than that in the original case. Therefore, the control objective is achieved, showing the load shifting ability of DEWH control. The estimated temperature is lower than the measured value during control and the minimum temperature of the controlled case is higher than that in the original case. This validates the proposed method in successful maintaining the end-user comfort in the experiments.

2.6 Conclusion

This chapter proposes an individual DEWH state estimation method that requires no temperature measurements. Based on the analysis on hot-water consumption patterns and the proposed fuzzy logic membership function, hot-water consumption activities are identified. Worst case assumptions are made to estimate the worst cases (minimum

temperature). The estimated temperature keeps lower than the actual temperature. This shows the effectiveness of the worst case assumptions which can be used to maintain the end-user comfort.

Furthermore, the experiments are conducted on an actual DEWH. The estimated temperatures secure the end-user comfort during control. A simple example with the proposed state estimation method is also reported in this chapter to reduce the length of heating duration, validating the load shifting ability of the conventional DEWHs.

3 Peak Shaving

3.1 Introduction

In power systems, peak shaving refers to leveling out peaks in electricity use by residential, industrial, and commercial power consumers, which benefits grid stability and cost savings. The peak periods of DEWH demand are consistent with the peak periods in power systems [32]. Hence, the reduction of DEWHs demand during peak durations will help to reduce the peak demand in power systems. The goal of this chapter is to develop an algorithm for peak shaving with DEWHs.

In this chapter, the conventional DEWHs are controlled without temperature measurements. The estimated information based on the proposed method in Chapter 2 can be the reference for control selections and maintaining the end-user comfort. The subsequent hot-water consumption is modeled with a temperature drop weight matrix.

The chapter is organized as follows. In Section 3.2, a temperature drop weight matrix is introduced to show the effect of the subsequent hot-water consumption. In Section 3.3, the customer satisfaction prediction index (CSPI) is introduced to show the control priority of the DEWHs. Section 3.4 details the proposed algorithm for peak shaving. Section 3.5 presents the peak shaving results verifying the effectiveness of the proposed algorithm. Section 3.6 concludes this chapter.

3.2 Temperature Drop Weight Matrix

The knowledge of human behaviors helps to minimize the impact on the hot-water availability while controlling DEWHs [48], [82], [83]. Preparing enough thermal energy for the subsequent hot-water consumption activities will reduce the risk of affecting the end-user comfort. In Section 2.3.3, the hot-water consumption activities are identified with the worst case assumptions. The residual hot-water above the consumed volume of the identified activity is assumed to be drawn out with a constant flow rate during the investigated hour.

From Equation (2.6), the temperature drop rate is caused by the standby heat loss and the subsequent hot-water consumption (draw out with the average flow rate), and can be written as:

$$w = \frac{A(T_{aa} - T_{am})}{c\rho V} + \frac{F}{V}(T_{out} - T_{in}) \quad (3.1)$$

where w is the temperature drop rate in $^{\circ}\text{C}/\text{min}$, A is the surface area of the DEWH, R is the thermal resistance of the insulation material, T_{am} is the ambient temperature around DEWH, c is the specific heat capacity of water, ρ is the density of water, V is the volume of the tank, T_{aa} is the estimated temperature of the DEWH after an identified activity occurs (as Equation (2.16)), F is the draw out hot-water flow rate in lpm , T_{out} is the temperature of draw out hot-water, and T_{in} is the temperature of inlet cold-water. As analyzed in Chapter 2, the average flow rate is small, and thus the temperature drop rate is small as well.

The weight matrix, denoted by \mathbf{W} , consists of all the temperature drop rates of the DEWHs.

$$\mathbf{W} = [w_1 \quad w_2 \quad \dots \quad w_n]' \quad (3.2)$$

where n is the total number of the DEWHs.

DEWHs can be classified into five groups according to their states and estimated temperatures. The available control commands for each group are presented in Table 3.1.

Table 3.1 Available Control Commands

Group	Thermostat	Relay	Estimated Temp.	Available Command
1	Off	-	-	On
2	On	On	$T \geq TL$	On/Off
3	On	On	$T < TL$	On
4	On	Off	$T \geq T_{tole}$	On/Off
5	On	Off	$T < T_{tole}$	On

where T_{tole} is the tolerance temperature.

The DEWHs are controllable when their thermostats are on, and are uncontrollable when their thermostats are off. According to that, we know:

1. For DEWHs in Group 1: they are uncontrollable regardless the relay states, and only on-signals are allowed till their thermostats turn on.
2. For DEWHs in Group 2: their estimated temperatures are no less than their lower limits, and their relays are on. On-signals or off-signals can be sent to these DEWHs to control their demand.

3. For DEWHs in Group 3: their estimated temperatures are less than their lower limits, and their relays are on. On-signals can be kept sending to these DEWHs to let heat them, which helps to avoid control DEWHs frequently.
4. For DEWHs in Group 4: their estimated temperatures are not less than their tolerance temperatures ($T \geq T_{tole}$), and their relays are off. On-signals or off-signals can be sent to these DEWHs to control their demand.
5. For DEWHs in Group 5: their estimated temperatures are less than their tolerance temperatures, and their relays are off. Only on-signals are allowed to maintain the end-user comfort.

3.3 Customer Satisfaction Prediction Index

The temperature of a DEWH when its thermostat turns on can be estimated by Equation (2.16), and the DEWH can be kept on until its internal temperature reaches its upper limit.

The whole heating duration can be estimated as:

$$D_{full} = \frac{(TH - T_{aa})c\rho V}{P_{rate} - wc\rho V} \quad (3.3)$$

where P_{rate} is the rated power of the DEWH, and D_{full} is the whole heating duration.

Given a constant T_{aa} (which depends on large hot-water consumption activities), D_{full} increases with the increase of w and the decrease of T_{aa} , which means more hot-water is

used. As w is small, D_{full} is positive.

As shown in Figure 3.1, the whole heating process can be represented by two parts. In the first part, the DEWH is heated from the minimum temperature to its lower limit; the heating duration in this part is denoted by D_{part1} . In the second part, the DEWH is heated from its lower limit to its upper limit; the heating duration in this part is denoted by D_{part2} .

$$D_{full} = D_{part1} + D_{part2} \quad (3.4)$$

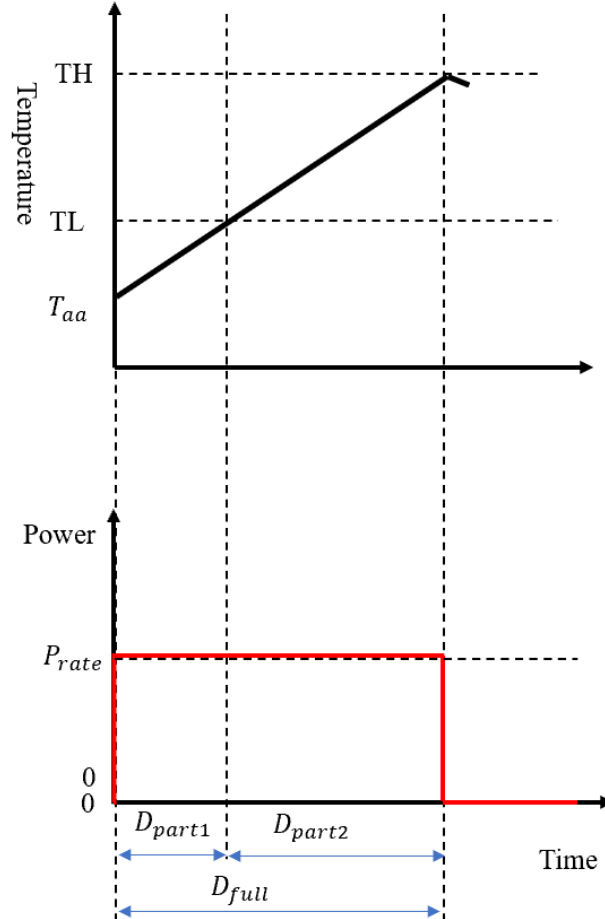


Figure 3.1 Temperature and power demand during a heating duration

According to Equation (3.2), the durations D_{part1} and D_{part2} can be calculated by:

$$\begin{cases} D_{part1} = \frac{(TL - T_{aa})c\rho V}{P_{rate} - wc\rho V} \\ D_{part2} = \frac{(TH - TL)c\rho V}{P_{rate} - wc\rho V} \end{cases} \quad (3.5)$$

Note that D_{part1} and D_{part2} are dependent on the temperature drop weight w . When there are no shower or bath activities (with large hot-water consumption in a short period), the internal temperature remains no lower than its lower limit and D_{part1} is zero.

Five hot-water consumption activities are conducted on an actual DEWH using consumed volumes of 0 liters, 7 liters, 15 liters, 35 liters, and 45 liters, respectively. The five activities are initiated after the DEWH reaches its lower limit, and the start temperatures are set to 45 °C (the Consumer Product Safety Commission recommends setting the DEWH temperature at no more than 49°C to prevent scalding in America [84]). The electricity costs are lower with a lower setpoint, because of the reduction in the standby heat loss. As the temperature of water in a DEWH is distributed from high on top to low at bottom, the outlet temperature is high enough to prevent bacteria growth [39] [85]. Figures 3.2 and 3.3 show the corresponding currents and temperatures, indicating that the required heating duration has a direct relationship with the consumed volume of hot-water activities. More hot-water consumption requires a longer heating duration, which causes a lower minimum temperature.

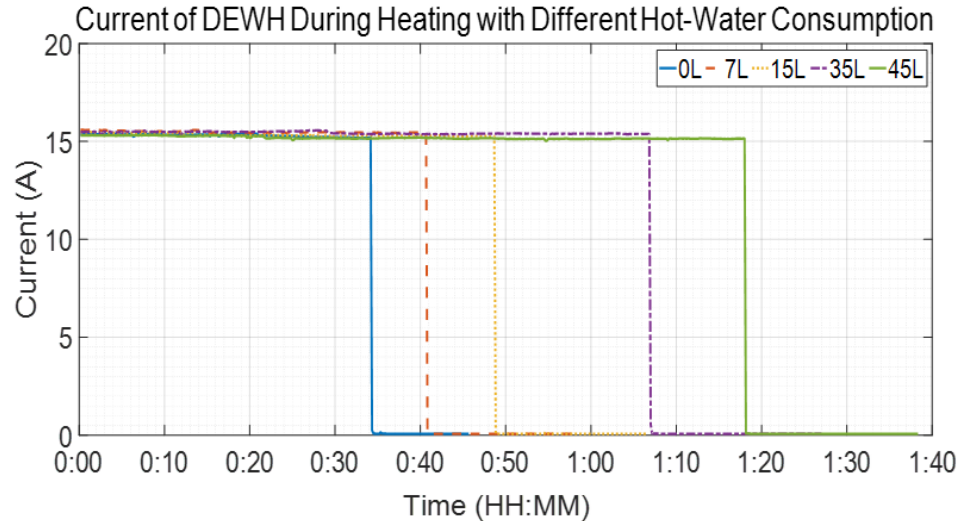


Figure 3.2 Current of the DEWH during each case study

The end-user comfort is directly related to the temperature of a DEWH, and thus the hot-water consumption and heating duration. To consider the effects of the subsequent hot-water consumption and heating duration, CSPI as presented in Equation (3.6), is proposed to sort the priority of the investigated DEWHs for controls.

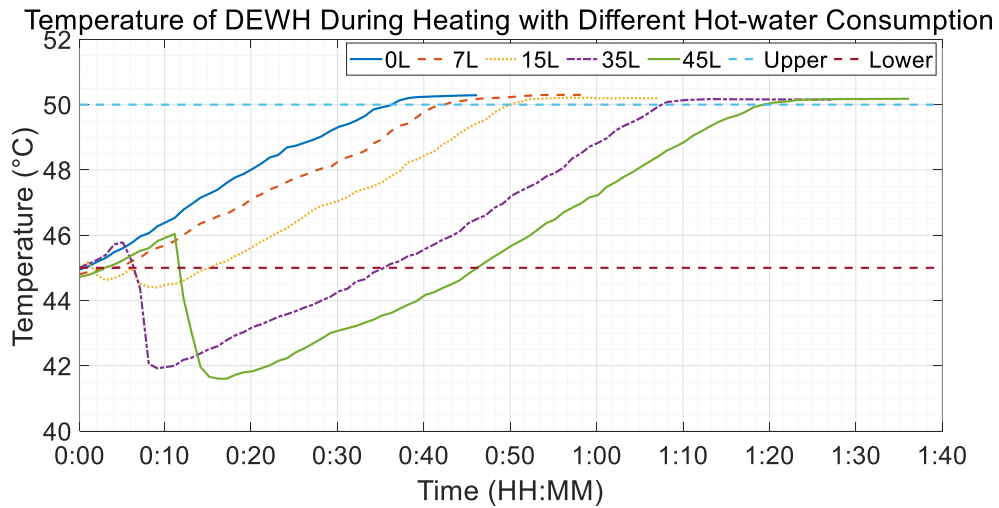


Figure 3.3 Temperature of the DEWH during each case study

$$C_{CSPi,i} = \frac{D_{cum,i} - D_{part1,i}}{D_{part2,i}} \quad (3.6)$$

where $D_{cum,i}$ is the cumulative heating duration for the i^{th} DEWH since the thermostat is turned on, and $D_{part1,i}$ and $D_{part2,i}$ are the required heating durations of the DEWH.

The C_{CSPi} increases during heating. When $D_{cum} < D_{part1}$, C_{CSPi} is negative, indicating that the estimated temperature is lower than the lower limit. When $D_{cum} > D_{part1}$, C_{CSPi} is positive, indicating that the estimated temperature is higher than the lower limit. When $D_{cum} = D_{full}$, C_{CSPi} reaches its maximum value which is 1, indicating that the estimated temperature is equal to the upper limit. When $D_{cum} = 0$, C_{CSPi} is the minimum. Combine Equations (3.5) and (3.6), the minimum C_{CSPi} is:

$$\min C_{CSPi,i} = -\frac{TL_i - T_{aa,i}}{TH_i - TL_i} \quad (3.7)$$

where TH_i and TL_i are the upper and lower temperature limits of the i^{th} DEWH, and $T_{aa,i}$ is the estimated temperature of the DEWH after an identified activity.

From Equation (2.16), T_{aa} is decreased with the increase of consumed volume of the large hot-water consumption activity (shower or bath). Knowing C_{CSPi} is decreased with T_{aa} according to Equations (3.5) - (3.7), we conclude that the C_{CSPi} reflects the effect of the hot-water consumption.

An example is presented in Figure 3.4 to show C_{CSPi} during the heating duration. In the example, 45 liter hot-water is drawn out in 9 minutes with a flow rate of 5 *lpm*. When the

DEWH thermostat turns on, C_{CSPI} is the minimum. It increases during heating with a linear slope. C_{CSPI} reaches its maximum value when the thermostat turns off.

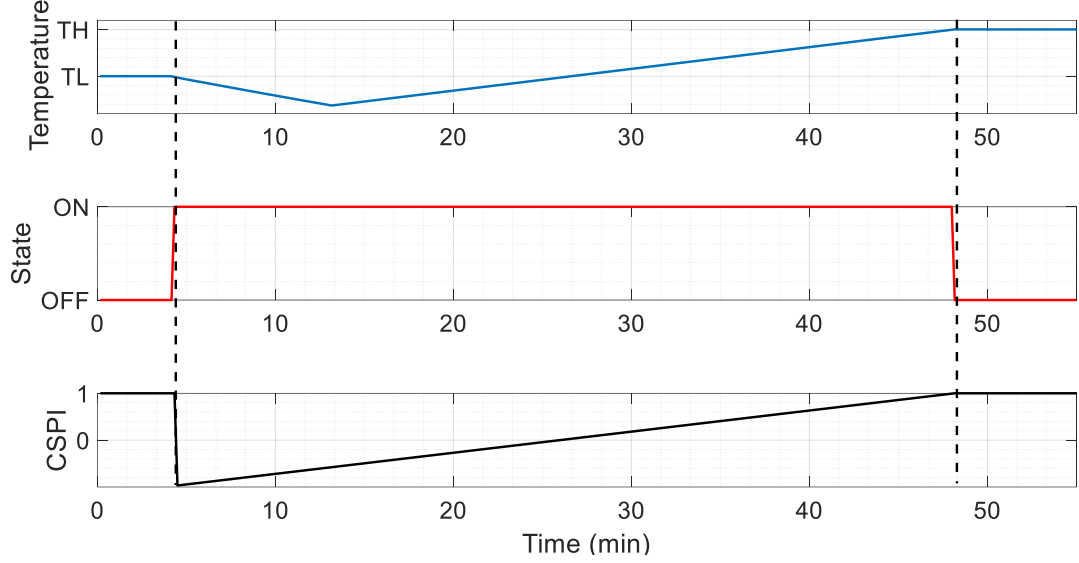


Figure 3.4 Example of an activity

When the DEWH is turned off by control actions, it stops consuming electricity power from power systems. The internal temperature drops due to the hot-water consumption and standby heat loss, which increases the required heating time. As shown in Figure 3.5, the cumulative heating time (D_{cum}) for the whole heating duration is $D_{part1} + D_{part2} + D_{add}$, which is more than that in Figure 3.1 ($D_{part1} + D_{part2}$). D_{add} is the increased heating time due to control actions. CSPI of the DEWH under control should be modified to incorporate the effect of control actions:

$$C_{CSPI,i} = \frac{D_{cum,i} - D_{part1,i} - c\rho V_i \frac{D_{elap,i} - D_{cum,i}}{60P_{rate,i}} w_i}{D_{part2,i}} \quad (3.8)$$

where $D_{elap,i}$ is the time elapsed of the i^{th} DEWH since the thermostat is turned on, and

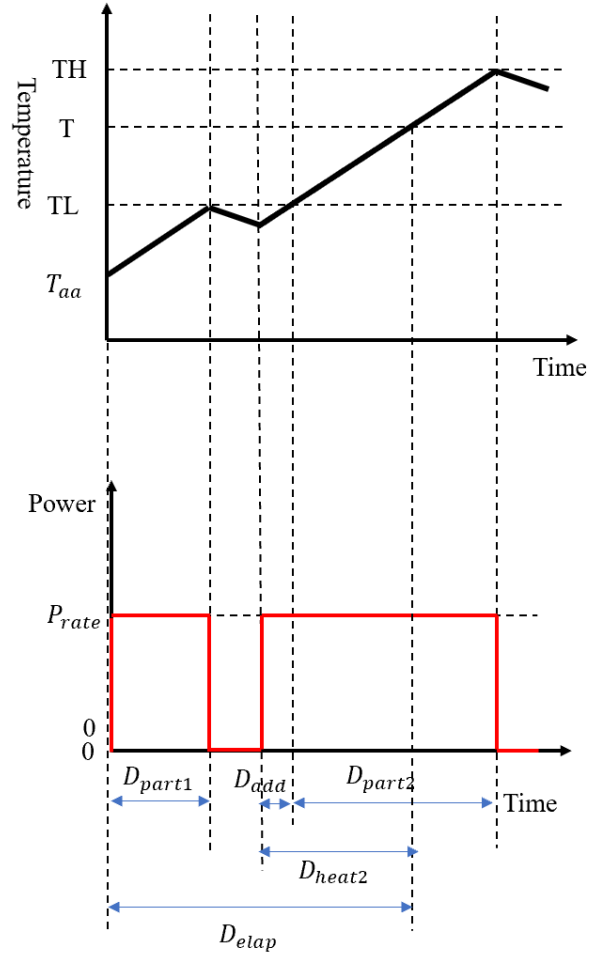


Figure 3.5 Temperature and power demand with control actions

$D_{elap,i} \geq D_{cum,i}$. If the DEWH is never controlled off by the relay, $D_{elap,i} = D_{cum,i}$. As shown in Figure 3.5, the DEWH temperature is heated to T when the time elapsed is D_{elap} , the cumulative heating duration D_{cum} is equal to $D_{part1} + D_{heat2}$, and $D_{elap} > D_{cum}$.

When the thermostat stays on and a new hour begins, the hourly hot-water demand changes. The estimated temperature and flow rate are updated with the proposed state estimation method in Chapter 2. Whereby, weight w , D_{part1} , D_{part2} and C_{CSPI} can be updated in the above equations as well.

3.4 Proposed Peak Shaving Algorithm

Based on the CSPI, a control algorithm for peak shaving is introduced, and the pseudocode of the proposed algorithm is shown in Figure 3.6. The detailed process is as follows:

Algorithm
1: Estimate states \mathbf{S} and identify states of thermostats \mathbf{M} .
2: Update weight matrix \mathbf{W} .
3: Calculate heating duration \mathbf{D}^k of DEWHs.
4: Update \mathbf{G}_{CSPI}^k .
5: Select controllable DEWHs, then sort them.
6: Generate control signals.
7: Apply control signals \mathbf{CS} to DEWHs.

Figure 3.6 Pseudocode of the proposed algorithm

Step 1. The states of DEWHs are estimated based on the variations from smart meter data.

$\mathbf{S} = \{s_1^k, s_2^k, \dots, s_N^k\}$ represents DEWHs' states, where N is the total number of DEWHs, s_i^k is the state of the i^{th} DEWH at the k^{th} sample, and $s_i^k = 0$ when the DEWH is off or $s_i^k = 1$ when the DEWH is on. The thermostats' state $\mathbf{M} = \{Thm_1^k, Thm_2^k, \dots, Thm_N^k\}$ can be identified by DEWHs and their relays states, as shown in Chapter 2. Thm_i^k is the thermostat state of the i^{th} DEWH at the k^{th} sample, and $Thm_i^k = 0$ when the thermostat is off or $Thm_i^k = 1$ when the

thermostat is on.

Step 2. Update the weight matrix \mathbf{W} : if the thermostats are changed or the estimated average flow rates are changed (in a new hour), their weights should be updated with Equation (3.1); else, let $w_i^k = w_i^{k-1}$, where w_i^k is the temperature drop rate of the i^{th} DEWH at the k^{th} sample.

Step 3. Calculate heating duration $\mathbf{D}^k = \{D_{cum,1}^k, D_{cum,2}^k, \dots, D_{cum,N}^k\}$ of DEWHs with \mathbf{S} and \mathbf{M} , which can be expressed as:

$$D_{cum,i}^k = \begin{cases} D_{cum,i}^{k-1} + \Delta t, & \text{when } Thm_i^k = 1 \& s_i^k = 1 \\ D_{cum,i}^{k-1}, & \text{when } Thm_i^k = 1 \& s_i^k = 0 \\ 0, & \text{when } Thm_i^k = 0 \end{cases} \quad (3.9)$$

where $D_{cum,i}^k$ is the cumulative heating duration of the i^{th} DEWH at k^{th} sample interval, and Δt is the time interval.

Step 4. Update $\mathbf{G}_{CSPi}^k = \{C_{CSPi,1}^k, C_{CSPi,2}^k, \dots, C_{CSPi,N}^k\}$ with Equation (3.8), $C_{CSPi,i}^k$ is the CSPI of the i^{th} DEWH at the k^{th} sample. The elapsed time $\mathbf{D}_{elap}^k = \{D_{elap,1}^k, D_{elap,2}^k, \dots, D_{elap,N}^k\}$ is varying with time, which can be expressed as:

$$D_{elap,i}^k = \begin{cases} D_{elap,i}^{k-1} + \Delta t, & \text{when } Thm_i^k = 1 \\ 0, & \text{when } Thm_i^k = 0 \end{cases} \quad (3.10)$$

where $D_{elap,i}^k$ is the elapsed time of i^{th} DEWH at the k^{th} sample.

Step 5. Select controllable DEWHs with \mathbf{M} and \mathbf{G}^k , and these DEWHs can be turned off

to reduce the peak demand. These controllable DEWHs should be from Group 2 in Table 3.1. For these DEWHs in Group 2, their estimated temperature should be no less than their lower limits. In other words, their *CSPI* cannot be negative.

The control signals are defined as $\mathbf{CS}^k = \{CS_1^k, CS_2^k, \dots, CS_N^k\}$, where CS_i^k is the control signal for the i^{th} DEWH at the k^{th} sample, is presented in Equation (3.11). Identify the control availability of each DEWH, $\mathbf{C} = \{C_1^k, C_2^k, \dots, C_N^k\}$, with Equation (3.12), where C_i^k is the control availability for the i^{th} DEWH at the k^{th} sample. $C_i^k = 0$ indicates that the DEWH is uncontrollable, and $C_i^k = 1$ represents controllable.

$$CS_i^k = \begin{cases} 1, & \text{DEWH receives on - signal} \\ 0, & \text{DEWH receives off - signal} \end{cases} \quad (3.11)$$

$$C_i^k = \begin{cases} 1, & \text{when } Thm_i^k = 1 \& CS_i^{k-1} = 1 \& C_{CSPI,i}^k \geq 0 \\ 0, & \text{else} \end{cases} \quad (3.12)$$

All these controllable DEWHs ($C_i^k = 1$) are sorted in the ascent order of CSPI. Only these controllable DEWHs can be sent off-signals to reduce the demand.

Step 6. Generate control actions for the controllable DEWHs to reduce demand. The detail process as follows:

At first, for the DEWHs belonging Group 5, i.e., whose estimated temperatures are lower than their tolerance temperatures, their relays should be turned on to maintain

the end-user comfort. These DEWHs are in a set \mathbf{B} :

$$\mathbf{B} = (\mathbf{CS}^{k-1} == 0) \cap (\mathbf{CSPI}^k < C_{CSPI,tole}) \quad (3.13)$$

where $C_{CSPI,tole}$ is the tolerance CSPI for DEWHs, which can be expressed as:

$$C_{CSPI,tole} = \frac{T_{tole} - TL}{TH - TL} \quad (3.14)$$

On-signals are sent to all the DEWHs in set \mathbf{B} , and the total demand will be increased. The increased demand is necessary to maintain the end-user comfort, and its value is:

$$P_{back} = \sum_{j=1}^b P_{rate,j} \quad (3.15)$$

where b is the total number of DEWHs which are in set \mathbf{B} , and $P_{rate,j}$ is the rated power of j^{th} DEWH in the set.

Then, the objective of the control algorithm is to reduce demand to achieve the desired demand for peak shaving, and the objective function can be written as:

$$\begin{aligned} \min & \left| P_{obj} - P_{back} - \sum_{q=1}^p P_{rate,q} CS_q^k \right| \\ \text{s.t.} & \begin{cases} \text{If } C_q^k = 0, CS_q^k = 0 \\ \text{If } C_q^k = 1, CS_q^k = 0 \text{ or } 1 \\ \text{If } CS_q^k = 0, CS_{q+1}^k = 0 \\ \text{If } CS_q^k = 1, CS_{q+1}^k = 0 \text{ or } 1 \end{cases} \end{aligned} \quad (3.16)$$

where P_{obj} is the desired demand of DEWHs (see Equations (3.17) and (3.18) for details), p is the number of controllable DEWHs, and q means q^{th} DEWHs in the sorted list. These controllable DEWHs can be sent off-signals. The DEWHs with

high CSPIs can be turned off for a long period, hence, it avoids changing their relay states frequently.

Solving the objective function to generate control signals for these controllable DEWHs. The detailed process is shown in Appendix I.

Step 7. Apply the control actions to the DEWHs. The DEWHs in set \mathbf{B} receive on-signals and the controllable DEWHs receive control signals in Step 6. Other DEWHs maintain their previous control signals.

The desired demand of DEWHs P_{obj} is the direct objective of the control. Low peak demand benefits grid stability and reduces costs [86]–[88]. Hence, the peak demand is expected to be as low as possible. However, the available capacity of controllable DEWHs is limited because the DEWHs in set \mathbf{B} must be turned on taking into account the end-user comfort.

These desired demands determine the electrical energy from power systems to the DEWHs. The electrical energy converts to the thermal energy, part of which is consumed by hot-water consumption and the rest is stored in the water in the tank. Therefore, Equation (3.17) holds.

$$\sum_{i=1}^f P_{obj,i} \Delta t = \sum_{i=1}^f \sum_{j=1}^N Q_{com,i,j} + c\rho \sum_{j=1}^N V_j (T_{end,i} - T_{start,j}) \quad (3.17)$$

$$s. t. \begin{cases} T_{in,j} \leq T_{start,j} \leq TH_j \\ T_{tole,j} \leq T_{end,j} \leq TH_j \end{cases}$$

where i is the i^{th} sampling interval, f is the total number of sampling intervals during control, Δt is the time interval, and Q_{com} is the thermal energy consumed by the hot-water consumption activity and standby heat loss during a sampling interval. V_j is the tank volume of the j^{th} DEWH, $T_{start,j}$ is the start temperature, which should be between the upper limit and the cold-water temperature. $T_{end,j}$ is the temperature after controls, which should be between the upper limit and the tolerance temperature.

During the peak shaving control, the required electrical energy will be increased after peak periods due to the requirement of the end-user comfort. Such a natural response to the control is called payback effect [89]–[91]. To reconcile the potential payback effect, constraints (3.18) for P_{obj} should be satisfied:

$$\begin{cases} \sum_{i=1}^f P_{obj,i} \Delta t \leq \sum_{i=1}^f \sum_{j=1}^N Q_{com,i,j} + c\rho \sum_{j=1}^N V_j (TH_j - T_{in,j}) \\ \sum_{i=1}^f P_{obj,i} \Delta t \geq \sum_{i=1}^f \sum_{j=1}^N Q_{com,i,j} + c\rho \sum_{j=1}^N V_j (T_{tole,j} - TH_j) \end{cases} \quad (3.18)$$

If P_{obj} is unreasonable (i.e., if all the DEWHs are controlled off for a long duration), the payback effect may lead to an undesired new peak after controls.

The DEWH which has more thermal energy stored in the tank could contribute more to peak shaving. Hence, sufficiently heating the DEWH before peak periods is favorable. When all the DEWHs are fully heated, P_{obj} is the minimum.

3.5 Case Study Results

In this section, the proposed algorithm is tested using 20,000 DEWHs (19,999 simulated DEWH models and the actual DEWH). Table 3.2 summarized the parameters of DEWHs. The DEWHs are divided into five types, each type has 4,000 DEWHs with two kinds of temperature settings (each setting has 2,000 DEWHs). The temperature setpoints are different in different areas, such as 52°C in American, 60 °C in Canada [92]. But, the Consumer Product Safety Commission recommends setting the temperature at no more than 49°C to prevent scalding in America [84]. Based on the recommendations, two

Table 3.2 Parameters of DEWHs in Case Study

Type	TL(°C)	TH(°C)	P_{rate} (W)	V (L)
1	45	50	3000	160
1	50	55	3000	160
2	45	50	3000	200
2	50	55	3000	200
3	45	50	4500	279
3	50	55	4500	279
4	45	50	6000	320
4	50	55	6000	320
5	45	50	9000	455
5	50	55	9000	455

different deadbands (45°C to 50°C, and 50°C to 55°C) are used for the investigation in the thesis.

The simulated models are based on Equation (2.6). Figure 3.7 shows a comparable heating performance between a real DEWH and a simulated one which has the same parameters (tank volume, rated power, lower and upper temperature limits). The minimum temperatures affect the end-user comfort, and are approximately equal in the figure. The differences between the real and the simulated DEWHs are caused by measurement noises, the internal water flow (when cold-water enters the DEWH, there will be water convection), and variations of the voltage [93]. The differences are small, which validates the simulated models.

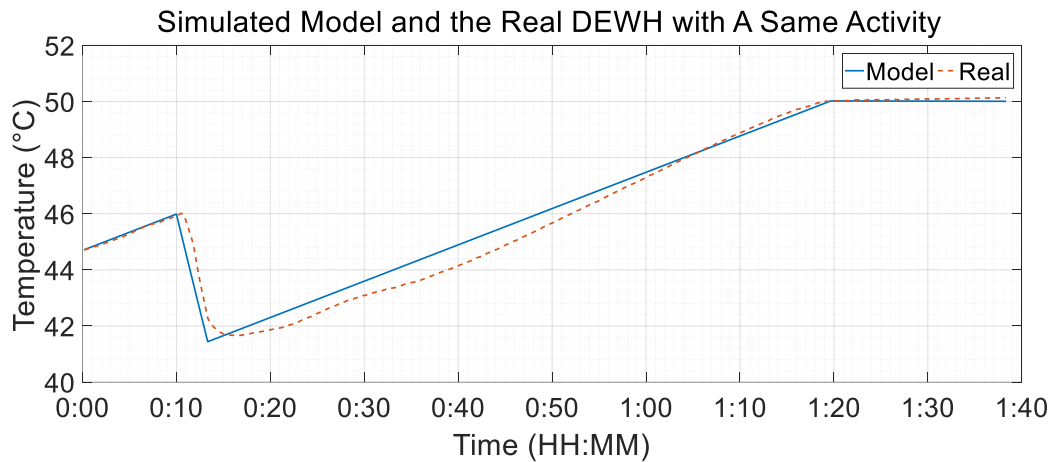


Figure 3.7 Comparison of the real DEWH and its simulated model

The hot-water consumption data is generated by the CREST model [81] that was used in Section 2.5. The hot-water consumption data for each DEWH is selected based on the number of residents. The number of residents varies from 1 to 5 in the model, the more the residents in the house, the larger the DEWH tank to prepare enough hot-water for each

user. Therefore, the hot-water consumption of the DEWH varies. Normally, the consumption increases with the number of residents [63], [65], [66]. Hence, there have many different patterns in the generated hot-water consumption data.

Figure 3.8 shows the total hot-water consumption of all DEWHs for three workdays. In each day there are two demand peaks: the morning peak and the evening peak. The hourly hot-water consumption patterns are estimated based on the probabilities in the CREST demand model.

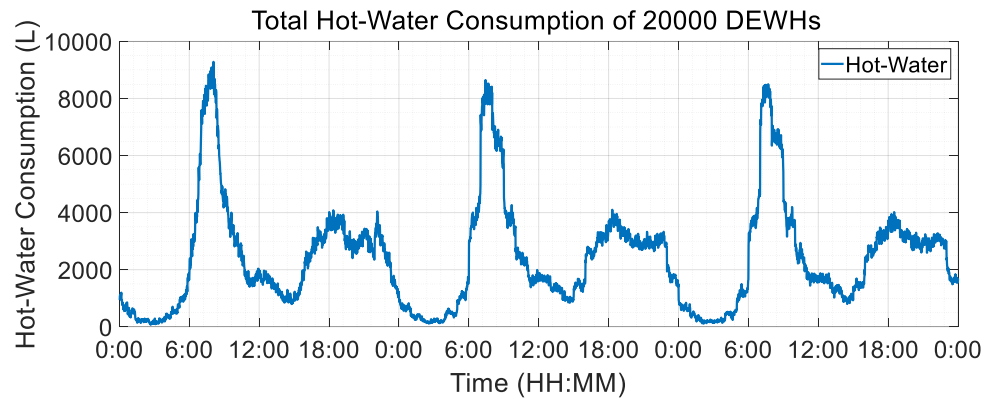


Figure 3.8 Hot-water consumption of the DEWHs system in three workdays

In this thesis, the investigated high demand peak periods are from the “time-of-day” (TOD) policy of Nova Scotia Power (NS Power), Canada, which defines peak periods as being from 7 am to 12 pm, and 4 pm to 11 pm every weekday [94].

The simulated DEWH model has a 10-second time resolution. The time resolution of the proposed control algorithm is one minute which is practical for real-world power systems.

3.5.1 Peak Shaving

Figure 3.9 shows the electric power consumption results of the DEWHs system. The ‘Original’ line is the power demand without any control, which is called the original case in the thesis. The peak demand is about 21.8 MW (the total rated power of DEWHs is 102 MW) during the morning peaks and 9.6 MW during the evening peaks.

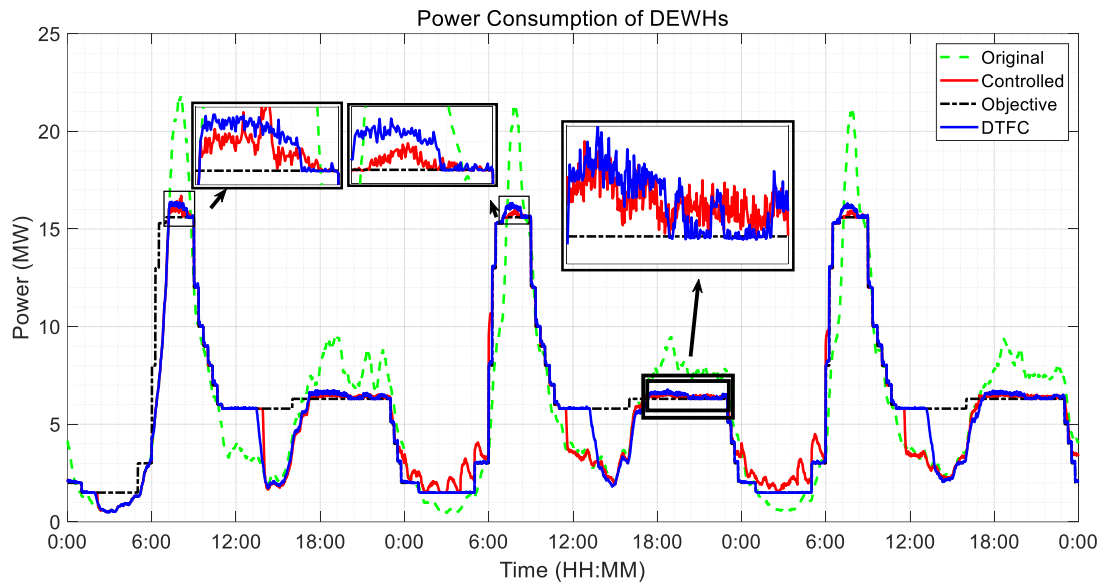


Figure 3.9 Power consumption of the DEWHs system

The ‘Controlled’ line is the power demand with the proposed control algorithm. The morning peak is about 16.6 MW (first day) and 16 MW (subsequent days), while the evening peak is about 6.6 MW. Only those DEWHs whose thermostats are on can be controlled off for peak shaving. The number of the controllable DEWHs is limited at the beginning, and therefore the available peak shaving capacity is limited. Hence, as shown in Figure 3.9, the peak shaving capacity of the first day is smaller than the subsequent days.

On average, the proposed algorithm achieves the peak load reduction by 5.23 MW (24% of the morning peak demand in the original case) for the morning peaks and 3 MW (31.3% of the evening peak demand in the original case) for the evening peaks.

A direct temperature feedback control (DTFC) method [22] is employed to compare with the proposed algorithm, its annotation is ‘DTFC’ in the figures. The DTFC method has been implemented in practice for pilot projects, and the temperature information is used to select control actions. The end-user comfort can be maintained by temperature measurements of DEWHs in the DTFC, which makes the DTFC a good benchmark for providing the performance of the proposed algorithm in this thesis. The peak shaving ability of the DTFC is similar to the proposed algorithm. The “Objective” in Figure 3.9 is the desired curve for control algorithms.

The measurements of hourly electricity consumption for the original case, the DTFC, and the proposed algorithm are shown in Figure 3.10. The peak shaving methods aim at shifting electricity consumption from peak periods without affecting end-users. Therefore, the thermal energy consumed by hot-water consumption activities is not changed by control actions. Hence, the total electricity consumption should be approximately equal as shown in Figure 3.10.

Table 3.3 is the consumed electricity of each case during different periods. The peak shaving algorithms reduce the peak demand by shifting it to standard and off-peak periods. With the TOU electricity price of NS Power, the daily electricity cost saving by the

proposed algorithm and the DTFC is more than \$ 1,000 per day (the electricity cost is about \$ 25,000 per day in the original case). Furthermore, some jurisdictions have a punitive rate structure (when the peak demand exceeds a threshold value, a penalty will be imposed) [95], [96]. With the reduction of peak demand, the penalty may be avoided by the proposed algorithm, resulting in attractive economic benefits.

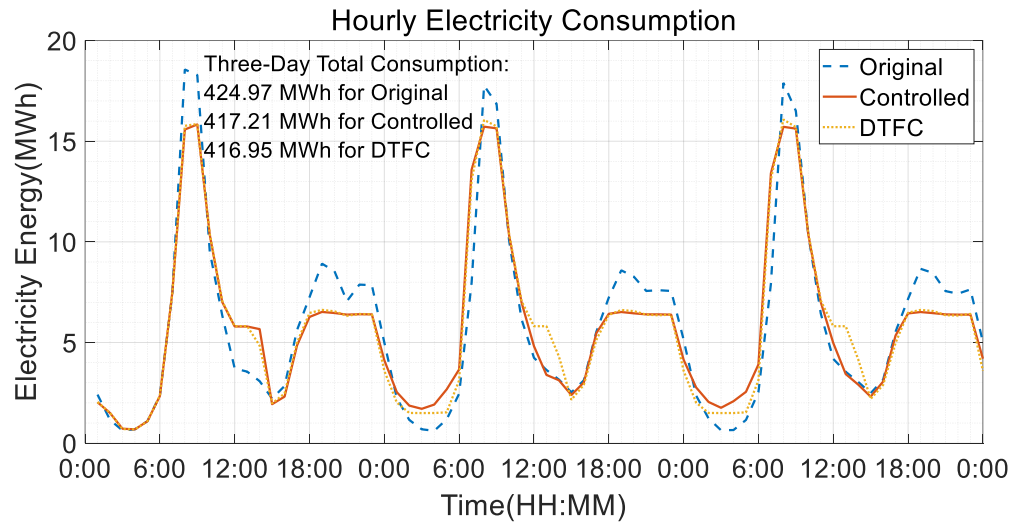


Figure 3.10 Hourly electricity consumption

In this thesis, three temperature zones are used to show the comfort levels and available power shifting capacity. The three temperature zones are defined as: a) Zone 1, where the temperature of a DEWH is between its upper and lower limit; b) Zone 2, where the DEWH temperature is between its lower limit and the tolerance temperature; and c) Zone 3, where the DEWH temperature is lower than its tolerance temperature. The end-user comfort will be satisfied when the DEWH temperature is maintained in Zone 1 or Zone 2. Meanwhile, if the DEWH temperature drops to Zone 3, the end-user comfort may be affected. Large hot-water consumption during a short period will cause significant temperature drops,

Table 3.3 Electricity Consumption

		M-Peak (MWh)	Standard (MWh)	E-Peak (MWh)	Off-Peak (MWh)
Day 1	Original	56.26	11.77	53.05	20.58
	Controlled	54.40	16.11	42.57	19.87
	DTFC	54.81	17.79	41.70	19.59
Day 2	Original	55.15	12.42	52.34	21.47
	Controlled	53.70	12.67	43.33	32.00
	DTFC	54.59	17.72	41.79	23.38
Day 3	Original	55.45	12.22	52.43	21.50
	Controlled	53.70	12.57	43.22	32.55
	DTFC	54.63	18.50	41.71	27.38

NS Power defines peak time from 7 am to 12 pm (M-Peak) and 4 pm to 11 pm (E-peak), standard time from 12 pm to 4 pm, and off-peak time from 11 pm to 7 am.

M-peak here is from 7am to 12 pm, E-peak here is from 4 pm to 11pm.

which may lead to DEWH temperature down to Zone 3. Hence, the DEWH temperature in Zone 3 is undesired but unavoidable in practical applications [76].

For a DEWH without any control actions, the temperature will be maintained in Zone 1 for most of the time. If more DEWHs can be controlled to maintain their temperatures in Zone 2, more controllable capacity for peak shaving can be provided. DEWHs in Zone 3 are not used to provide peak shaving services. Therefore, the total controllable capacity for peak shaving is highly dependent on the DEWHs in Zone 1 and Zone 2.

The percentages of DEWHs in Zone 2 for three cases are shown in Figure 3.11. The proposed algorithm and the DTFC make more DEWHs operated in Zone 2 than the original case during the peak periods. In all cases, the percentages of DEWHs in Zone 2 are limited during standard and off-peak periods. This is so because the proposed control method allows DEWHs to keep heating until they are automatically turned off by their thermostats.

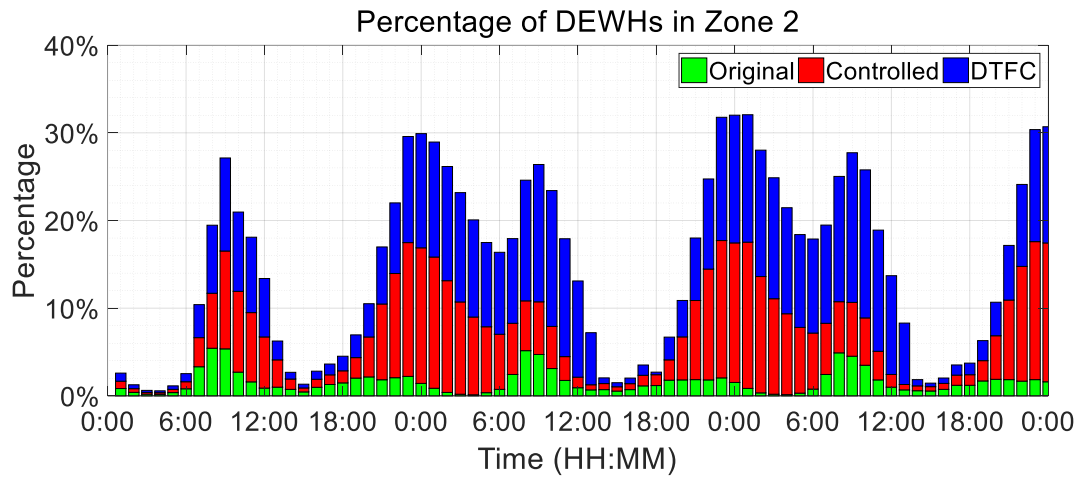


Figure 3.11 Percentage of DEWHs in Zone 2 during each hour

When the relay is on, the state of a DEWH is switched from on to off when its temperature reaches its upper limit. At this instant, the estimated temperature can be reset to its upper limit, and the previous estimation error is deleted, which will help to eliminate the cumulative estimation errors caused by unexpected activities. When the relay is on, the state of the DEWH is switched from off to on when its temperature reaches its lower limit. At this instant, the estimated temperature can be reset to its lower limit. By the two adjustments, the DEWH state estimation can be calibrated.

3.5.2 End-User Comfort

The end-user comfort is the most important constraint for the DLC [97], and it can be represented and analyzed with the temperature of DEWHs.

Figure 3.12 shows the percentages of DEWHs that are in Zone 3 in different cases. Compared with the percentages of the original case, the proposed method slightly increases the maximum percentage, but they are very close in most of the times. Hence, the end-user comfort is well maintained by the proposed algorithm. As the DTFC does not consider hot-water consumption, the percentage increase is more than that of the proposed algorithm. The proposed algorithm is better than the DTFC method.

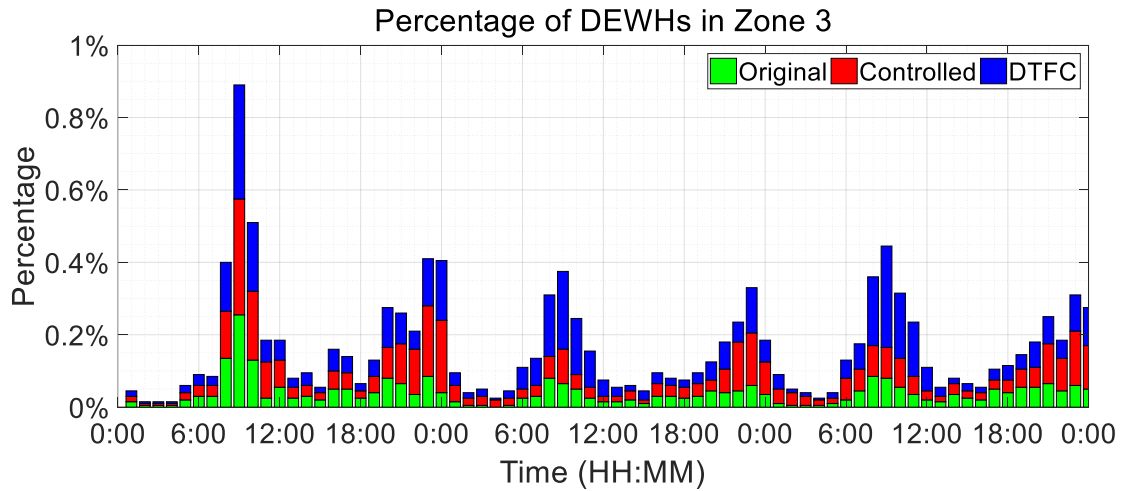


Figure 3.12 Percentage of DEWHs in Zone 3 during each hour

Figure 3.13 shows the maximum temperature drop of the DEWHs for each case. The maximum temperature drop is defined as the minimum temperature minus its lower limit. It is noteworthy that the temperature can drop beyond the lower limit when heavy hot-

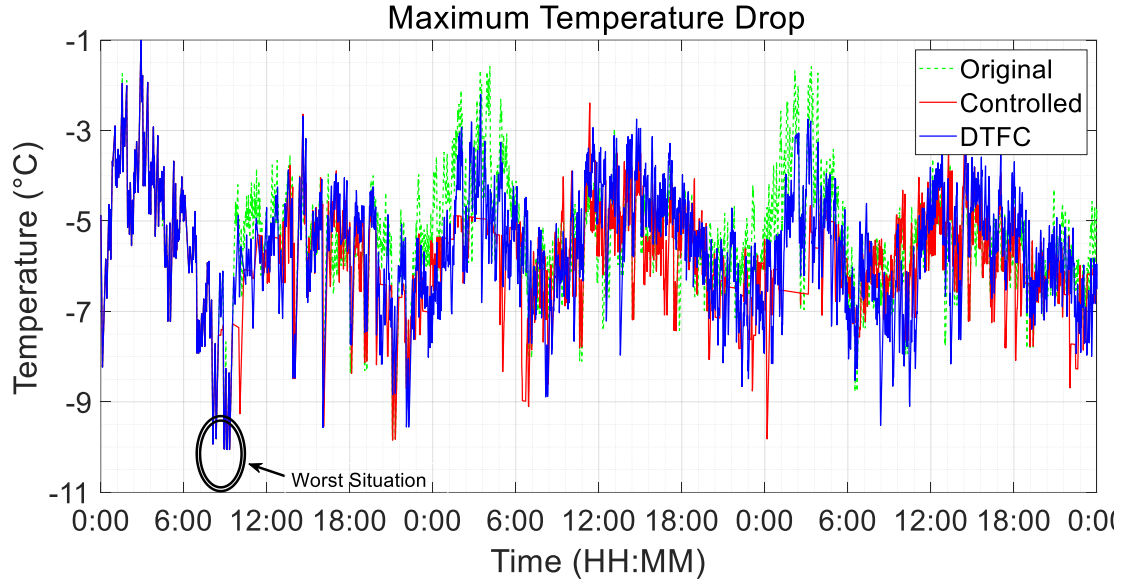


Figure 3.13 Maximum temperature drops of the DEWHs system

water consumption activities occur in a short period.

The worse situations are the same in Figure 3.13. The minimum temperature with the proposed control algorithm is the same as the minimum temperatures in the original case and in the DTFC case. Hence, the proposed algorithm has no additional damaging impact on the end-user comfort.

Figure 3.14 shows the CSPI of an DEWH during control. The tolerance temperature for the DEWH is 45 °C. There only two durations when the DEWH is in Zone 3 (the same for the controlled case and the original case), but the DEWH is heating (as the shown in the DEWH state). Hence, the CSPI can provide references for control. When the CSPI is lower than the tolerance value (-1 in Figure 3.14), the DEWH is turned on to maintain the end-user comfort; and the DEWH can be turned off until the CSPI is positive. Based on the

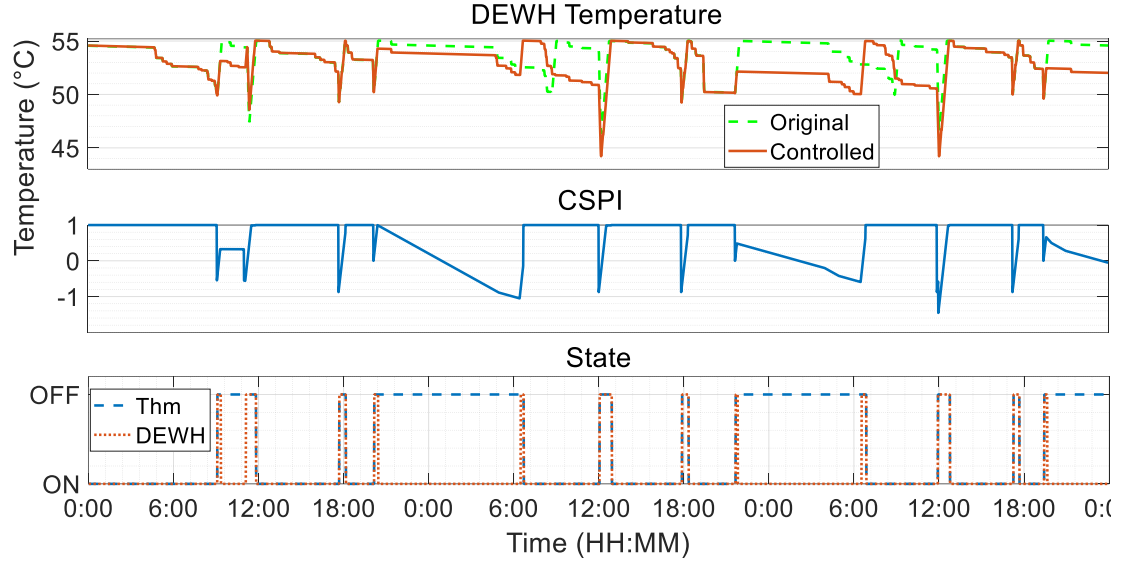


Figure 3.14 A DEWH information during control

thermostat state (Thm in Figure 3.14) and DEWH state, the DEWH is controllable only when its thermostat is on. When the thermostat is off, the DEWH is uncontrollable (the CSPI is adjusted to 1).

In summary, the proposed algorithm is better than the benchmarking DTFC method in terms of maintaining the end-user comfort, without the requirement for temperature measurements.

3.5.3 Randomness of Human Behaviors

The actual hot-water consumption may exceed the patterns due to the unexpected hot-water consumption caused by random human behaviors. The unexpected consumption will affect the accuracy of the weight matrix \mathbf{W} , and could lead to undesired temperature drop that negatively affects the end-user comfort. The proposed algorithm inherently mitigates the

impact through two mechanisms: a) the worst case assumptions for the estimation of hot-water consumption in Section 2.3.3; b) the estimated temperature adjustments as presented in the last paragraph of Section 3.5.1.

There are many DEWHs whose hot-water consumption are higher than their patterns in the previous case study of peak shaving. The volume of unexpected consumption is defined as:

$$V_{un} = V_{actual} - V_{pattern} \quad (3.19)$$

where V_{un} is the volume of the unexpected hot-water consumption, V_{actual} is the volume of actual hot-water consumption, and $V_{pattern}$ is the volume of hourly hot-water consumption. Figure 3.15 shows the maximum volume of the unexpected hot-water consumption of all the DEWHs in the case study. The maximum volume of the unexpected hot-water consumption is from 30 liters to 85 liters, which is high enough for the most intense water uses like bath or shower.

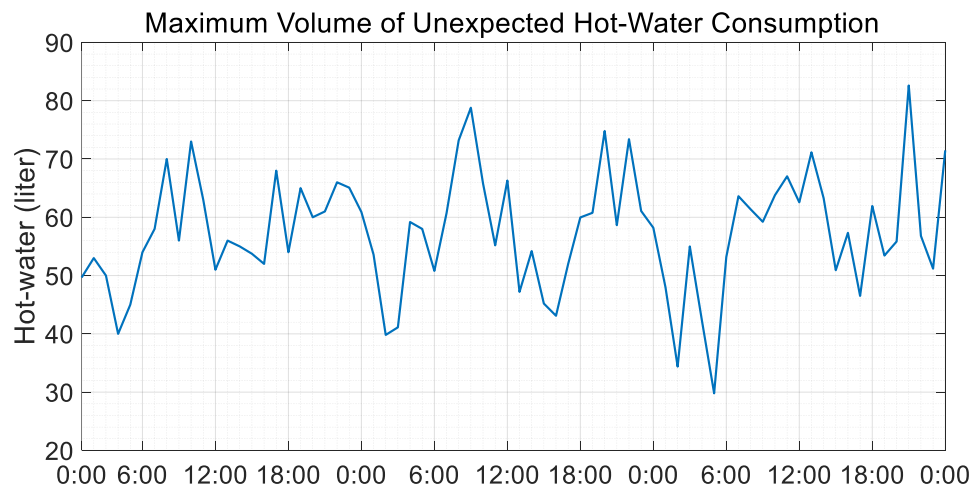


Figure 3.15 Maximum hot-water consumption excessive of the patterns

Figure 3.16 shows that the hot-water consumption of more than 7% DEWHs exceeds their patterns during peak periods.

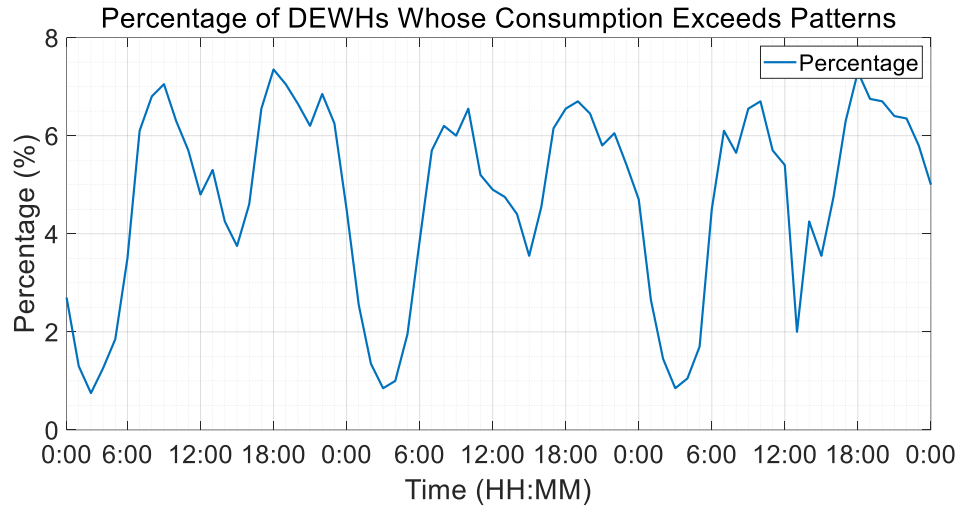


Figure 3.16 Percentage of DEWHs whose hot-water consumption exceeds patterns

Section 3.5.2 has shown the success in maintaining the end-user comfort. It can be concluded that the proposed algorithm performs well with the two mechanisms that mitigate the unexpected impact of random human behaviors, which is important for the implementation of the proposed algorithm in practice.

Furthermore, the defined tolerance temperature values are lower than the lower limit of a DEWH, but are still higher than the acceptable temperature for the human body (40 °C [98]). The acceptable scenario at worst is that the DEWH's outlet water temperature is equal to the acceptable temperature. Hence, using the tolerance temperature can secure the end-user comfort with an additional volume of hot-water consumption above of that of the

acceptable scenario. The additional volume can be calculated by:

$$V_{add} = \frac{V(T_{tole} - T_{body})}{T_{tole} - T_{in}} \quad (3.20)$$

where T_{body} is the acceptable temperature for the human body and is equal to 40 °C [71] [98]. Then the available volume of hot-water is about 10% to 20% of the tank volumes of DEWHs.

Thus, it is tenable to conclude that the proposed control algorithm can maintain the end-user comfort with random human behaviors.

3.6 Conclusion

In this chapter, a control algorithm without temperature measurements is proposed for peak shaving. A time-variant weight matrix is generated based on the state estimation method presented in Chapter 2, and is used to consider the subsequent hot-water consumption. Based on the weight matrix, *CSPI* is employed to evaluate the control priority of DEWHs.

The case study presented in Section 3.5 illustrates that the proposed algorithm is able to reduce peak demands significantly even without any temperature measurement. The morning peaks are reduced by 24% while the evening peaks are reduced by 31.3%. The proposed algorithm outperforms the DTFC method in terms of the end-user comfort.

The proposed control method can tackle the negative impact of random human behaviors

on end-user comfort with two inherent mechanisms: the worst case assumptions and the estimated temperature adjustments. The results validate the effectiveness.

4 Frequency Control

4.1 Introduction

With the increasing penetration of volatile RERs [25], more ancillary services are required in power systems to maintain the generation/load balance. Frequency control is an important kind of ancillary services. Frequency control services are mainly from on-line generators, whereas flexible loads can in principle provide these services, too. With the large thermal energy storage capacities, DEWHs can not only be used to provide peak shaving services but also can be used to provide frequency control services.

In power systems, a power mismatch between generation and load leads to a grid frequency deviation. The frequency decreases when the generation is lower than the demand, and it increases when the generation is higher than the demand. If there is no frequency control service for the power mismatch, the grid frequency diverges until a critical point, resulting in a blackout. Hence, frequency control is necessary for power systems. In traditional power systems, the power mismatch can be eliminated by the control of generation.

Generally, three levels of frequency control are used, primary, secondary, and tertiary control. The three levels of frequency are shown in Figure 4.1 [99]. The primary frequency control (PFC) is activated immediately when a frequency deviation occurs, which maintains the stability of the power system. Then the secondary frequency control (SFC) takes over to restore the grid frequency to the nominal value, and the consumed reserves

by the PFC are released. If the grid frequency is not restored after the SFC, the tertiary frequency control is required. The tertiary frequency control is used to restore the frequency and release the reserves that are consumed by the PFC and SFC.

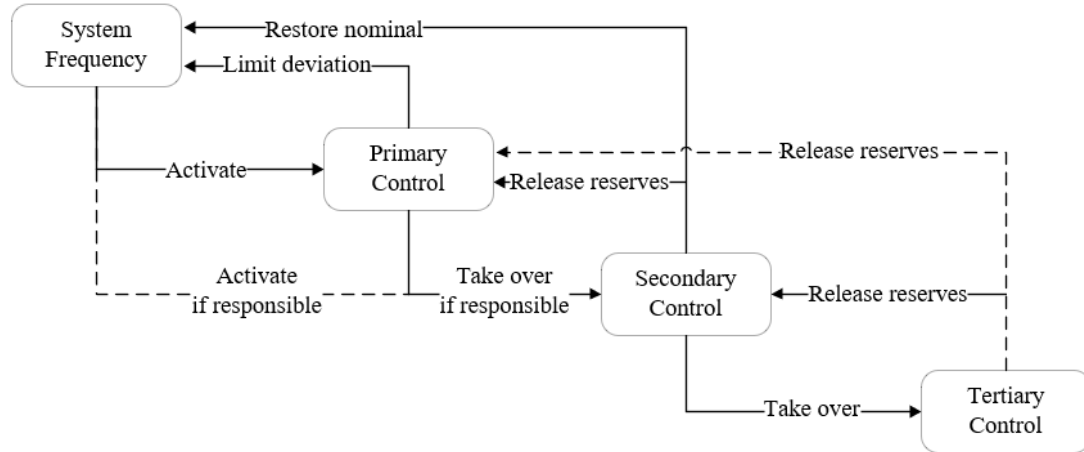


Figure 4.1 Frequency control in power systems

PFC is the first active response of resources to arrest the grid frequency deviations. Governors for PFC are continuously active, automatic, not driven by a centralized system, and respond instantaneously (in seconds). PFC adapts generation proportionally to the frequency deviation from the nominal grid frequency, thereby maintaining the grid frequency within permissible limits while a steady-state frequency deviation remains. The steady-state deviation is governed by the mismatch and characteristics of the power system [99].

SFC is employed to eliminate the steady-state deviation. SFC has a central controller to modify the active power, aiming at restoring the grid frequency to its nominal value [99].

SFC operates slower than the PFC, in a timeframe of minutes. The actions of SFC will take place continually in response to minor frequency deviations and power mismatches.

When the grid frequency cannot be restored to its nominal value. In this case, the tertiary frequency control service is required. The tertiary control is any automatic or manual change in the working points of the participating generating units. Hence, the tertiary control can be regarded as optimal switching problems [100], which is not considered in this thesis. Due to the delays of more than seconds in communications and controls of DEWHs, DEWHs are employed to provide the SFC services in this thesis.

When the SFC is provided, the grid frequency is restored to its nominal value by steering the area control error (ACE) to zero. ACE is the difference between scheduled and actual electrical generation within a control area in the power system, taking frequency bias into account. The ACE can be expressed as:

$$ACE = P_{measure} - P_{program} + K(f_{measure} - f_o) \quad (4.1)$$

where ACE is the area control error, $P_{measure}$ is the sum of the instantaneous measured active power, $P_{program}$ is the resulting programmed exchange with all the neighboring control areas, K is the K-factor of the control area in MW/Hz, $f_{measure}$ is the measured frequency of the control area, and f_o is the nominal frequency.

If the ACE is positive, the generation is higher than the load and should be decreased to provide frequency control services. If the ACE is negative, the generation should be

increased. To make ACE be zero, SFC resources should provide a desired correcting power, which can be written as:

$$\Delta P = -\beta \cdot ACE - \frac{1}{T_r} \int ACE dt \quad (4.2)$$

where β is the proportional factor of SFC in the control area, and T_r is the integration time constant of the secondary controller in the area.

Traditionally, frequency control services are provided through the generation-following-load paradigm. Nowadays, the frequency control can also be achieved by load controls. If the desired correcting power is positive, the load demand should be decreased. If the desired correcting power is negative, the load demand should be increased.

To respond to the desired correcting power, several reserve products in the electricity market should be chosen through bidding. These providers offer their reserves for frequency control [22]. Typically, the providers are remunerated separately for the accepted reserve capacity in the auction or the requested reserve energy by the SO.

In this thesis, DEWHs are aggregated as a virtual frequency control provider (VFCP). The VFCP is an SFC provider in the power system, bidding and providing SFC as an individual entity. If the desired correcting power is positive, the VFCP provides the SFC by decreasing its demand. If the desired correcting power is negative, the VFCP provides the SFC by increasing its demand.

The chapter is organized as follows. In Section 4.2, the VFCP framework is presented, and the available capacity of the VFCP is analyzed. The available energy level (AEL) model of the VFCP is also presented in this section. The proposed algorithms are described in Section 4.3. The frequency control services are implemented for different cases in Section 4.4 to show the frequency control performances with the VFCP. Last, Section 4.5 concludes this chapter.

4.2 Virtual Frequency Control Provider

The VFCP consists of a number of DEWHs, a centralized controller, and a capacity calculator. The framework of the VFCP is shown in Figure 4.2. The meter of each house is used to measure the total domestic power consumption. The power consumption of each house is sent to the capacity calculator, the DEWH state can be identified by the identification methods in [67], [76]. The capacity calculator is used to generate the available capacity for frequency control. The available capacity will be sent to the SO. The control signals are generated by the controller to respond to the requirement (desired correcting power) from the SO. The requirement should not be higher than the available capacity. The control signals are sent to each external relay to control DEWHs in the VFCP.

A baseline is introduced to represent the power demand of the VFCP without control. The baseline can be forecasted through some typical methods [31], [101], [102]. When the VFCP power is controlled lower than the baseline, the process can be regarded as the

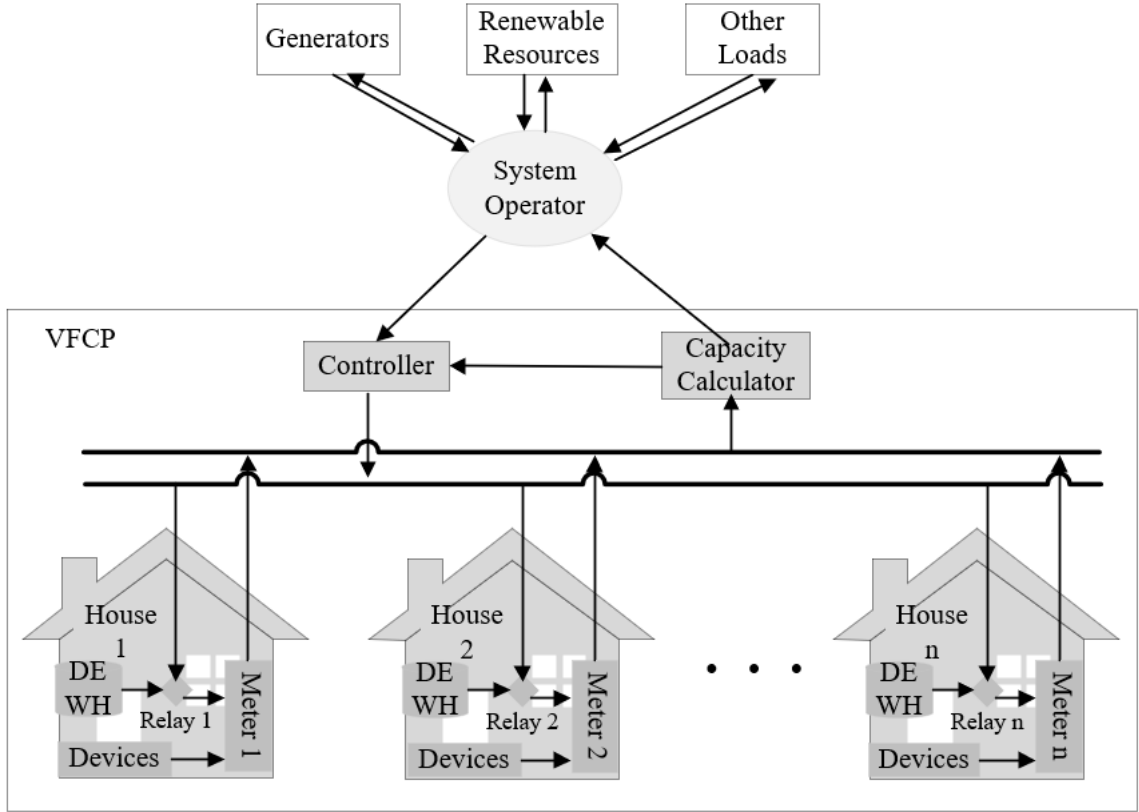


Figure 4.2 Framework of the VFCP

discharging process of a battery. When the VFCP power is higher than the baseline, the process is considered as the charging process of a battery.

Although the energy stored in the VFCP is related to the thermal energy stored in DEWHs, the estimated temperature cannot be used to show the available capacity for frequency control directly. Because the thermostats are uncontrollable for conventional DEWHs, only these DEWHs whose thermostats are on can be controlled to provide frequency control services. These DEWHs whose thermostats are off cannot be controlled; hence, they can be regarded as fully heated, and their AELs are 1. Then the AEL of each DEWH in the VFCP can be expressed as:

$$AEL_i(t) = \begin{cases} 1, & \text{when } Thm_i(t) = 0 \\ \frac{T_i(t) - TL_i}{TH_i - TL_i}, & \text{when } Thm_i(t) = 1 \end{cases} \quad (4.3)$$

where $AEL_i(t)$ is the available energy level of the i^{th} DEWH at time t , T is the estimated temperature of the DEWH, TL is the lower limit, TH is the upper limit, and Thm is the thermostat state, $Thm = 1$ when the thermostat is on or $Thm = 0$ when the thermostat is off.

The maximum AEL of a DEWH is 1, and the minimum value may be negative (the temperature can be lower than the lower limit, as shown in Chapter 2 and Chapter 3). The tank sizes and rated power of DEWHs in the VFCEP are different, the heating duration and consumed electrical energy are also different. The AEL_{VFCEP} of the VFCEP is:

$$AEL_{VFCEP}(t) = \frac{\sum_{i=1}^N AEL_i(t) V_i / P_{rate,i}}{\sum_{i=1}^N V_i / P_{rate,i}} \quad (4.4)$$

where N is the total number of DEWHs in the VFCEP, i means the i^{th} DEWH, V is the volume of the DEWH tank, and P_{rate} is the rated power of the DEWH.

These DEWHs with AEL values ($0 \leq AELs < 1$) can be turned off to reduce the VFCEP power.

If a DEWH relay has been controlled off and its AEL reaches AEL_{tole} ($AEL_{tole} = \frac{T_{tole} - TL}{TH - TL}$,

where T_{tole} is the tolerance temperature), the relay must be turned on to maintain the end-user comfort. The available control actions are related to the AEL of a DEWH and its relay state, as illustrated in Figure 4.3:

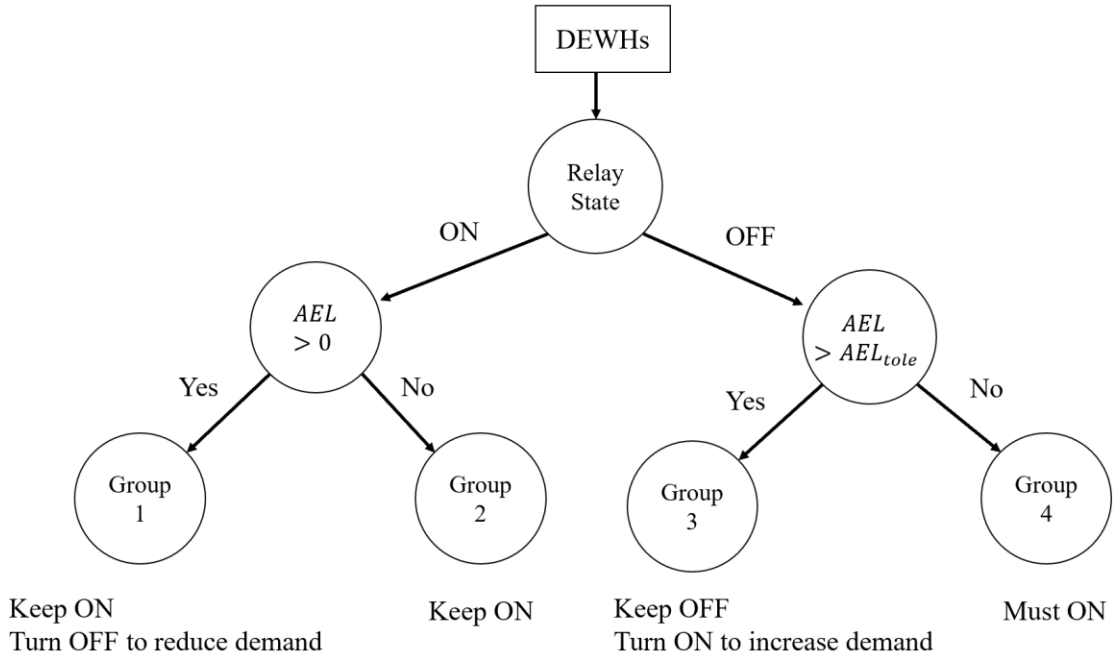


Figure 4.3 Available control action relates to AEL and relay state

- 1) Group 1: DEWHs whose relays are on and their $AELs > 0$. These DEWHs can be turned off to reduce the VFCP demand or kept on.
- 2) Group 2: DEWHs whose relays are on and AELs are not positive. These DEWHs must be kept on avoid control DEWHs frequently.
- 3) Group 3: DEWHs whose relays are off and AELs are higher than a threshold. These DEWHs can be turned on to increase the VFCP demand or kept off.
- 4) Group 4: DEWHs whose relays are off and AELs are not higher than the threshold. These DEWHs must be turned on to maintain the end-user comfort.

The available capacity of the VFCP for frequency control is dependent on the DEWHs' states and their relay states. The SO requires frequency control services should not exceed the available capacity. The SO sends the desired correcting power to the VFCP. The desired

correcting power can be positive, zero, or negative. The positive desired correcting power requires the VFCP to decrease its demand (ramp-down), and the negative desired correcting power requires the VFCP to increase its demand (ramp-up).

The VFCP power is:

$$P_{VFCP}(t) = \sum_{l=1}^{g1(t)} P_{rate,l} + \sum_{k=1}^{g2(t)} P_{rate,k} \quad (4.5)$$

where $g1$ and $g2$ are the numbers of DEWHs in Group 1 and Group 2. l means the l^{th} DEWH in Group 1, and k means the k^{th} DEWH in Group 2.

The ramp-up power reaches the maximum when all the DEWHs in Group 1, Group 2, Group 3, and Group 4 have received on-signals. The maximum ramp-up power can be expressed as:

$$\begin{aligned} P_{up,max}(t) = & \sum_{l=1}^{g1(t)} P_{rate,l} + \sum_{k=1}^{g2(t)} P_{rate,k} + \sum_{n=1}^{g3(t)} P_{rate,n} \\ & + \sum_{j=1}^{g4(t)} P_{rate,j} - P_{VFCP}(t) \end{aligned} \quad (4.6)$$

where $g3$ and $g4$ are the numbers of DEWHs in Group 3 and Group 4. n means the n^{th} DEWH in Group 3, and j means the j^{th} DEWH in Group 4. Combining Equations (4.5) and (4.6), the maximum ramp-up power is dependent on the cumulative power of these DEWHs in Group 3 and Group 4.

$$P_{up,max}(t) = \sum_{n=1}^{g3(t)} P_{rate,n} + \sum_{j=1}^{g4(t)} P_{rate,j} \quad (4.7)$$

The ramp-down power reaches the maximum when the DEWHs in Group 2 and Group 4 receive on-signals and the DEWHs in Group 1 and Group 3 receive off-signals. The maximum ramp-down power (negative value) can be expressed as:

$$P_{down,max}(t) = \sum_{k=1}^{g2(t)} P_{rate,k} + \sum_{j=1}^{g4(t)} P_{rate,j} - P_{VFCP}(t) \quad (4.8)$$

Combining Equations (4.5) and (4.8), the maximum ramp-down power can be re-written as:

$$P_{down,max}(t) = \sum_{j=1}^{g4(t)} P_{rate,j} - \sum_{l=1}^{g1(t)} P_{rate,l} \quad (4.9)$$

Hence, the maximum ramp-down power of the VFCP is dependent on the cumulative power of these DEWHs in Group 4 minus that in Group 1.

The tolerance temperature in this thesis is set as five degrees lower than its lower limit, the same as that in Chapter 3. The $AE L_{tole}$ is negative, as shown in Figure 4.3. The maximum ramp-up and ramp-down power are generated by the capacity calculator and sent to the SO. The maximum ramp-up and ramp-down power will be used by the SO to determine the desired power with the requirements for frequency control.

$$P_{down,max}(t) \leq -\Delta P(t) \leq P_{up,max}(t) \quad (4.10)$$

4.3 Proposed Frequency Control Algorithm

4.3.1 Frequency Control with Tolerance

DEWHs in Group 1 can be turned off to reduce the VFCEP power. DEWHs in Group 3 can be turned on to increase the VFCEP power. DEWHs in Group 4 must be turned on to maintain the end-user comfort and increase the VFCEP power. DEWHs in Group 2 must be kept on. Hence, the controllable DEWHs for frequency control are these DEWHs in Group 1 and Group 3.

After the VFCEP receives the desired correcting power from the SO, a control algorithm is required to generate control signals for DEWHs. The desired correcting power should meet the requirement in Equation (4.10). If the desired power exceeds the available capacities, it will be modified as shown in Equation (4.11). The control objective is to increase/decrease the VFCEP power to match the negative/positive desired correcting power.

$$-\Delta P(t) = \begin{cases} P_{up,max}(t), & \text{when } -\Delta P(t) > P_{up,max}(t) \\ P_{down,max}(t), & \text{when } -\Delta P(t) < P_{down,max}(t) \\ -\Delta P(t), & \text{else} \end{cases} \quad (4.11)$$

The DEWH groups (Group 1-4) should be synergistically managed to meet the control objective. At first, these DEWHs in Group 4 must be turned on to maintain the end-user comfort, which will increase the VFCEP power. Then, the desired correcting power for other groups (Group 1, Group 2 and Group 3) can be adjusted as:

$$\Delta P_{adjust}(t) = -\Delta P(t) - \sum_{j=1}^{g^4(t)} P_{rate,j} \quad (4.12)$$

where ΔP_{adjust} is the adjusted power, j means the j^{th} DEWH in Group 4, and ΔP is the desired correcting power from the SO. As DEWHs in Group 2 must be kept on, the adjusted

power is responded by DEWHs in Group 1 or Group 3.

If $\Delta P_{adjust} < 0$, DEWHs in Group 1 are selected to be turned off to reduce the demand. Otherwise, DEWHs in Group 3 are selected to be turned on to increase the demand. ΔP_{adjust} can be achieved by:

$$\Delta P_{adjust}(t) = \begin{cases} \sum_{n=1}^{g3(t)} P_{rate,n} CS_n, & \text{when } \Delta P_{adjust}(t) \geq 0 \\ \sum_{l=1}^{g1(t)} P_{rate,l} (CS_l - 1), & \text{when } \Delta P_{adjust}(t) < 0 \end{cases} \quad (4.13)$$

where n means the n^{th} DEWHs in Group 3, l means the l^{th} DEWHs in Group 1, $g1$ is the number of DEWHs in Group 1, $g3$ is the number of DEWHs in Group 3, and CS_n is the control signal for n^{th} DEWH in Group 3. $CS_n = 1$ indicates the DEWH receives on-signal, and $CS_n = 0$ indicates the DEWH receives off-signal.

Figure 4.4 is the schematic representation of the VFCEP to provide the SFC services. The proposed algorithm is based on the previous classification in Figure 4.3 (where Group 3 and Group 4 are classified by the tolerance AEL_{tole}). Hence, the algorithm is called frequency control with tolerance (FCWT) in this thesis. Its pseudocode is shown in Figure 4.5. The detailed description is as follows:

Step 1. Get the desired correcting power from the SO.

Step 2. Obtain the adjusted power. At first, classify DEWHs into Group 1 - 4. Then

$\Delta P_{adjust}(t)$ is generated by Equation (4.13).

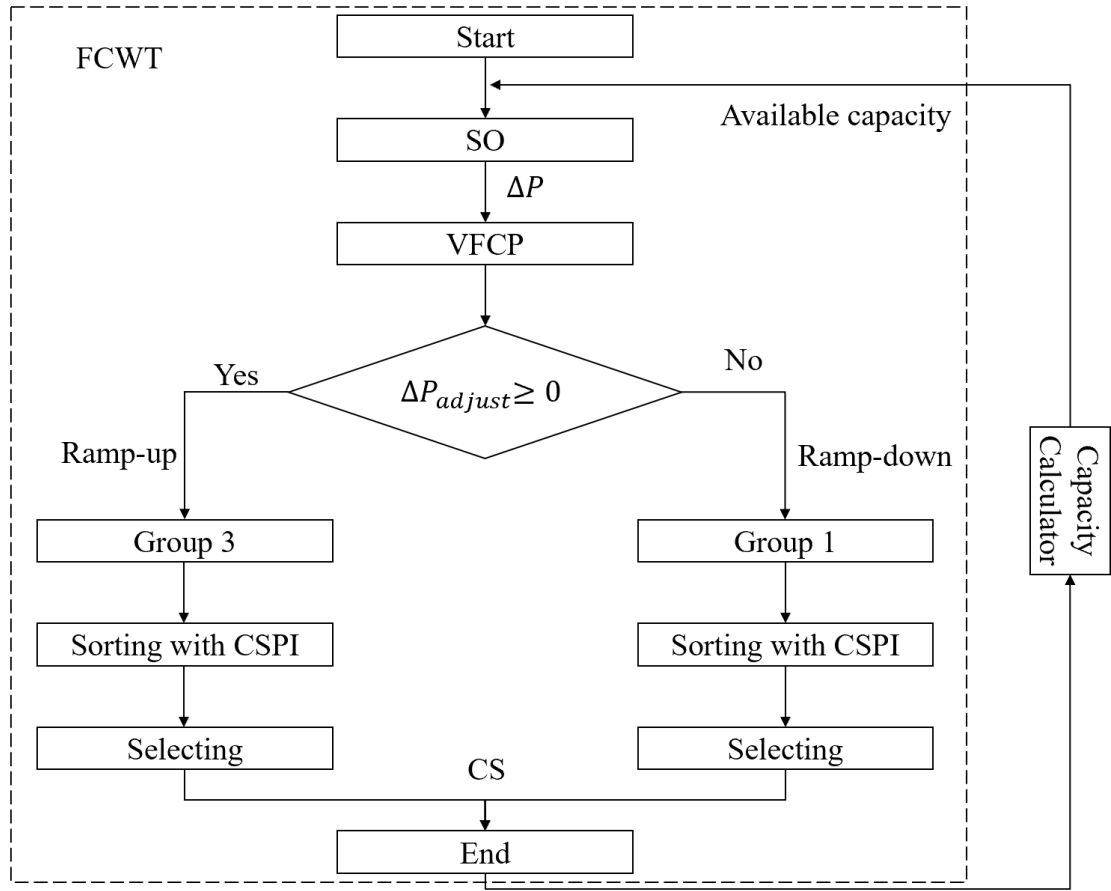


Figure 4.4 Schematic representation of FCWT

Step 3. If $\Delta P_{adjust}(t) \geq 0$, the VFCP power should be increased, go to Step 3.1; else, the VFCP power should be decreased, go to Step 3.2.

Step 3.1. Select DEWHs in Group 3 to respond to the positive $\Delta P_{adjust}(t)$,

- a). Sort the DEWHs of Group 3 according to their CSPIs by descending (Chapter 3 shows how to generate CSPI).

Algorithm: FCWT

Do

Step 1: Get the desired correcting power $\Delta P(t)$ from the SO.

Step 2: Obtain the adjusted power $\Delta P_{adjust}(t)$.

Step 3: If $\Delta P_{adjust}(t) \geq 0$, go to Step 3.1; else, go to Step 3.2.

Step 3.1: Select DEWHs in Group 3 for control.

- a). Sort DEWHs in Group 3 according to CSPIs by descending.
- b). Generate control actions.

Step 3.2: Select DEWHs in Group 1 for control.

- a). Sort DEWHs in Group 1 according to CSPIs by ascending.
- b). Generate control actions.

Step 4: Apply control actions to the VFPC; calculate and send available capacities.

End

Figure 4.5 Pseudocode of FCWT

b). Generate control actions for DEWHs in Group 3 by solving Equation (4.14).

These DEWHs with lower CSPIs have higher priorities to be turned on. The solution has the same process as shown in the Appendix I.

$$\begin{aligned} \min & \left| \Delta P_{adjust}(t) - \sum_{n=1}^{g3(t)} P_{rate,n} CS_n \right| \\ \text{s. t. } & \begin{cases} \text{if } CS_{n-1} = 1, CS_n = 1 \\ \text{if } CS_{n-1} = 0, CS_n = 0 \text{ or } 1 \end{cases} \end{aligned} \quad (4.14)$$

where $g3$ is the number of DEWHs in Group 3, and n means the n^{th} DEWH in the sorted order.

Step 3.2 Select DEWHs in Group 1 to respond to the negative $\Delta P_{adjust}(t)$.

- a). Sort the DEWHs of Group 1 according to their CSPIs by ascending.
- b). Generate control actions for DEWHs in Group 1 by solving Equation (4.15).

These DEWHs with higher CSPIs have higher priorities to be turned off.

$$\begin{aligned} \min & \left| \Delta P_{adjust}(t) + \sum_{l=1}^{g1(t)} P_{rate,l}(1 - CS_l) \right| \\ \text{s. t. } & \begin{cases} \text{if } CS_{l-1} = 0, CS_l = 0 \\ \text{if } CS_{l-1} = 1, CS_l = 0 \text{ or } 1 \end{cases} \end{aligned} \quad (4.15)$$

where $g1$ is the number of DEWHs in Group 1, and l means the l^{th} DEWH in the sorted order.

Step 4. Apply the generated control actions in Step 2 and Step 3 on the VFCEP. The available capacities (the maximum ramp-up and ramp-down power) are calculated with Equations (4.7) and (4.9). The SO will then receive the available capacities as references for the next desired correcting power.

4.3.2 Frequency Control with Adaptive Criterion

As shown in Equation (4.6), the maximum ramp-up power is increased with the increase in the cumulative power of these DEWHs of which the thermostats are on. Letting DEWHs be controlled off before their temperatures reach their upper temperature limits will

increase the maximum ramp-up power. However, when the VFCEP is responding to $\Delta P_{adjust} \geq 0$ in the FCWT, some DEWHs in Group 1 may reach their upper limits and the thermostats turn off. Coordinately controlling Group 1 and Group 3 (i.e., controlling them together to respond to a requirement) can help in avoiding the thermostats to turn off. Thus, the maximum ramp-up power can be increased.

An adaptive criterion, AEL_{adapt} , is proposed for the coordination between Group 1 and Group 3. When a relay of a DEWH is off and its AEL is lower than AEL_{adapt} , the DEWH must be turned on. The adaptive AEL_{adapt} should satisfy:

$$AEL_{tole} \leq AEL_{adapt} \leq 0 \quad (4.16)$$

The increased power of the DEWHs of which $AEL \leq AEL_{adapt}$ in Group 3 is P_{up} , and $P_{up} \geq \Delta P_{adjust}$. Then the DEWHs in Group 1 with high AELs are controlled to reduce the power by $(P_{up} - \Delta P_{adjust})$. Compared to the FCWT, both Group 1 and Group 3 are used for control, which avoids DEWHs to reach their upper limits. Hence, the maximum ramp-up power is increased due to the use of AEL_{adapt} .

As $AEL_{adapt} \geq AEL_{tole}$, the DEWHs are turned on to heat before their estimated temperatures drop to the tolerance temperatures. Hence, the adaptive AEL_{adapt} avoids the DEWH temperatures to drop too low.

From Equation (4.9), it is clear that the maximum ramp-down power (negative value) is

increased with the decrease in the cumulative power of the DEWHs in Group 4. As DEWHs are turned on when their AEL reach AEL_{adapt} , the cumulative power of DEWHs in Group 4 is reduced. The maximum ramp-down power is increased by AEL_{adapt} , and the detailed analysis is shown in Appendix II.

Hence, the available capacities for frequency control and the minimum temperature are increased with the adaptive AEL_{adapt} . A frequency control algorithm is proposed with AEL_{adapt} , which is called frequency control with adaptive criterion (FCWA) in this thesis.

Figure 4.6 is the schematic representation of the FCWA. Its pseudocode is shown in Figure 4.7. The detailed description is as follows:

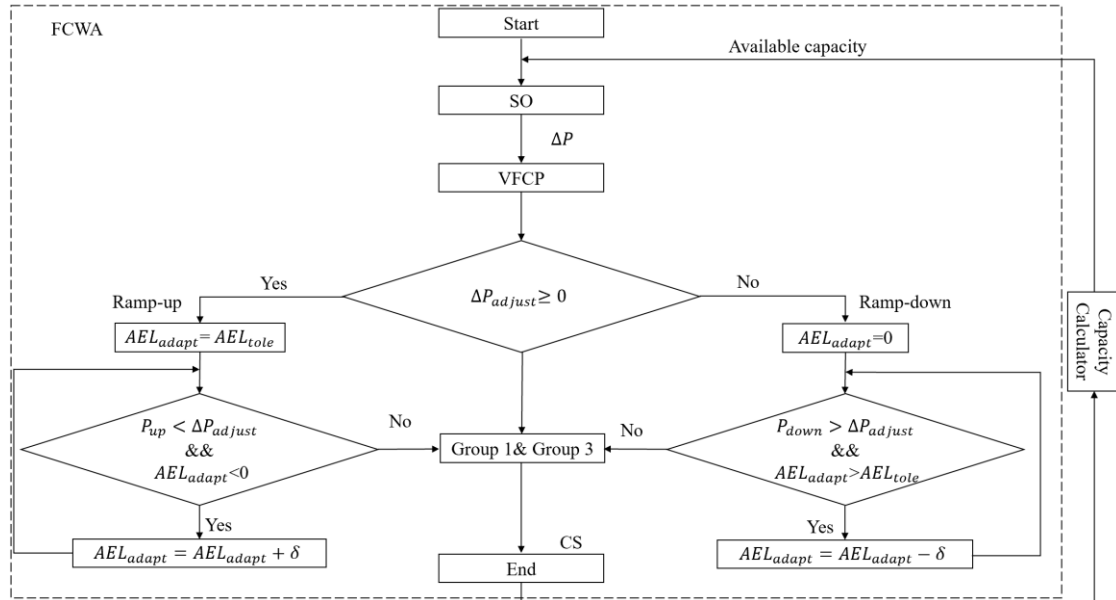


Figure 4.6 Schematic representation of FCWA

Algorithm: FCWA

Do

Step 1: Get the desired correcting power $\Delta P(t)$ from the SO.

Step 2: Adjust the adjusted power $\Delta P_{adjust}(t)$.

Step 3: If $\Delta P_{adjust}(t) \geq 0$, go to Step 3.1; else, go to Step 3.2.

Step 3.1: Set initial AEL_{adapt} as AEL_{tole} .

- a). Calculate the increased power, P_{up} .
- b). If $P_{up} < \Delta P_{adjust}(t)$ & $AEL_{adapt} < 0$, update AEL_{adapt} , repeat a); else, go to c).
- c). Generate control signals for these DEWHs with $AEL \leq AEL_{adapt}$, then go to Step 4.

Step 3.2: Set initial AEL_{adapt} as zero.

- a). Calculate the decreased power, P_{down} .
- b). If $P_{down} > \Delta P_{adjust}(t)$ & $AEL_{adapt} > AEL_{tole}$, update AEL_{adapt} , go to a); else, go to c).
- c). Generate control signals for these DEWHs with $AEL \leq AEL_{adapt}$, then go to Step 4.

Step 4: Select DEWHs for control.

Step 5: Apply control actions to the VFCEP; calculate and send the available capacities.

End

Figure 4.7 Pseudocode of FCWA

Step 1. – Step 2. The same with Step 1- Step 2 in the FCWT.

Step 3. If the $\Delta P_{adjust}(t) \geq 0$, the VFCEP power should be increased, go to Step 3.1; else, the VFCEP power should be decreased, go to Step 3.2.

Step 3.1. Increase the VFCEP power to respond to a positive $\Delta P_{adjust}(t)$. At first, the initial value of the adaptive AEL_{adapt} is set as the minimum value, AEL_{tole} .

a). Calculate the increased power, P_{up} , which is the total demand of DEWHs with off relays and $AEL_{tole} \leq AEL \leq AEL_{adapt}$.

$$P_{up} = \text{sum}(\mathbf{P}.*((\mathbf{AEL} \geq AEL_{tole}) \& (\mathbf{AEL} \leq AEL_{adapt}) \& (\mathbf{RS} == 0))) \quad (4.17)$$

where $\mathbf{P} = [P_{rate,1}, P_{rate,2}, \dots, P_{rate,N}]^T$, which is the rated power of each DEWH in the VFCEP. N is the number of DEWHs in the VFCEP. $\mathbf{RS} = [RS_1, RS_2, \dots, RS_N]^T$, which shows the relay state of each DEWH. $\mathbf{AEL} = [AEL_1, AEL_2, \dots, AEL_N]^T$, which shows the AEL of each DEWH.

b). If $P_{up} < \Delta P_{adjust}(t)$ and $AEL_{adapt} < 0$, update AEL_{adapt} with Equation (4.18) to increase P_{up} .

$$AEL_{adapt} = AEL_{adapt} + \delta \quad (4.18)$$

where δ is set as 0.1 in the thesis.

If $P_{up} \geq \Delta P_{adjust}(t)$ or $AEL_{adapt} = 0$, go to c).

c). Select the DEWHs of which relays are off and their AEL s between AEL_{tole} and AEL_{adapt} . These DEWHs are candidates for on-signals. Two kinds of controllable DEWHs are classified: 1). DEWHs of which relays are off and AEL s are higher than AEL_{adapt} ; and 2). DEWHs of which relays are on and AEL s between 0 and 1 (Group 1). An objective for the two kinds of DEWHs is calculated by Equation (4.19), and then go to Step 4.

$$P_{obj}(t) = \Delta P_{adjust}(t) - P_{up} \quad (4.19)$$

Step 3.2. Decrease the VFCEP power to respond to a negative $\Delta P_{adjust}(t)$. At first, the initial value of the adaptive AEL_{adapt} is set as zero.

a). Calculate the decreased power P_{down} , which consists of two parts, and can be written as:

$$P_{down} = -P_1 + P_{up} \quad (4.20)$$

where P_1 is the power of these DEWHs of which relays are on and their AELs are not negative (DEWHs of which in Group 1). It can be expressed as:

$$P_1 = \text{sum}(\mathbf{P}.* ((\mathbf{AEL} \geq 0) \& (\mathbf{AEL} < 1) \& (\mathbf{RS} == 1))) \quad (4.21)$$

P_{up} is the increased power of these DEWHs of which relays are off and their AELs between AEL_{tole} and AEL_{adapt} , as shown in Equation (4.17).

b). If $P_{down} > \Delta P_{adjust}(t)$ and $AEL_{adapt} > AEL_{tole}$, decrease the AEL_{adapt} to reduce the increased power P_2 with:

$$AEL_{adapt} = AEL_{adapt} - \delta \quad (4.22)$$

If $P_{down} \leq \Delta P_{adjust}(t)$ or $AEL_{adapt} = AEL_{tole}$, go to c).

c). The same with Step 3.1.c).

Step 4. Generate control signals for the controllable DEWHs. If the $P_{obj}(t) \geq 0$, the power of these DEWHs should be increased, go to Step 4.1; else, the power should be decreased, go to Step 4.2.

Step 4.1. If $P_{obj}(t) \geq 0$, more DEWHs should be sent on-signals to increase the VFPC power. These DEWHs of which relays are off and AELs are higher than AEL_{adapt} are sorted in a descending order by their CSPIs. Solving Equation (4.23) to generate control actions for these sorted DEWHs.

$$\begin{aligned} \min & \left| P_{obj}(t) - \sum_{i=1}^{k1(t)} P_{rate,i} CS_i \right| \\ \text{s. t. } & \begin{cases} \text{if } CS_{i-1} = 1, CS_i = 1 \\ \text{if } CS_{i-1} = 0, CS_i = 0 \text{ or } 1 \end{cases} \end{aligned} \quad (4.23)$$

where $k1$ is the number of DEWHs in the order, and i means the i^{th} DEWHs.

Step 4.2. If $P_{obj} < 0$, more DEWHs should receive off-signals to decrease the VFPC power. These DEWHs with on relays and $AEL > 0$ are selected for control (DEWHs of which in Group 1), they are sorted in an ascending order by their CSPIs. Solving Equation (4.24) to generate control actions for these sorted DEWHs.

$$\begin{aligned} \min & \left| P_{obj}(t) + \sum_{i=1}^{g1(t)} P_{rate,i} (1 - CS_i) \right| \\ \text{s. t. } & \begin{cases} \text{if } CS_{i-1} = 0, CS_i = 0 \\ \text{if } CS_{i-1} = 1, CS_i = 0 \text{ or } 1 \end{cases} \end{aligned} \quad (4.24)$$

where $g1$ is the number of DEWHs in the order, and i means the i^{th} DEWHs.

Step 5. The same with Step 4 of FCWT.

4.4 Case Study Results

In this Section, case studies with 20,000 DEWHs were used to validate the proposed frequency control methods. These DEWHs had the same parameters and hot-water consumption settings as those in Chapter 3. An IEEE 34-node test feeder [103] is a typical test model in the power system analyses and therefore was employed in the case studies. The diagram of the test feeder is shown in Figure 4.8. Load and renewable generation data were from the Pennsylvania-New Jersey-Maryland Interconnection (PJM) [104]. The electricity consumption of the VFCE takes up 6.4% of the total energy demand of the whole test feeder. The transient stability analysis tool of CYME, a power engineering software, was used to show the frequency deviations. The simulation time step of CYME is 0.0167 seconds.

The operation states of power systems can be divided into the normal and contingency states. The frequency control services are required to maintain or restore power systems to the normal state. Figure 4.9 shows the relationships between states and the required services [105], [106]. The normal state is characterized by the satisfaction of the equality and inequality constraints, and by a sufficient level of stability margins in transmissions and generations [105], [106]. The system has the ability to defend a single contingency event (such as a generator lost) [105].

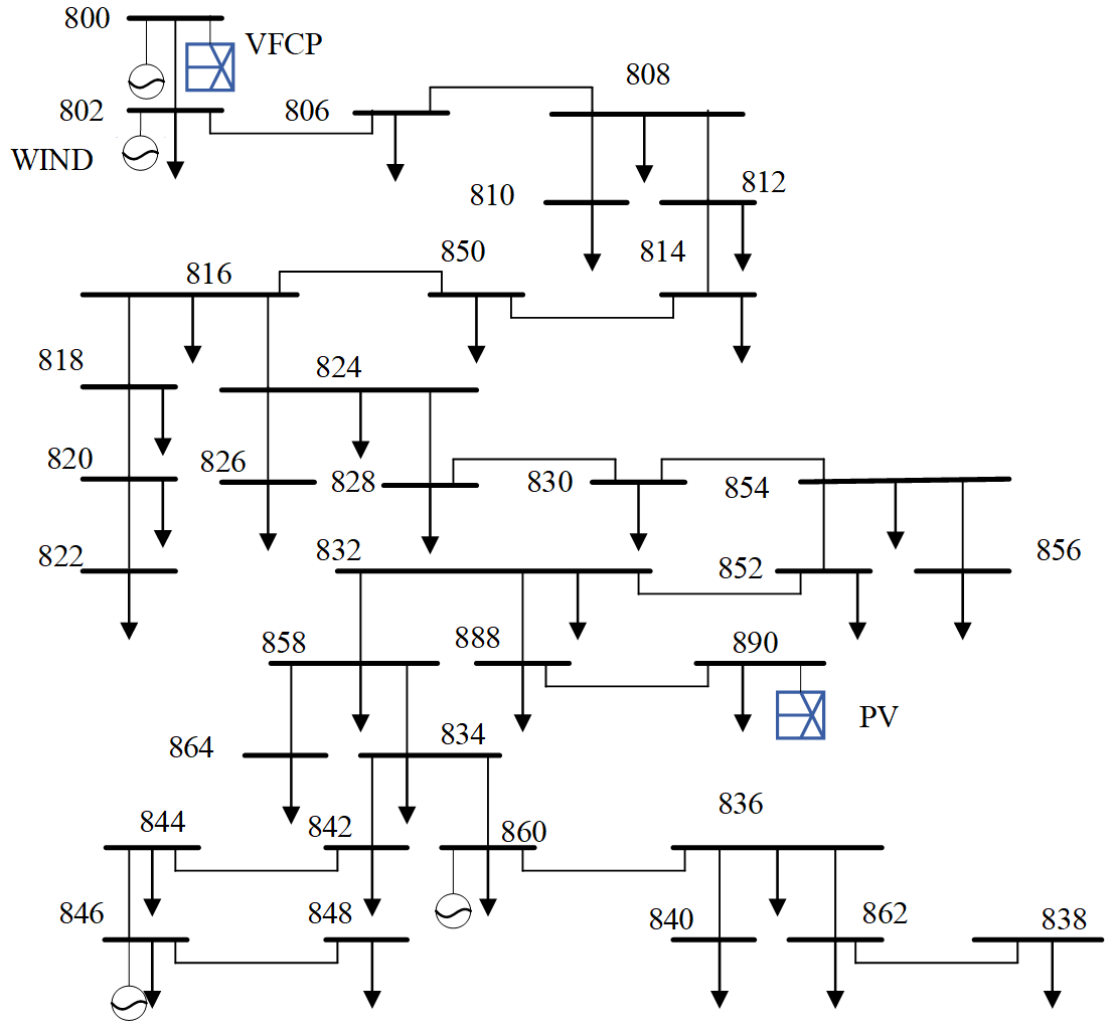


Figure 4.8 Diagram of IEEE 34-bus system

The normal state can be classified into the normal secure state and normal insecure state [106]. During the normal insecure state, all operating inequality constraints are still satisfied but the power system is vulnerable to contingencies. There are four basic types of inequality constraints in power systems: the generator real power limit, generator reactive power limit, load bus voltage limit, and line flow constraint, as shown in Equation (4.25).

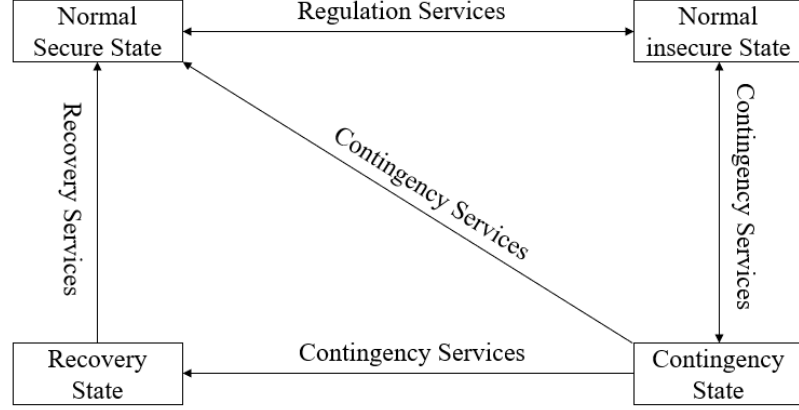


Figure 4.9 Power system operation states and required services

$$\begin{cases} P_{g,min} \leq P_g \leq P_{g,max} \\ Q_{g,min} \leq Q_g \leq Q_{g,max} \\ V_{bus,min} \leq V_{bus} \leq V_{bus,max} \\ I_{min} \leq I \leq I_{max} \end{cases} \quad (4.25)$$

where P_g , Q_g , V_{bus} , and I are the generator real power, generator reactive power, load bus voltage, and line flow respectively. $P_{g,min}$ and $P_{g,max}$ are the minimum and maximum real power generation of the generator. $Q_{g,min}$ and $Q_{g,max}$ are the minimum and maximum reactive power generation of the generator. $V_{bus,min}$ and $V_{bus,max}$ are the minimum and maximum voltage limitations of the bus. I_{min} and I_{max} are the minimum and maximum flow limitations of the bus. Regulation services are required to restore the system to its normal secure state.

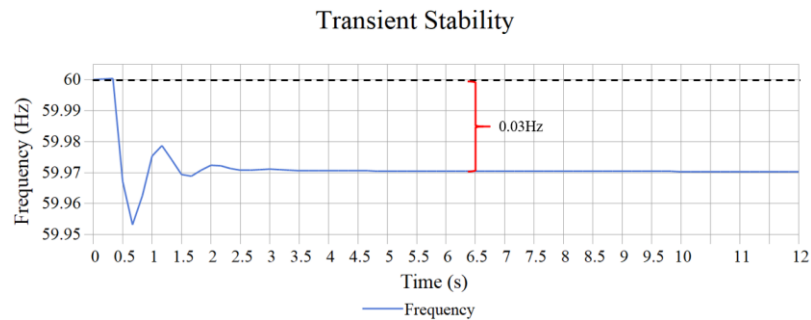
When these operating inequality constraints are not satisfied, the power system is operated in a contingency state, and contingency services are required to correct and bring the power system into a normal state. When the system is under a recovery state, recovery services are required to bring the system into a normal state. In this thesis, the VFCP that provides

SFC services are analyzed for both normal and contingency conditions.

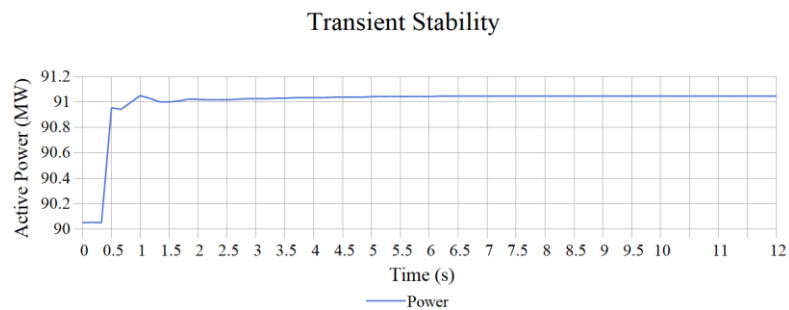
4.4.1 Frequency Control Under Normal Conditions

4.4.1.1 For Renewable Generation

The renewable generation fluctuates in practice. When an amplitude of -1 MW fluctuation occurs, the grid frequency drops by 0.03 Hz (on Bus 800) as shown in Figure 4.10(a). Other on-line generators increase their generations to match the fluctuation, and the total generation is shown in Figure 4.10(b). The increased generation is 1MW, and the response time is less than 2 seconds. However, the reserve from on-line generators is reduced. The



(a)

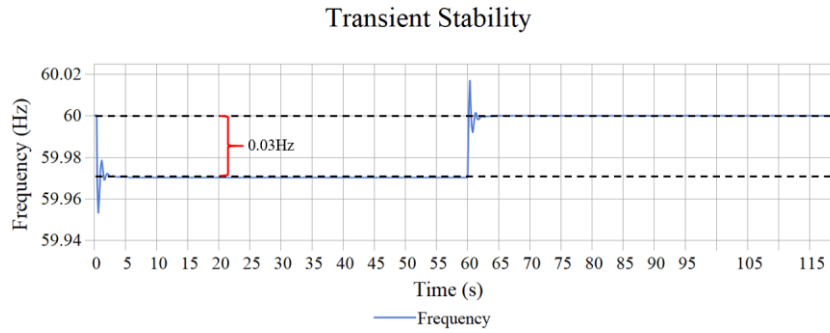


(b)

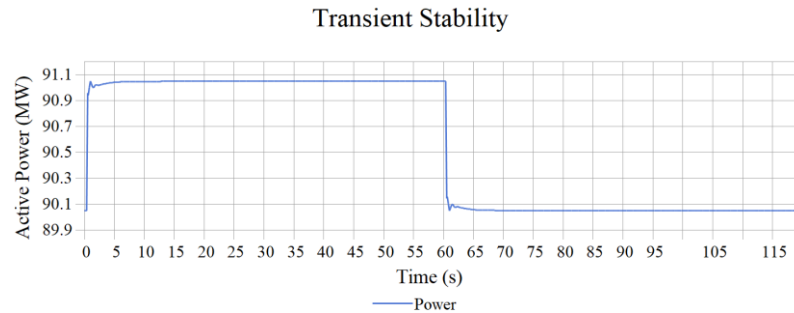
Figure 4.10 Frequency and generation without the VFCEP in CYME

system is in the normal state with less security due to the grid frequency deviation.

Figure 4.11(a) shows the grid frequency has been restored to its nominal value (60 Hz), with the VFCP. The generation of on-line generators is shown in Figure 4.11(b). It is clear that the total generation of other generators is recovered to the previous value, and the reserve that used by the PFC is released. The system security is recovered.



(a)



(b)

Figure 4.11 Frequency and generation with the VFCP in CYME

Next, the VFCP is used to compensate the power mismatch between the actual and forecasted generation along time. The renewable generation data from PJM is shown in Figure 4.12. The actual renewable generation is lower than the forecast generation in most

of the times.

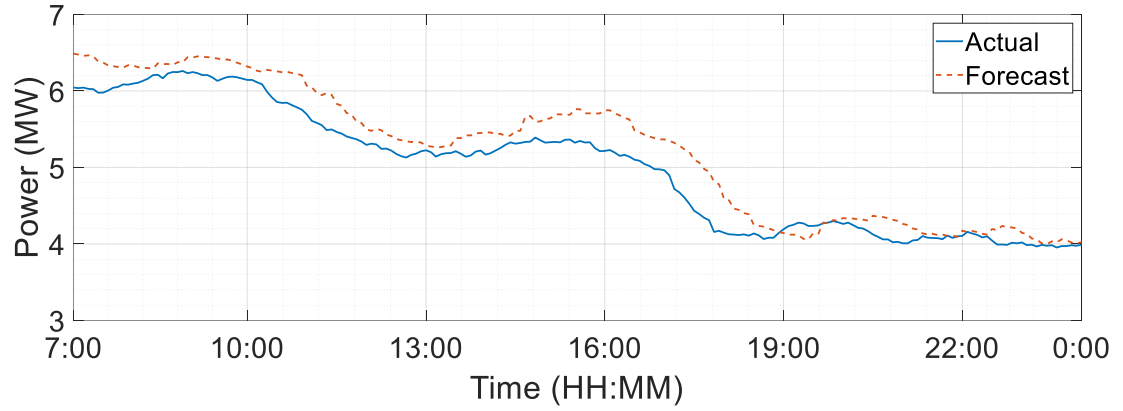


Figure 4.12 Actual and forecast renewable generation

Grid frequency deviations are caused by the power mismatches between the actual and forecasted renewable generations. Then the SO requires the VFCEP to recover the mismatches to maintain the grid frequency. The Ref in Figure 4.13 is the reference power for the VFCEP to match the mismatches. The VFCEP keeps discharging when the actual generation is lower than the forecast generation, and vice versa.

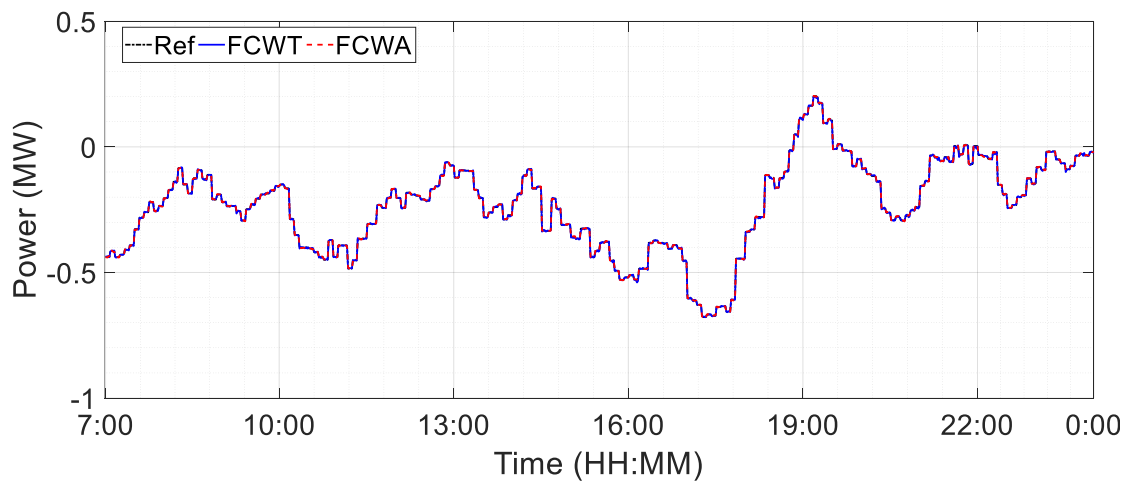


Figure 4.13 Charging/discharging power of the VFCEP

Figure 4.14 presents the tracking errors to distinguish the tracking results of the FCWT and FCWA. The tracking errors are minor compared to the total demand of the VFCEP. The tracking errors of the FCWA are smaller than the errors of the FCWT. Root-mean-square (RMS) power tracking error as a percentage of the total steady-state power consumption [107] is selected to evaluate the tracking performance, given by:

$$RMS = \frac{\sqrt{\frac{1}{L} \sum_{i=1}^L (P_{actual,i} - P_{Ref,i})^2}}{P_{avg}} \quad (4.26)$$

where $P_{actual,i}$ is the actual power demand of the i^{th} sample, P_{Ref} is the reference power demand, L is the length of the tracking duration, and P_{avg} is the average actual power demand of the duration. The FCWT and FCWA have similar RMS values (0.034% for the FCWT and 0.025% for the FCWA), which are very small.

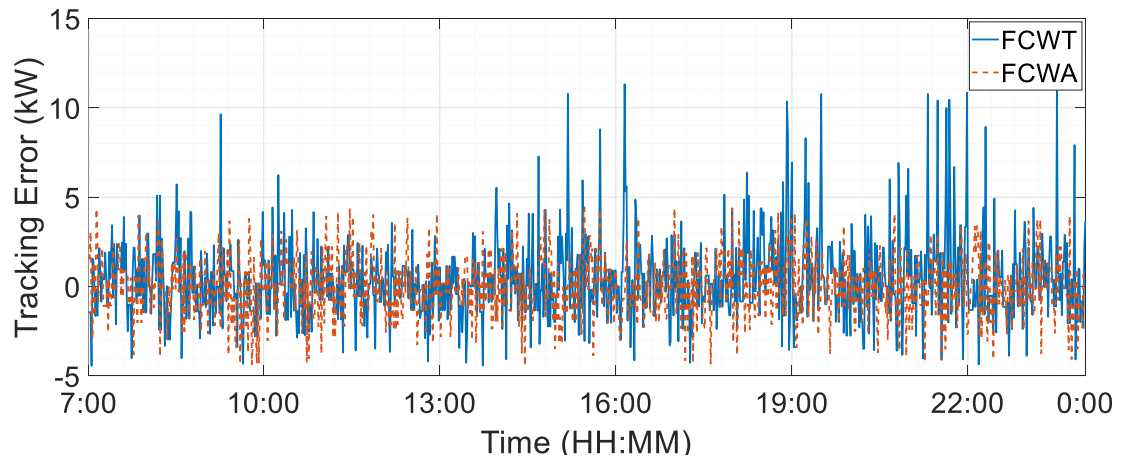


Figure 4.14 Tracking errors of the two proposed algorithms

As stated in Section 4.3.2, the available capacities of the FCWA are larger than the FCWT, this statement is verified by the results shown in Figure 4.15. As the ramp-down power is provided by turning off DEWHs in the VFCP, the maximum ramp-down power should be limited to the VFCP demand (the cumulative power of DEWHs in Group 1 and Group 2, but only DEWHs in Group 1 can be turned off). The VFCP demand depends on the baseline and the committed reserve for services. The baseline is unchanged during control; the committed reserve for services depends on the requirements from the SO, which is also unchanged by control. Therefore, the VFCP demand should not be changed by control actions. Hence, the ramp-down capacities of the FCWT and FCWA are both limited during control, as shown in Figure 4.15. The FCWA controls more DEWHs in Group 1 to increase the available capacity, but the increase is limited.

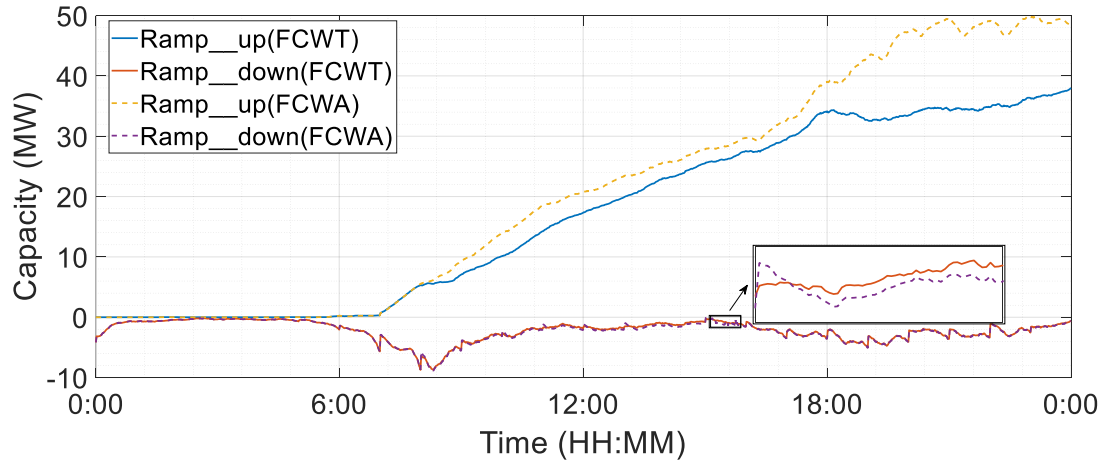


Figure 4.15 Available capacities of the VFCP

The ramp-up power is provided by turning on DEWHs in the VFCP, and the maximum ramp-up power depends on the cumulative power of controllable DEWHs in the VFCP. With the proposed algorithms, more DEWHs can be controllable, which increases the

ramp-up power. As shown in Figure 4.15, the FCWA has more ramp-up capacity than the FCWT.

If all the DEWHs are controllable, the ramp-up power is maximum. However, we cannot control all the DEWHs in the VFCEP at the same time, because DEWHs are controlled based on the estimated information with the worst case assumptions. DEWHs may be heated to their upper limits before being controlled off (these DEWHs become uncontrollable). Hence, the ramp-up power should be limited too.

It is noted that the DEWHs in the VFCEP need to be fully heated to eliminate the estimate errors during control in off-peak periods (as shown in Chapter 3 to eliminate the estimated errors from the unexpected hot-water consumption). This is necessary for maintaining the end-user comfort without temperature measurements. Then the ramp-up and ramp-down capacities will be decreased during the off-peak periods (from 11 pm to 7 am as shown in Chapter 3). When a DEWH is fully heated, it can be used to provide service again when its thermostat reaches its lower limit.

When the VFCEP is employed as an SFC reserve resource, the mismatches between the actual and forecast renewable generations can be compensated with both proposed control algorithms. The VFCEP helps to smooth the fluctuations caused by renewable generations, with no additional reserves required.

4.4.1.2 Regulation Services

Regulation services correct for short-term deviations that might affect the stability of the power system. The minute-to-minute deviations between generations and loads are reduced and eventually eliminated by regulation services. These deviations come from generations and loads in practice. For the test model, the required regulation service capacities are 800 kW (4 am to 8 am and 4 pm to 0 am) and 525 kW (other durations) [104], which are shown as the Up and Down lines in Figure 4.16. The test regulation signals from PJM [104] are used to test the frequency regulation services from the VFCEP using the two proposed algorithms.

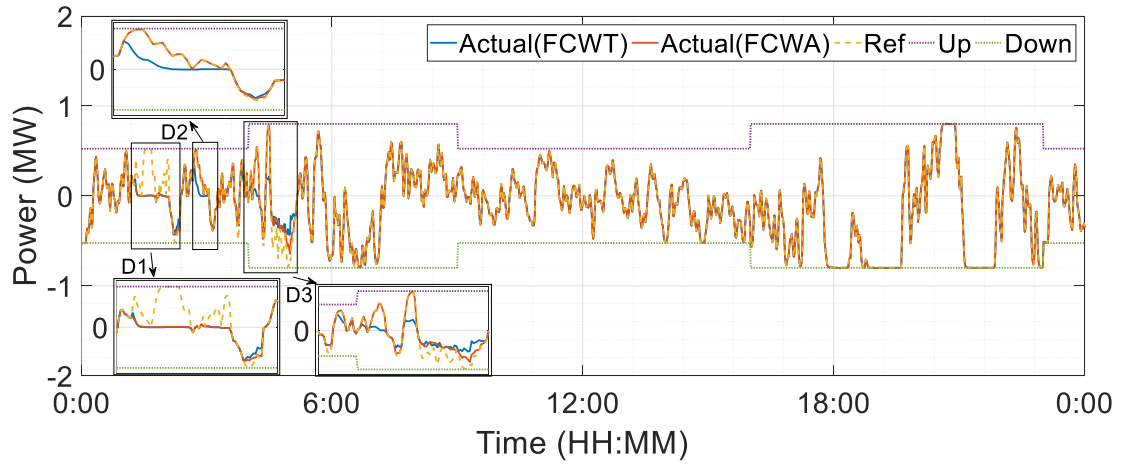


Figure 4.16 Regulation services by the VFCEP

The results presented in Section 3.5.1 illustrates that the demand of DEWHs before 6:00 is small, the minimum demand can be low to 0.37 MW, which is lower than the required regulation capacity. Hence, the available capacities may not meet the objectives.

The Actual (FCWA) line in Figure 4.16 shows the charging/discharging power of the

VFCP by the FCWA. With Equation (4.27), the RMS value of FCWA is about 1.14% and 1.75% for FCWT, the FCWA has a smaller error. With FCWA, there are two durations (D1 and D3) in which the VFCP cannot provide enough capacities to respond to the objectives for regulation. The Actual (FCWT) line is the result of the FCWT. There are three durations (D1, D2, and D3) in which the VFCP cannot provide enough capacities to respond to the objectives for regulation. Except for these durations, the VFCP closely tracks the desired correcting power to provide regulation services.

Figure 4.17 shows the available ramp-up and ramp-down capacities that are sent to the SO. During D1, the available ramp-up capacities for both algorithms are almost zero. During D2, the available ramp-up capacity is almost zero for the FCWT, but the FCWA has enough capacities to respond to the objectives. During D3, the ramp-down capacities of both algorithms cannot meet the requirements at the half part, and the FCWA has more capacity in the first half part. The ramp-up capacity of the FCWA is more than the requirements for

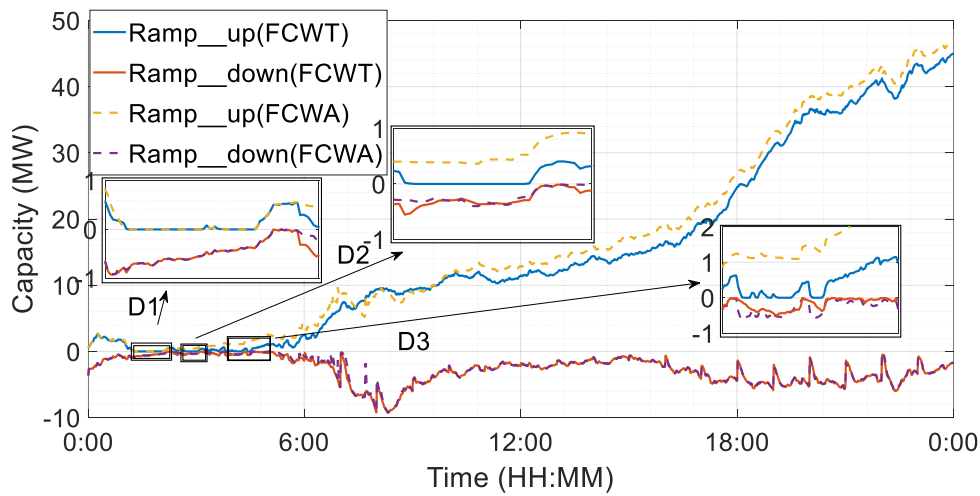


Figure 4.17 Available ramp-up and ramp-down capacities

regulation, but the FCWT does not have enough ramp-up capacity in some areas. Hence, the FCWA has more available capacities for frequency control than the FCWT based on the same initial conditions. The available capacities for frequency control are increased by the adaptive AEL_{adapt} .

Although the proposed FCWA algorithm increases the available capacity, the power demand of the VFCP before 6:00 am is small and the available capacities are still not enough. This is because the DEWHs become uncontrollable after the thermostats are automatically turned off. Nonetheless, the ramp-up and ramp-down capacities can be increased by including more DEWHs in the VFCP.

Except for the durations D1, D2 and D3, the two algorithms have enough ramp-up and ramp-down regulation capacities. The VFCP tracks the reference power and provides regulation services.

The frequencies of the test model (on Bus 800) with the deviations between generations and loads are shown in Figure 4.18. Without the VFCP to provide SFC (woVFCP), the generators provide the PFC and maintain the frequency by consuming reserves from on-line generators. The FCWT (wFCWT) and FCWA (wFCWA) maintain the grid frequency by providing frequency control services with the VFCP. The FCWA outperforms the other two cases with lower frequency deviations.

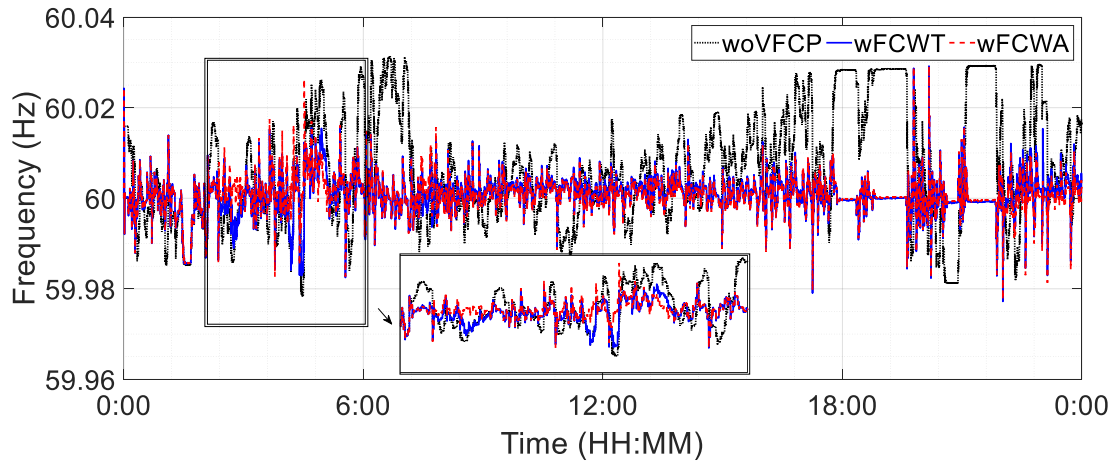


Figure 4.18 Frequency of the test model

Figure 4.19 shows the maximum temperature drop in each case (minimum temperature minus the lower limit). The $\min T(\text{FCWA})$ is the maximum temperature drop with the FCWA, $\min T(\text{FCWT})$ is the maximum temperature drop with the FCWT, and $\min T$ is the maximum temperature drop without any control actions. It is clear that the $\min T(\text{FCWT})$ and $\min T$ are closed to each other. The maximum temperature drop with the FCWA is less

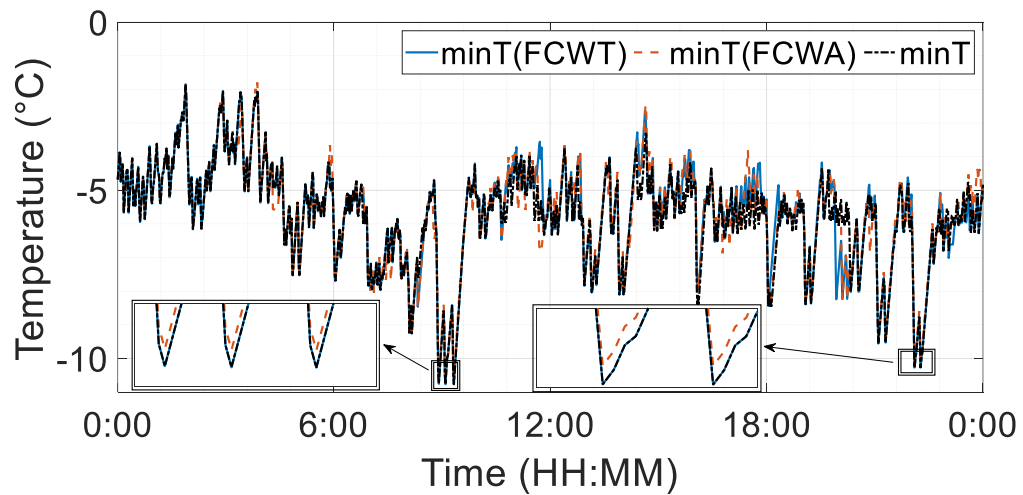


Figure 4.19 Maximum temperature drop during regulation

than the other two cases. Hence, the FCWA helps to maintain the end-user comfort.

Therefore, the FCWA not only enables more available capacities for frequency control, but also reduces the maximum temperature drop for maintaining end-user comfort.

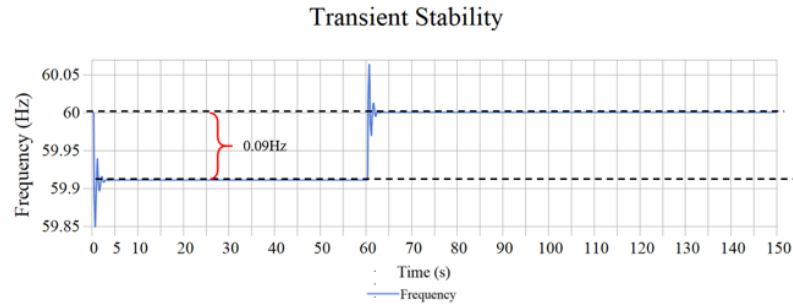
4.4.2 Frequency Control Under Contingency Conditions

The VFCP can be used to restore the grid frequency for contingency events. In general, the contingency services are required to provide services for at least 30 minutes.

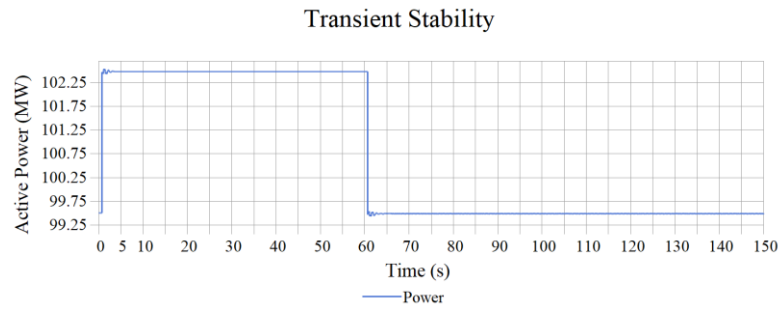
Figure 2.20 shows an example of using the VFCP to provide frequency control services under a contingency condition. The contingency event is 3MW generation loss on Bus 846 at 7:30, leading to a 0.074 Hz frequency drop. The grid frequency is restored to the nominal value by the VFCP. Figure 4.20(b) shows the total generation of other on-line generators is increased when the generator is lost. The total generation is recovered to the previous value when the VFCP starts to provide contingency services.

Figure 4.21 shows the VFCP is discharged by 3 MW for 0.5 hours from 7:30 am to 8 am with the proposed algorithms FCWT and FCWA. Both algorithms provide enough capacity for frequency control services under the contingency condition.

The available ramp-up and ramp-down capacities are shown in Figure 4.22. There still are enough capacities for other ancillary services, such as regulation services. The available



(a)



(b)

Figure 4.20 Frequency and generation in CYME after a contingency event

capacities of the FCWA are more than that of the FCWT.

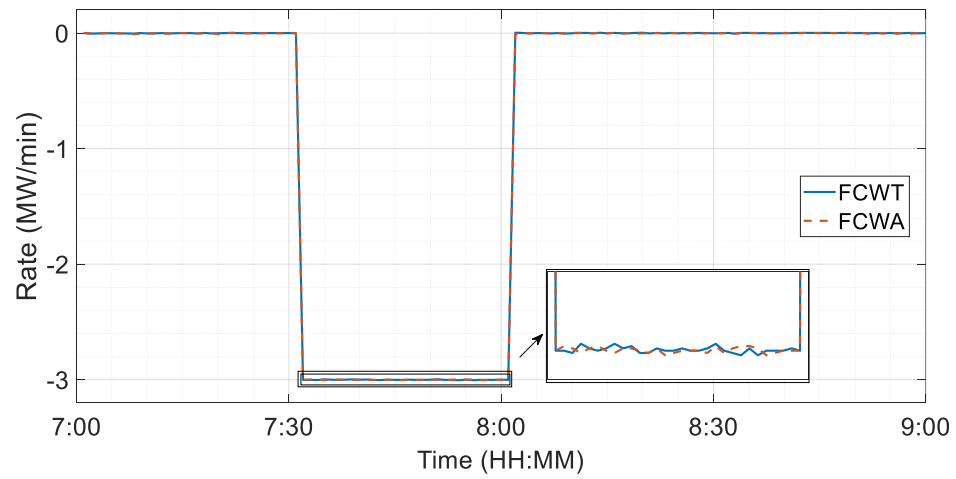


Figure 4.21 Discharging power of the VFCEP for the contingency event

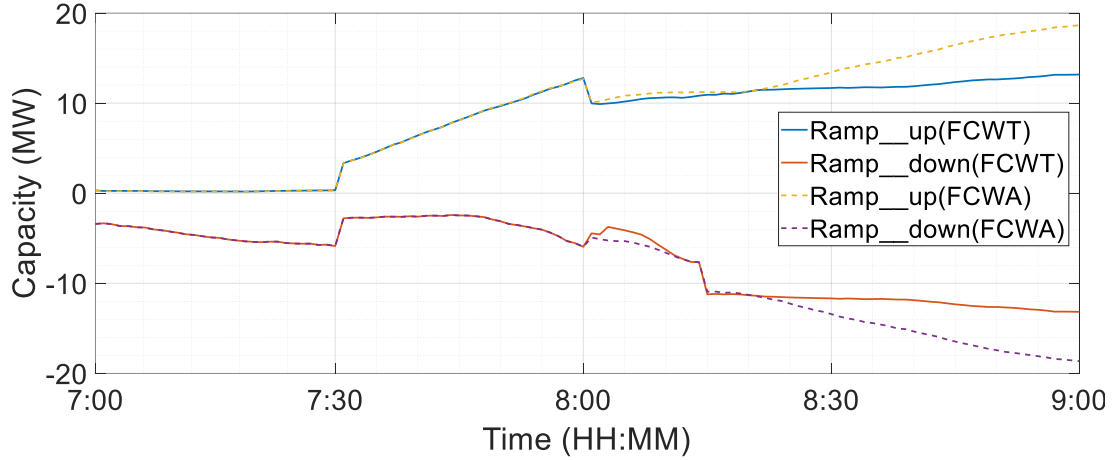


Figure 4.22 Available capacities of the VFCP

4.5 Conclusion

This chapter proposes a framework, VFCP, for frequency control. The VFCP sends available ramp-up and ramp-down capacities to the SO, and responds to the desired correcting power from the SO to maintain the grid frequency. The control actions are selected based on the state estimation method in Chapter 2, without requirements of temperature measurements.

Two control algorithms are proposed for VFCP to provide frequency control services with direct DEWH control. Due to the communications and control delays in more than seconds, the VFCP is used for SFC only. FCWT directly selects DEWHs of which in Group 1 and Group 3 to respond to the desired correcting power from the SO. FCWA allows more DEWHs' temperatures to be close to their lower limits with an adaptive AEL_{adapt} , thus increasing the available capacities for frequency control and benefiting the end-user comfort.

5 Conclusions and Future Work

5.1 Summary of this Thesis

This thesis investigated the potential of using conventional DEWHs with an external control relay to provide power system services including peak shaving and frequency control, without temperature measurements.

A state estimation method for individual DEWHs without temperature measurements was proposed in Chapter 2. Based on hot-water consumption patterns and worst case assumptions, the hot-water consumption activity was identified with a fuzzy logic membership function. Then residual hot-water above of the identified activity was treated as drawn out with an average flow rate. The DEWH temperature was estimated based on the activity, average flow rate and relay state. The estimated temperature was used in the control algorithms for peaks shaving and frequency control.

Chapter 3 presented a method that allowed DEWHs to reduce peak demand without temperature measurements. The DEWH temperatures were estimated by using the state estimation method in Chapter 2. A proposed index—CSPI was introduced to show the control priority of DEWHs with the estimated DEWH temperature and subsequent hot-water consumption. The end-user comfort was maintained during the control.

Chapter 4 presented two frequency control algorithms using conventional DEWHs without

temperature measurements. DEWHs were aggregated as a frequency control resource to provide frequency control services in an aggregated way. The VFCEP consisted of DEWHs, a centralized controller, and a capacity calculator. DEWHs were classified into different groups based on their thermostat states, relay states, and AELs. FCWT responded to the desired correcting power by turn on DEWHs in Group 3 or turn off DEWHs in Group 1. FCWA was based on FCWT, with the adaptive AEL_{adapt} . FCWA allow more DEWHs' temperature to be close to their lower limits, which increased the available capacities for frequency control and benefitted the end-user comfort.

5.2 Conclusions

The main contributions of the thesis include state estimation and control methodologies to enable conventional DEWHs to provide peak shaving and frequency control services. The conclusions and contributions are summarized as follows:

- (1) The end-user comfort is maintained without temperature measurements during control, which helps to recruit more end-users for deploying the proposed algorithms in practice.
- (2) The proposed algorithms minimize the impact of the uncertainty and randomness of hot-water consumption on temperature estimation. The randomness of hot-water behaviors are normal in practice, which may lead to a lower temperature. This is critical for any direct load control methods for conventional DEWHs without temperature measurements.

- (3) The CSPI is proposed to determine the control priority of DEWHs, which is based on the cumulative heating duration of each DEWH. Then, the control priority can be used to maintain the end-user comfort with minimized relay switching actions. The CSPI employs the heating duration instead of temperature information, which removes the requirements of temperature measurements during control. The impact of hot-water consumption is taken into consideration in the CSPI, which helps to control effectively.
- (4) A control algorithm for peak shaving is proposed based on the CSPI. An experimental demonstration verifies the effectiveness in peak shaving. The peak demands are reduced by 24.0% for morning peaks and 31.3% for evening peaks. The case study results also show the end-user comfort is maintained during control.
- (5) The VFCEP framework is proposed to aggregate and manage DEWHs as a centralized frequency control resource. VFCEP can participate in the electricity market as an individual service provider for bidding and providing services. The VFCEP generates frequency control reserves by make full use of DEWHs instead of adding online generators, which saves costs and benefits to utilities.
- (6) Two control algorithms, FCWA and FCWT, are proposed in the VFCEP framework to provide the SFC. The proposed algorithms help to reduce and eventually eliminate the frequency deviations. The FCWA with an adaptive criterion have more available capacities for frequency control than the FCWT.

5.3 Future Work

There are many avenues to continue the work in this thesis. The future researches include:

- The worst case assumptions in Chapter 2 are used to estimate the lowest temperature. More accurate analyses on worst cases are required, which helps make full use of the available capacity from DEWHs.
- Based on the development of communication technologies, more and more data become available for making long-term load forecasts of aggregated DEWHs. Then long-term objectives can be optimized and scheduled.
- Hot-water consumption analyses and forecasts are required to prepare sufficient thermal energy for end-user, which help make full use of the capacity form DEWHs and maintain the end-user comfort. Machine learning based approaches and other advanced algorithms can be used to analyze and forecast the hot-water consumption.
- DEWH states should be identified to make accurate control actions. With the increasingly available data, load identification methods can be improved in future.

References

- [1] Ebrhim Vaahedi, “Power system generation load balance,” in *Practical Power System Operation*, Ltd, Mar. 2014, pp. 105–118.
- [2] *Global Energy & CO2 Status Report, the Latest Trends in Energy and Emissions in 2018*, International Energy Agency, Paris, France, Mar. 2019.
- [3] Z. Wang and S. Wang, “Grid power peak shaving and valley filling using vehicle-to-grid systems,” *IEEE Trans. Power Deliv.*, vol. 28, no. 3, pp. 1822–1829, Jul. 2013.
- [4] *Intermittency Analysis Project: Appendix B, Impact of Intermittent Generation on Operation of California Power Grid*, GE Energy Consulting, Report CEC-500-2007-081-APB, 2007.
- [5] C. C. Zhou, “Thermal, power and electrical engineering ,” *2013 2nd International Conference on Energy and Environmental Protection (ICEEP 2013)*, April 19 - 21, 2013, Guilin, China. pp. 1-5.
- [6] Michael Lippert, Saft, “Key steps must be followed to find the optimum sized megawatt-scale Li-ion energy storage system for a large wind or solar plant,” *Energy Storage, Renewable Energy, Solar*, vol.22, no. 9, Sept. 2017, pp. 26-27.
- [7] H. Yang, S. Yang, Y. Xu, E. Cao, M. Lai, and Z. Dong, “Electric vehicle route optimization considering time-of-use electricity price by learnable Partheno-genetic algorithm,” *IEEE Trans. Smart Grid*, vol. 6, no. 2, pp. 657–666, Mar. 2015.
- [8] Severin Borenstein, Michael Jaske, Arthur Rosenfeld, “*Dynamic pricing, advanced metering, and demand response in electricity markets*, ” Univ. California Energy Ins., Berkeley, California, Oct. 2002.
- [9] *20% Wind Energy by 2030 Increasing Wind Energy's Contribution to U.S. Electricity*

- Supply*, Natl. Renew. Energy Lab. NREL US Dep. Energy Renew. Energy Consult. Serv. Energy. Inc., Dec. 2008.
- [10] *About Renewable Energy*, Natural Resources Canada, [Online] Available: <https://www.nrcan.gc.ca/energy/energy-sources-distribution/renewables/about-renewable-energy/7295>.
- [11] J. Sun, M. Li, Z. Zhang, T. Xu, J. He, H. Wang, G. Li, “Renewable energy transmission by HVDC across the continent: system challenges and opportunities,” *CSEE J. Power Energy Syst.*, vol. 3, no. 4, pp. 353–364, Dec. 2017.
- [12] Arthouros Zervos, “Renewables 2019 global status report, a comprehensive annual overview of the state of renewable energy,” REN21, *Renewables Now, Wien Energies Solar Thermal System*, Vienna, Austria, 2019.
- [13] *Renewables 2020 Analysis and Forecasts to 2025*, International Energy Agency, Paris, France, May 2020.
- [14] Kerry Thoubboron, “The Advantages and Disadvantages of Renewable Energy,” *Energy Sage*, Oct. 25, 2018.
- [15] M. Liu, F. L. Quilumba, and W. Lee, “Dispatch scheduling for a wind farm with hybrid energy storage based on wind and LMP forecasting,” *IEEE Trans. Ind. Appl.*, vol. 51, no. 3, pp. 1970–1977, May 2015.
- [16] S. Buhan, Y. Özkazanç, and I. Çadircı, “Wind pattern recognition and reference wind mast data correlations with NWP for improved wind-electric power forecasts,” *IEEE Trans. Ind. Inform.*, vol. 12, no. 3, pp. 991–1004, Jun. 2016.
- [17] Y. Wang, N. Zhang, Q. Chen, D. S. Kirschen, P. Li, and Q. Xia, “Data-driven

- probabilistic net load forecasting with high penetration of behind-the-meter PV,” *IEEE Trans. Power Syst.*, vol. 33, no. 3, pp. 3255–3264, May 2018.
- [18] S. Ghosh, S. Rahman, and M. Pipattanasomporn, “Distribution voltage regulation through active power curtailment with PV inverters and solar generation forecasts,” *IEEE Trans. Sustain. Energy*, vol. 8, no. 1, pp. 13–22, Jan. 2017.
- [19] H. Hao, Y. Lin, A. S. Kowli, P. Barooah, and S. Meyn, “Ancillary service to the grid through control of fans in commercial building HVAC systems,” *IEEE Trans. Smart Grid*, vol. 5, no. 4, pp. 2066–2074, Jul. 2014.
- [20] I. Beil, I. Hiskens, and S. Backhaus, “Frequency regulation from commercial Building HVAC demand response,” *Proc. IEEE*, vol. 104, no. 4, pp. 745–757, Apr. 2016.
- [21] H. Huang and F. Li, “Sensitivity analysis of load-damping characteristic in power system frequency regulation,” *IEEE Trans. Power Syst.*, vol. 28, no. 2, pp. 1324–1335, May 2013.
- [22] E. Vrettos, *Control of residential and commercial loads for power system ancillary services*, PhD. dissertation, Dipl. -Ing. National Technical University of Athens, Greece, 2016.
- [23] H. Hui, Y. Ding, W. Liu, Y. Lin, and Y. Song, “Operating reserve evaluation of aggregated air conditioners,” *Appl. Energy*, vol. 196, pp. 218–228, Jun. 2017.
- [24] Mikael Amelin, “Frequency control,” Electrical Engineering, KTH Royal Ins. Tech., [Online] Available: <https://www.kth.se/social/upload/52e0c925f2765446480bda2b/L5-L6.pdf>.
- [25] Y. V. Makarov, C. Loutan, J. Ma, and P. de Mello, “Operational impacts of wind generation on California power systems,” *IEEE Trans. Power Syst.*, vol. 24, no. 2, pp.

1039–1050, May 2009.

- [26] T. Ericson, “Direct load control of residential water heaters,” *Energy Policy*, vol. 37, no. 9, pp. 3502–3512, Sep. 2009.
- [27] R. George, K. G. Harikrishnan, G. Zacharia, and N. Augustine, “Peak hour load control & overcurrent monitoring system,” *International Research Journal of Engineering and Technology*, vol. 3, no. 6, pp. 2392-2395, Jun. 2016.
- [28] F. Ruelens, B. J. Claessens, S. Quaiyum, B. D. Schutter, R. Babuška, and R. Belmans, “Reinforcement learning applied to an electric water heater: From theory to practice,” *IEEE Trans. Smart Grid*, vol. 9, no. 4, pp. 3792–3800, Jul. 2018.
- [29] F. Ruelens, B. J. Claessens, S. Vandael, B. D. Schutter, R. Babuška, and R. Belmans, “Residential demand response of thermostatically controlled loads using batch reinforcement learning,” *IEEE Trans. Smart Grid*, vol. 8, no. 5, pp. 2149–2159, Sep. 2017.
- [30] C. Perfumo, E. Kofman, J. H. Braslavsky, and J. K. Ward, “Load management: Model-based control of aggregate power for populations of thermostatically controlled loads,” *Energy Convers. Manag.*, vol. 55, pp. 36–48, Mar. 2012.
- [31] X. Gong, J. L. Cardenas-Barrera, E. Castillo-Guerra, B. Cao, S. A. Saleh, and L. Chang, “Bottom-up load forecasting with Markov-based error reduction method for aggregated domestic electric water heaters,” *IEEE Trans. Ind. Appl.*, vol. 55, no. 6, pp. 6401–6413, Nov-Dec., 2019.
- [32] K. Al-jabery, Z. Xu, W. Yu, D. C. Wunsch, J. Xiong, and Y. Shi, “Demand-side management of domestic electric water heaters using approximate dynamic programming,” *IEEE Trans. Comput.-Aided Des. Integr. Circuits Syst.*, vol. 36, no.

- 5, pp. 775–788, May 2017.
- [33] *Energy Use Handbook 1990 to 2015*, Natural Resources Canada, Ottawa, Canada, 2018.
- [34] A. Sepulveda, L. Paull, W. G. Morsi, H. Li, C. P. Diduch, and L. Chang, “A novel demand side management program using water heaters and particle swarm optimization,” in *2010 IEEE Electrical Power Energy Conference*, Aug. 2010, pp. 1–5.
- [35] A. Moreau, “Control strategy for domestic water heaters during peak periods and its impact on the demand for electricity,” *Energy Procedia*, vol. 12, pp. 1074–1082, 2011.
- [36] M. Pfeiffer, *Load control strategies for electric water heaters with thermal stratification*, Semester Thesis, EEH - Power Systems Lab., Swiss Federal Ins. of Tech. Zurich, Zurich, Spring. 2011.
- [37] *Energy Star Water Heater Demand Response Test Procedure Check-In 1*, U. S. Department of Energy, Washington, U. S. A., Aug. 2019.
- [38] David Podorson and E Source, “Grid interactive water heaters - How water heaters have evolved into a grid scale energy storage medium,” *the 2016 ACEEE Summer Study on Energy Efficiency in Buildings*, 2016.
- [39] *Designing, Operating, and Simulating Electric Water Heater Populations for the Smart Grid*, CanmetENERGY, Varennes, Quebec, Canada, 2013.
- [40] Ken Eklund, “Assessment of Demand Response Potential of Heat Pump Water Heaters,” *Washington State University Energy Program*, Olympia, WA, Sep. 2015.
- [41] R. Diao, S. Lu, M. Elizondo, E. Mayhorn, Y. Zhang, and N. Samaan, “Electric water

- heater modeling and control strategies for demand response,” in *2012 IEEE Power and Energy Society General Meeting*, Jul. 2012, pp. 1–8.
- [42] S. Iacovella, K. Lemkens, F. Geth, P. Vingerhoets, G. Deconinck, R. DHulst, K. Vanthournout, “Distributed voltage control mechanism in low-voltage distribution grid field test,” in *2013 4th IEEE PES Innovative Smart Grid Technologies EUROPE (ISGT EUROPE)*, Oct. 2013.
- [43] J. Wang, H. Zhang, and Y. Zhou, “Intelligent under frequency and under voltage load shedding method based on the active participation of smart appliances,” *IEEE Trans. Smart Grid*, vol. 8, no. 1, pp. 353–361, Jan. 2017.
- [44] N. Ruiz, I. Cobelo, and J. Oyarzabal, “A direct load control model for virtual power plant management,” *IEEE Trans. Power Syst.*, vol. 24, no. 2, pp. 959–966, May 2009.
- [45] T. M. Calloway and C. W. Brice, “Physically-based model of demand with applications to load management assessment and load forecasting,” *IEEE Trans. Power Appar. Syst.*, no. 12, pp. 4625–4631, 1982.
- [46] A. Gomes, C. H. Antunes, and A. G. Martins, “A multiple objective evolutionary approach for the design and selection of load control strategies,” *IEEE Trans. Power Syst.*, vol. 19, no. 2, pp. 1173–1180, 2004.
- [47] S. Koch, J. L. Mathieu, and D. S. Callaway, “Modeling and control of aggregated heterogeneous thermostatically controlled loads for ancillary services,” in *Power Systems Computation Conference*, 2011, pp. 1–7.
- [48] F. Aguirre, F. H. Magnago, and J. M. Alemany, “Constructing hot water load profile: An agent-based modeling approach,” *IEEE Trans. Sustain. Energy*, pp. 1–1, June. 2018.

- [49] H. Kazmi, S. D'Oca, C. Delmastro, S. Lodeweyckx, and S. P. Corgnati, "Generalizable occupant-driven optimization model for domestic hot water production in NZEB," *Appl. Energy*, vol. 175, pp. 1–15, Aug. 2016.
- [50] R. Spur, D. Fiala, D. Nevrala, and D. Probert, "Influence of the domestic hot-water daily draw-off profile on the performance of a hot-water store," *Appl. Energy*, vol. 83, no. 7, pp. 749–773, Jul. 2006.
- [51] R. Spur, D. Fiala, D. Nevrala, and D. Probert, "Performances of modern domestic hot-water stores," *Appl. Energy*, vol. 83, no. 8, pp. 893–910, Aug. 2006.
- [52] M. H. Nehrir, B. J. LaMeres, and V. Gerez, "A customer-interactive electric water heater demand-side management strategy using fuzzy logic," in *Power Engineering Society 1999 Winter Meeting, IEEE*, 1999, vol. 1, pp. 433–436.
- [53] Q. Hu and F. Li, "Hardware design of smart home energy management system with dynamic price response," *IEEE Trans. Smart Grid*, vol. 4, no. 4, pp. 1878–1887, Dec. 2013.
- [54] Ning Lu and S. Katipamula, "Control strategies of thermostatically controlled appliances in a competitive electricity market," in *IEEE Power Engineering Society General Meeting 2005*, vol. 1, pp. 202–207, Jun. 2005.
- [55] J. Kondoh, N. Lu, and D. J. Hammerstrom, "An evaluation of the water heater load potential for providing regulation service," *IEEE Trans. Power Syst.*, vol. 26, no. 3, pp. 1309–1316, Aug. 2011.
- [56] X. Gong, E. Castillo-Guerra, J. L. Cardenas-Barrera, B. Cao, S. A. Saleh, and L. Chang, "Robust hierarchical control mechanism for aggregated thermostatically controlled loads," *IEEE Trans. Smart Grid*, vol. 12, no.1, pp. 453–467, Jan. 2021.

- [57] D. S. Callaway and I. A. Hiskens, “Achieving controllability of electric loads,” *Proc. IEEE*, vol. 99, no. 1, pp. 184–199, Jan. 2011.
- [58] Z. A. Obaid, L. M. Cipcigan, M. T. Muhssin, and S. S. Sami, “Development of a water heater population control for the demand-side frequency control,” in *2017 IEEE PES Innovative Smart Grid Technologies Conference Europe (ISGT-Europe)*, Sep. 2017, pp. 1–6.
- [59] K. Elamari and L. A. C. Lopes, “Frequency based control of electric water heaters in small PV-diesel hybrid mini-grids,” in *2012 25th IEEE Canadian Conference on Electrical and Computer Engineering (CCECE)*, Apr. 2012, pp. 1–4.
- [60] A. Haider, W. Stark, and T. K. A. Brekken, “Electric hot water heater primary frequency control,” in *2018 IEEE Energy Conversion Congress and Exposition (ECCE)*, Sep. 2018, pp. 2670–2675.
- [61] T. Masuta and A. Yokoyama, “Supplementary load frequency control by use of a number of both electric vehicles and heat pump water heaters,” *IEEE Trans. Smart Grid*, vol. 3, no. 3, pp. 1253–1262, Sep. 2012.
- [62] M. Shaad, C. P. Diduch, M. E. Kaye, and L. Chang, “A basic load following control strategy in a direct load control program,” in *2015 IEEE Electrical Power and Energy Conference (EPEC)*, Oct. 2015, pp. 339–343.
- [63] W. B. DeOreo and P. W. Mayer, “The end uses of hot water in single family homes from flow trace analysis,” *Water Research Foundation, Aquacraft Inc Rep. Undated*, 2000.
- [64] *Residential End Uses of Water, Version 2: Executive Report*, Water Research Foundation, Alexandria, USA, Apr. 2016.

- [65] H. Farahbakhsh, V. I. Ugursal, and A. S. Fung, "A residential end-use energy consumption model for Canada," *Int. J. Energy Res.*, vol. 22, no. 13, pp. 1133–1143, 1998.
- [66] C. Aguilar, D. J. White, D. L. Ryan, "*Domestic water heating and water heater energy consumption in Canada*," Canadian Building Energy End-Use Data and Analysis Centre, Apr. 2005.
- [67] P. Pijnenburg, S. A. Saleh, and P. McGaw, "Performance evaluation of the ZIP model-phaselet frame approach for identifying appliances in residential loads," *IEEE Trans. Ind. Appl.*, vol. 52, no. 4, pp. 3408–3421, Jul. 2016.
- [68] *Quantifying the energy and carbon effects of water saving full technical report*, Environment Agency, Little Hillm Orcop, Hereford, Apr. 2009.
- [69] E. McKenna and M. Thomson, "High-resolution stochastic integrated thermal–electrical domestic demand model," *Appl. Energy*, vol. 165, no. Supplement C, pp. 445–461, Mar. 2016.
- [70] S. Xiang, L. Chang, B. Cao, Y. He, and C. Zhang, "A Novel Domestic Electric Water Heater Control Method," *IEEE Trans. Smart Grid*, vol. 11, no. 4, pp. 3246–3256, Jul. 2020.
- [71] N. G. Paterakis, O. Erdinç, A. G. Bakirtzis, and J. P. S. Catalão, "Optimal household appliances scheduling under day-ahead pricing and load-shaping demand response strategies," *IEEE Trans. Ind. Inform.*, vol. 11, no. 6, pp. 1509–1519, Dec. 2015.
- [72] V. Dufresne, *The Value of Demand Response in a Hydro-Dominated Power Grid – The Example of Quebec, Canada*, Master dissertation, Carleton University, Ottawa, Canada, 2016.

- [73] *Water Heating Data Collection and Analysis, Residential End Use Monitoring Program (REMP)*, Commonwealth of Australia, 2012.
- [74] Linqi Zhu, Chong Zhang, Chaomo Zhang, Zhansong Zhang, Xueqing ZHou, Weinan Liu, Boyuan Zhu, “A new and reliable dual model- and data-driven TOC prediction concept: A TOC logging evaluation method using multiple overlapping methods integrated with semi-supervised deep learning,” *Journal of Petroleum Science and Engineering*, vol. 188, pp. 1-16, May. 2020.
- [75] Arnaldo Sepulveda, *Soft computing methods for the implementation of aggregated load control of domestic electric water heaters*, Master dissertation, Univ. New Brunswick, 2009.
- [76] L. Paull, H. Li, and L. Chang, “A novel domestic electric water heater model for a multi-objective demand side management program,” *Electr. Power Syst. Res.*, vol. 80, no. 12, pp. 1446–1451, Dec. 2010.
- [77] M. Shad, A. Momeni, R. Errouissi, C. P. Diduch, M. E. Kaye, and L. Chang, “Identification and estimation for electric water heaters in direct load control programs,” *IEEE Trans. Smart Grid*, vol. 8, no. 2, pp. 947–955, Mar. 2017.
- [78] Minimum Hot Water Needs for a Dishwasher [Online], Available: <https://homeguides.sfgate.com/minimum-hot-water-needs-dishwasher-84557.html>.
- [79] How Long is a Dishwasher Cycle [Online], Available: <https://www.finishdishwashing.ca/en/benefits-of-dishwasher/efficiency/>.
- [80] *Residential end uses of water*, American Water Works Association Research Foundation, 1999.
- [81] I. Richardson, M. Thomson, and D. Infield, “A high-resolution domestic building

- occupancy model for energy demand simulations,” *Energy Build.*, vol. 40, no. 8, pp. 1560–1566, Jan. 2008.
- [82] M. A. Zuniga Alvarez, K. Agbossou, A. Cardenas, S. Kelouwani, and L. Boulon, “Demand response strategy applied to residential electric water heaters using dynamic programming and K-Means clustering,” *IEEE Trans. Sustain. Energy*, pp. 1–1, Feb. 2019.
- [83] T. Sonnekalb and S. Lucia, “Smart hot water control with learned human behavior for minimal energy consumption,” in *2019 IEEE 5th World Forum on Internet of Things (WF-IoT)*, 2019, pp. 572–577.
- [84] Commission Acts On Hot Tap Water Scald Hazard, *U.S. Consumer Product Safety Commission*, Aug. 22, 2016.
- [85] Christiana O. Onabola, “Health and Safety Aspects of Demand Response on Electric Storage Water Heaters: A Mini Literature Review,” *UBC Sustainability Scholar*, Vancouver, Quebec, Canada, 2018.
- [86] H. Liang, Y. Liu, F. Li, and Y. Shen, “Dynamic economic/emission dispatch including PEVs for peak shaving and valley filling,” *IEEE Trans. Ind. Electron.*, vol. 66, no. 4, pp. 2880–2890, Apr. 2019.
- [87] J.-J. Shen, Q.-Q. Shen, S. Wang, J.-Y. Lu, and Q.-X. Meng, “Generation scheduling of a hydrothermal system considering multiple provincial peak-shaving demands,” *IEEE Access*, vol. 7, pp. 46225–46239, Mar. 2019.
- [88] M. J. E. Alam, K. M. Muttaqi, and D. Sutanto, “A controllable local peak-shaving strategy for effective utilization of PEV battery capacity for distribution network support,” *IEEE Trans. Ind. Appl.*, vol. 51, no. 3, pp. 2030–2037, May 2015.

- [89] A. Esmat, J. Usaola, and M. Á. Moreno, “Congestion management in smart grids with flexible demand considering the payback effect,” in *2016 IEEE PES Innovative Smart Grid Technologies Conference Europe (ISGT-Europe)*, 2016, pp. 1–6.
- [90] H. Vermeulen and T. Nieuwoudt, “Optimization of residential solar PV system rating for minimum payback time using half-hourly profiling,” in *2015 International Conference on the Domestic Use of Energy (DUE)*, 2015, pp. 215–221.
- [91] E. Georges, V. Lemort, B. Cornélusse, D. Ernst, Q. Louveaux, and S. Mathieu, “Direct control service from residential heat pump aggregation with specified payback,” in *2016 Power Systems Computation Conference (PSCC)*, 2016, pp. 1–7.
- [92] *Residential Electric Water Heater Owner's Manual Installation and Operating Instructions*, Giant Factories Inc, Montreal, Quebec, Canada, 2017.
- [93] Z. Xu, R. Diao, S. Lu, J. Lian, and Y. Zhang, “Modeling of electric water heaters for demand response: A baseline PDE model,” *IEEE Trans. Smart Grid*, vol. 5, no. 5, pp. 2203–2210, Sep. 2014.
- [94] Marcel Boter, “Higher electricity prices can unleash the value of Quebec's energy potential,” Montreal economic Ins., Apr. 2007.
- [95] OECD Economic Surveys Canada 2010, *Organization For Economic Co-operation and Development*, Canada, vol. 2010/14, Sept. 2010.
- [96] *A smart grid electricity price plan*, OSPE Energy Task Force, Ontario Society of Professional Engineers, Jun. 2015.
- [97] O. Erdinç, A. Taşcıkaraoğlu, N. G. Paterakis, Y. Eren, and J. P. S. Catalão, “End-user comfort oriented day-ahead planning for responsive residential HVAC demand aggregation considering weather forecasts,” *IEEE Trans. Smart Grid*, vol. 8, no. 1,

- pp. 362–372, Jan. 2017.
- [98] Benoît Lévesque, Michel Lavoie, and Jean Joly, "Residential water heater temperature: 49 or 60 degrees Celsius?", *Can J Infect Dis*, vol. 15, no. 1, pp. 11-12, Jan-Feb., 2004.
- [99] T. S. Borsche, A. Ulbig, and G. Andersson, "Impact of frequency control reserve provision by storage systems on power system operation," *IFAC Proc. Vol.*, vol. 47, no. 3, pp. 4038–4043, Jan. 2014.
- [100] M. Perninge and R. Eriksson, "Optimal tertiary frequency control in power systems with market-based regulation," *IFAC-PapersOnline.*, vol. 50, no. 1, pp. 4374–4381, Jul. 2017.
- [101] X. Gong, J. L. C. Barrera, L. Chang, E. C. Guerra, B. Cao, and S. Saleh, "Integrated multi-horizon power and energy forecast for aggregated electric water heaters," in *2018 IEEE Energy Conversion Congress and Exposition (ECCE)*, 2018, pp. 2628–2635.
- [102] F. L. Quilumba, W.-J. Lee, H. Huang, D. Y. Wang, and R. L. Szabados, "Using smart meter data to improve the accuracy of intraday load forecasting considering customer behavior similarities," *IEEE Trans. Smart Grid*, vol. 6, no. 2, pp. 911–918, Mar. 2015.
- [103] IEEE 34 node test model, IEEE PES AMPS DSAS Test Feeder Working Group, [Online]. Available: <https://site.ieee.org/pes-testfeeders/resources/>.
- [104] 30 Minute Uncertainty Data, Pennsylvania-New Jersey-Maryland (PJM), May 2019 [Online]. Available: <https://www.pjm.com/Search%20Results.aspx?#q=30-minute-uncertainty&sort=relevancy>.
- [105] L. Mili, "Taxonomy of the characteristics of power system operating states," 2nd

Nation Science Foundation Resilient and Sustainable Infrastructures (NSF RESIN) workshop, Jan. 2011.

- [106] A. Abur and A. G. Expósito, “Power System State Estimation: Theory and Implementation,” CRC Press, Mar.2004.
- [107] J. L. Mathieu, S. Koch, and D. S. Callaway, “State estimation and control of electric loads to manage real-time energy imbalance,” *IEEE Trans. Power Syst.*, vol. 28, no. 1, pp. 430–440, Feb. 2013.

Appendix I Solution of the Objective Function

For the objective function

$$\min \left| P_{obj} - P_{back} - \sum_{q=1}^p P_{rate,q} CS_q^k \right|$$

$$s.t. \begin{cases} \text{If } C_q^k = 0, CS_q^k = 0 \\ \text{If } C_q^k = 1, CS_q^k = 0 \text{ or } 1 \\ \text{If } CS_q^k = 0, CS_{q+1}^k = 0 \\ \text{If } CS_q^k = 1, CS_{q+1}^k = 0 \text{ or } 1 \end{cases}$$

where, P_{obj} is the desired demand of DEWHs, p is the number of controllable DEWHs, q is q^{th} DEWHs in the sorted list, P_{back} is the increased demand to maintain the end-user comfort, P_{rate} is the rated power, CS_q^k is the control signal on q^{th} DEWH at k^{th} sampling interval, and C_q^k is the control availability for q^{th} DEWH at k^{th} sampling interval. $C_q^k = 0$ indicates that the DEWH is uncontrollable, and $C_q^k = 1$ represents controllable. $CS_q^k = 0$ indicates that the DEWH receive off-signal, and $CS_q^k = 1$ represents the DEWH receive on-signal.

The solution process is:

Step 1. The function $\min |P_{obj} - P_{back} - \sum_{q=1}^p P_{rate,q} CS_q^k|$ is re-written as:

$$\sum_{q=1}^p P_{rate,q} CS_q^k \rightarrow P_{obj} - P_{back}$$

Step 2. Based on the constraints $s. t. \begin{cases} \text{If } C_q^k = 0, CS_q^k = 0 \\ \text{If } C_q^k = 1, CS_q^k = 0 \text{ or } 1 \end{cases}$, only these controllable.

These control signals for these controllable DEWHs should satisfy

$s. t. \begin{cases} \text{If } CS_q^k = 0, CS_{q+1}^k = 0 \\ \text{If } CS_q^k = 1, CS_{q+1}^k = 0 \text{ or } 1 \end{cases}$, then the re-written equation can be translated to:

$$P_{rate,1} + P_{rate,2} + \dots + P_{rate,r} \rightarrow P_{obj} - P_{back}.$$

Step 3. The r is obtained.

Step 4. The solution of CS^k is obtained with $CS_i^k = \begin{cases} 1, i = 1, 2, \dots, r \\ 0, i = r + 1, \dots, p \end{cases}$.

Appendix II Analysis of the Maximum Ramp-Down Power Is Increased by the Adaptive Criterion

To analyze the maximum ramp-down power is increased by the adaptive criterion.

The ramp-down power $P_{down,max}$ is negative, the maximum value:

$$P_{down,max}(t) = \sum_{k=1}^{g2(t)} P_{rate,k} + \sum_{j=1}^{g4(t)} P_{rate,j} - P_{VFCP}(t)$$

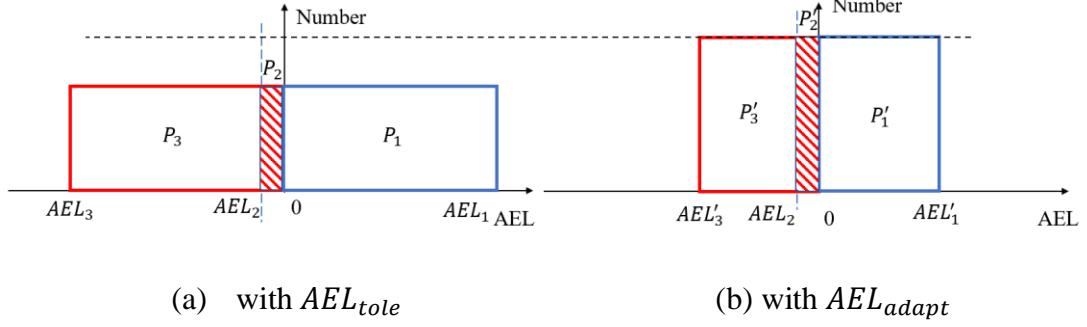
where $g2$, and $g4$ are the number of DEWHs in Group 2, and Group 4, respectively, k means the k^{th} DEWH in Group 2, and j means the j^{th} DEWH in Group 4. P_{VFCP} is the VFCP power, and P_{base} is the demand of the baseline. The VFCP is controlled to charge/discharge to respond to the desired correcting power for frequency control, it should not be changed by control actions.

Hence, the maximum ramp-down power is increased with the decrease in the cumulative power of these DEWHs in Group 2 and Group 4. As these DEWHs are turned on when their AELs are lower than AEL_{adapt} , they are directly changed from Group 3 to Group 2. Hence, there will be rarely DEWHs in Group 4, in other words, the cumulative power of these DEWHs in Group 4 is reduced.

As the VFCP power is:

$$P_{VFCP}(t) = \sum_{i=1}^{g1(t)} P_{rate,i} + \sum_{k=1}^{g2(t)} P_{rate,k}$$

where $g1$ is the number of DEWHs in Group 1, and i is the i^{th} DEWH in Group 1. The VFCP power can not be changed by control.



The figure show that with AEL_{adapt} , the AELs of DEWHs are controlled in a narrower range, the DEWH temperatures are closer to their lower limits. The VFCP power are equal.

$$\begin{cases} P_{VFCP}(t) = P_1(t) + P_2(t) + P_3(t) \\ P_{VFCP}(t) = P'_1(t) + P'_2(t) + P'_3(t) \end{cases}$$

Let us assume the cumulative power of the DEWHs in Group 1 for both cases are equal, then, they are equal in Group 2 too.

$$\begin{cases} P_1(t) = P'_1(t) \\ P_2(t) + P_3(t) = P'_2(t) + P'_3(t) \end{cases}$$

The DEWHs are heating and their AELs are increasing by $-AEL_2$ in a time interval, these DEWHs which $AEL_2 \leq AEL \leq 0$ will be changed from Group 2 to Group 1 at next interval. If we assume that no DEWH thermostat change in the time interval, and no control actions are applied, then the cumulative power of the DEWHs in Group 1 are:

$$\begin{cases} P_1(t+1) = P_1(t) + P_2(t) \\ P'_1(t+1) = P'_1(t) + P'_2(t) \end{cases}$$

And the cumulative power of the DEWHs in Group 2 are $P_3(t)$ and $P'_3(t)$. It is obvious that the cumulative power of these DEWHs in Group 2 is reduced. The maximum ramp-down power is increased by AE_{adapt} .

If we select the criterion as $AE = 0$, these DEWHs in Group 3 with $AE < 0$ are required to turn on, which will need to reduce the cumulative power of DEWHs in Group 1; in other words, the maximum ramp-down power is reduced. The available control capacity is smaller than that with AE_{adapt} .

Hence, the cumulative power of these DEWHs in Group 2 and Group 4 are reduced by AE_{adapt} , then, the maximum ramp-down power of the VFPC is increased.

Curriculum Vitae

Candidate's full name: Sheng Xiang

Universities attended (with dates and degrees obtained):

2007-2011, Bachelor of Science,
Electrical Engineering,
School of Electrical Engineering and Automation,
Hefei University of Technology,
Hefei, Anhui, China.

2011-2014, Master of Engineering,
Electrical Engineering,
School of Electrical Engineering and Automation,
Hefei University of Technology,
Hefei, Anhui, China.

2014-2016 Ph.D. Candidate,
Electrical Engineering,
School of Electrical Engineering and Automation,
Hefei University of Technology,
Hefei, Anhui, China.

2016-Present Pd.D. Candidate,

Electrical Engineering,
Department of Electrical and Computer Engineering,
University of New Brunswick,
Fredericton, NB, Canada.

Publications:

- (1) Sheng Xiang, Liuchen Chang, Bo Cao, Yigang He, Chaolong Zhang, "A novel domestic electric water heater control method," *IEEE Trans. Smart Grid*, vol. 11, no. 4, pp. 3246-3256, Jul. 2020.
- (2) Sheng Xiang, Liuchen Chang, Bo Cao, Yigang He, "Group-based control for domestic electric water heaters with quantum-inspired evolutionary algorithm," *IEEE Energy Conversion Congress & Expo, ECCE 2020*, Oct. 2020.
- (3) Sheng Xiang, Yigang He, Liuchen Chang, Kehan Wu, Chaolong Zhang, "An improved quantum-inspired evolutionary algorithm for knapsack problems," *Cloud Computing and Security, 3rd International Conference, ICCCS 2017*, pp: 694-708, 2017.
- (4) Sheng Xiang, Yigang He, "Optimal economic scheduling of electric power system based on elite group guided quantum-inspired evolutionary algorithm," *3rd International Conference on Information Science and Control Engineering*, pp: 1024-1028, 2016.
- (5) Chaolong Zhang, Yigang He, Lifeng Yuan, Sheng Xiang, "A multiple heterogeneous kernel RVM approach for analog circuit fault prognostic," *Cluster Computing*, vol. 22, supplement 2, pp: 3849-3861, Mar. 2019.
- (6) Chaolong Zhang, Yigang He, Lifeng Yuan, Sheng Xiang, "Analog circuit incipient

- fault diagnosis method using DBN based features extraction,” *IEEE Access*, vol. 6, pp: 23053- 23064, 2018.
- (7) Chaolong Zhang, Yigang He, Lifeng Yuan, Sheng Xiang, “Capacity prognostics of lithium-ion batteries using EMD denoising and multiple kernel RVM,” *IEEE Access*, vol. 5, pp: 12061- 12070, 2017.
- (8) Chaolong Zhang, Yigang He, Lifeng Yuan, Wei He, Sheng Xiang, Zhigang Li, “A novel approach for diagnosis of analog circuit fault by using GMKL-SVM and PSO,” *Journal of Electronic Testing*, vol. 32, no. 5, pp: 531-540, Oct. 2016.

Patents (Authorized):

- (1) CN106532721B, Yigang He, Sheng Xiang, Wei He, Luqiang Shi, Guolong Shi, Bing Li, Liulu He.
- (2) CN107702346B, Yigang He, Sheng Xiang, Chenchen Li, Lin Tao, Lei Zuo, Liulu He.
- (3) CN107202428A, Yigang He, Sheng Xiang, Zhigang Li, Hui Yang, Liulu He.
- (4) CN102946239B, Yigang He, Mu Li, Hongmin Li, Sheng Xiang.
- (5) CN102982376B, Yigang He, Wu Peng, Hongmin Li, Sheng Xiang.
- (6) CN104459560B, Yigang He, Chaolong Zhang, Lei Zuo, Sheng Xiang, Baiqiang Yin.
- (7) US10408882B2, Yigang He, Chaolong Zhang, Lei Zuo, Sheng Xiang, Baiqiang Yin.
- (8) CN104568208B, Yigang He, Fangming Deng, Lei Zuo, Baiqing Yin, Bing Li, Lifeng Yuan, Sheng Xiang, Wei He.
- (9) CN105610191B, Yigang He, Tao Wang, Baiqiang Yin, Zhigang Li, Wei He, Tiancheng Shi, Sheng Xiang, Yuanyuan Su.